The histone methyltransferase DOT1L: discovery of small-molecule inhibitors and its role in Wnt signaling

by

Garrett S. Gibbons

A dissertation submitted in partial fulfillment
of the requirements for the degree of
Doctor of Philosophy
(Molecular and Cellular Pathology)
in the University of Michigan
2014

Doctoral committee:

Assistant Professor Zaneta Nikolovska-Coleska, Chair
Assistant Professor Tomasz Cierpicki
Professor Eric R. Fearon
Professor Hollis D. Showalter

© Garrett S. Gibbons 2014

DEDICATION

This work is dedicated to my mother, Mary Jo Gibbons,
and her father, James Johnson.

ACKNOWLEDGEMENTS

I must express the utmost gratitude for the mentorship of Zaneta Nikolovska-Coleska. She has been supportive throughout our entire time together and has encouraged my growth as a scientist and as a person. The lessons she has provided me with during this thesis encompass more than technical skills, but personal life skills, work ethic, and dedication. I sincerely appreciate all the members of the lab, past and present, who provided technical and moral support as well as fostered intellectual growth and solidarity in times of challenges.

My thesis committee was instrumental in the guidance and completion of this thesis work. Eric R. Fearon and lab members provided guidance, cell lines and reagents for Wnt signaling experiments. Hollis D. Showalter contributed significant knowledge and guidance in addition to lab space and reagents for the synthesis of compounds. Tomasz Cierpicki and his lab members provided technical expertise for NMR experiments. Jay L. Hess and lab members contributed extensive expertise in the field of MLL leukemia biology and provided numerous cell lines and reagents. The staff of the molecular and cellular pathology department, Laura Hessler, Laura Labut, and the former director, Nick Lukacs, have been vital for my success as a graduate student at the University of Michigan.

Many collaborators have contributed greatly to this work and my training. In particular, Andrew Muntean provided valuable insight and discussion as well as performing colony forming unit assays. My colleagues, Meilan Liu, Adrienne Wang, Stephen Johnson, and Paul Marinec have each spent hours of their precious time to train me in technical skills and/or to demonstrating the type of scientist I hope to become. The faculty in the Department of Chemistry at Michigan Technological University, particularly, Pushpalaltha Murthy, Dallas Bates, Shiyue Fang, and David Chesney all took time to

mentor me as an undergraduate and provided me with experiences to be successful in my Ph.D. work. Undoubtedly, the spark of scientific interest was ignited within me by David “Kirb” Kirby as a high school student. The demonstration of scientific principles and inquiry were instrumental in setting me on a path towards scientific research.

I have received tremendous support from my family, in particular, my mother to whom I am eternally grateful. Her unconditional love and encouragement has continually driven my enthusiasm to follow this path laid before me. The unfortunate situations of those around me have transformed into a launch pad for creative thought, critical analysis, and scientific inquiry. The death of my father at a young age from a brain tumor unleashed a plethora of questions and fueled a young mind’s desire to better understand the world around it. Witnessing my grandfather experience the brutally slow and unyielding progression of Alzheimer’s disease until his death was the inspiration that lead to my path towards seeking therapies for diseases. My entire family has constantly encouraged me and for that I am grateful.

Lastly, I must thank a fellowship within the community that has taught me a set of principles and a new way of life, without whom I would not be here today. When I needed help, they were there to pass along to me what was so freely given to them. The friends I have today are absolutely necessary for my serenity and the ability to pursue this research. *Aloha ke akua*.

TABLE OF CONTENTS

LIST OF FIGURES

LIST OF ABBREVIATIONS

^{3}H – tritium isotope
AEP - AF4 and ENL family proteins
AF4 – MLLT2 mixed lineage leukemia translocated to chromosome 2 protein
AF6 – MLLT4 mixed lineage leukemia translocated to chromosome 4 protein
AF9 – MLLT3 mixed lineage leukemia translocated to chromosome 3 protein
AF10– MLLT10 mixed lineage leukemia translocated to chromosome 10 protein
ALL - acute lymphoblastic leukemia
AML - acute myeloid leukemia
APC – adenomatous polyposis coli
ASH2L – absent small or homeotic 2 like
Bcl-1 – B-cell lymphoma
BH3 – Bcl-1 homology domain 3
Boc – ditert-butoxylcarbonyl
CBCs – Crypt basal columnar cells
CBP – CREB binding protein
ChIP – chromatin immunoprecipitation
CK1 - casein kinase 1
DCE - dichloroethane
DMAP – 4- dimethylamino pyrimidine
DMSO - dimethylsulfoxide
DNA – deoxyribonucleic acid
DOT1L – Disruptor of Telomeric Silencing 1 Like
DotCom – DOT1L complex
EAP – ENL associated proteins
ELISA - enzyme linked immunosorbent assays
ENL – eleven nineteen leukemia protein
EPZ - Epizyme
FP - fluorescence polarization
FRET - fluorescence resonance energy transfer assays
GSK3 - glycogensynthase kinase 3
GST – glutathione s-transferase
GPR84 – G-protein coupled receptor 84
Hoxa9 – homeobox a9

H3K79 – Histone H3 Lysine 79
H3K79Me1 – monomethylated Histone H3 Lysine 79
H3K79Me2 – dimethylated Histone H3 Lysine 79
H3K79Me3 – trimethylated Histone H3 Lysine 79
H3 – histone H3
H4 – histone H4
H2A – histone H2A
H2B – histone H2B
His6- polyhistidine tag
HMDS - hexamethyldisilazane
HMTase- Histone Methyltransferase
HPLC – high performance liquid chromatography
i-fabp - intestinal fatty acid binding protein
IP - intraperitoneal
ISCs – intestinal stem cells
ITC- isothermal titration calorimetry
IV - intravenous
LEF – Lymphoid enhancer-binding factor
LRP - Lipoprotein receptor-related protein
MCL-1 – myeloid cell leukemia-1
MLL- Mixed lineage leukemia
MOF – MYST1 K (lysine) acetyltransferase 8
SAM – S-adenosyl methionine
SAH – S-adenosyl homocysteine
OM-LZ - octapeptide motif and leucine zipper
PAFc – polymerase associated factor complex
Pd/C – palladium on carbon
PHD – plant homeo domain
qRT-PCR – quantitative real time polymerase chain reaction
RBP5 – auxin binding protein 5
Rspo - R-spondin
SCF – stem cell factor
SEC – super elongation complex
Skp1 – s-phase kinase associated protein 1
SMAC – second mitochondrial derived activator of caspase
SP – standard precision
SMN - survival motor neuron
STD – saturation transfer difference
TCF – T-cell factor

TFA – trifluoroacetic acid
THF - tetrahydrofuran
TLC – thin layer chromatography
TMS – trimethylsilane
TMSOTf – trimethylsilyl trifluoromethansulfonate
TRRAP - Transformation/transcription domain-associated protein
UMD – University of Michigan Disruptor of H3K79 methylation
UV-vis – ultra violet- visible light spectrum
WDR5 – WD repeat domain 5
Wnt – wingless type
XIAP – x-linked inhibitor of apoptosis
XP – extra precision

ABSTRACT

Covalent post translational modifications of histone proteins are an important mechanism of epigenetic gene regulation that modulate chromatin structure. Methylation of histone lysine residues is one of several chemical marks that establish the “histone code” essential for proper temporal and spatial expression of gene programs required for cell fate determination in development. Dysregulation of histone methylation contributes to the development of numerous human diseases, particularly cancer. The sole histone H3 lysine 79 (H3K79) methyltransferase, DOT1L, is required for leukemogenic transformation in a subset of leukemias bearing translocations of the *MLL* gene. Human leukemias carrying *MLL* gene rearrangements aberrantly recruit DOT1L to leukemogenic genes leading to increased H3K79 methylation and their transcriptional activation. There are also reports that DOT1L plays a role in Wnt signaling, a pathway frequently dysregulated in colon cancer. Small molecule inhibitors of DOT1L are highly sought for the development of therapeutics in leukemia and as chemical tools to probe the role of DOT1L in other human diseases. We applied several approaches for the identification of DOT1L inhibitors, virtual screening, *de novo* design, and biochemical screening. Here we present the biochemical, biophysical, and cellular characterization of different classes of DOT1L inhibitors. Several S-adenosylmethionine (SAM) analogues have been identified as DOT1L inhibitors by virtual screening and we developed a novel pathway for synthesis of additional 5’ modified adenosine analogues. Additionally, we identified UMD-7, which inhibits H3K79 methylation by a unique mechanism of histone binding and phenocopies genetic loss of DOT1L. Employing a chemical biology approach the requirement for H3K79 methylation in Wnt signaling was investigated by inhibiting DOT1L with EPZ004777, a selective and potent SAM competitive inhibitor. Our findings indicate that H3K79 methylation is not essential for maintenance or activation of Wnt pathway target gene expression in colon cancer cell

lines. Furthermore, H3K79 methylation is not elevated in human colon carcinoma samples in comparison with normal colon tissue. Therefore, our findings indicate that inhibition of DOT1L histone methyltransferase activity is likely not a viable therapeutic strategy in colon cancer.

CHAPTER 1

INTRODUCTION

1.1 Epigenetics

1.1.1 Histone modifications: an epigenetic mechanism of gene regulation

Although the cells in our bodies contain the same genetic information in our genome, different cell types selectively express specific genes in a tightly regulated spatial and temporal manner throughout development. One important mechanism regulating this process is the compaction of DNA into the structure of chromatin. In eukaryotic cells, DNA is packaged into chromatin through interactions with histones proteins(*1*). A nucleosome, the basic unit of chromatin structure, is formed by 146 base pairs of DNA wound around an octamer of histone proteins consisting of two units of each histone H2A, H2B, H3, and H4 (*2*). Nucleosomes can further compact and supercoil to form transcriptionally inactive heterochromatin, or remain in an accessible open euchromatin structure (*3*). This process is coordinated by numerous post translational modifications of histone proteins such as methylation, acetylation, and ubiquitination of lysine residues, methylation of arginine residues, and phosphorylation of serine, threonine, or tyrosine residues(*4*).

The covalent modification of histone proteins constitutes a dynamic and heritable mechanism of gene regulation beyond the genomic information within DNA and is collectively referred to as the “histone code” (*5*). Deposition, recognition, and removal of covalent posttranslational modifications of histones are processes regulated by different classes of enzymes thought of as writers, readers, and erasers of the histone

code (Table 1) (*6*). Several examples of “writers” are histone methyltransferases that carry out methylation of histone arginine and lysine residues, acetylation of lysine residues by histone acetyltransferases, and phosphorylation of serine, threonine, or tyrosine residues are carried out by various kinases (*7*). Histone “reader” enzymes recognize covalent modifications of histones and recruit additional proteins such as transcription factors or other chromatin modifying enzymes as effectors to carry out the downstream biological function. Bromodomain, tudor domain, and chromodomain containing proteins recognize acetylated and methylated lysine residues while PHD containing proteins are a large family that recognize diverse substrates (*6*). Removal of histone marks are carried out by several different enzyme families such as the removal of acetylation by histone deacetylases and removal of methylation by histone demethylases.

The coordinated spatial and temporal expression of genes regulated by epigenetic modifications is essential for normal development and cell fate determination in the development of organisms. Histone modification plasticity allows cells to respond to environmental cues and thus rapidly adapt gene expression programs to reprogram cellular phenotypes. However, hijacking of these processes leading to dysregulated histone modification patterns is also central to the development of numerous human diseases including cancer, inflammation, and metabolic diseases (*6*).

1.1.2 Histone methyltransferases

Methylation of histone residues plays a key role in regulating gene transcription programs (*8*). The family of enzymes responsible for histone methylation is collectively known as histone methyltransferases (HMTases). Both arginine and lysine residues of histones can be methylated and are carried out by separate classes of enzymes known as protein arginine methyltransferases (PRMTs) or lysine methyltransferases (KMTs). PRMTs are Class I methyltransferases containing a seven-stranded β-sheet structure (*9*). They are capable of symmetrical or asymmetrical methylation of arginine residues depending on whether single methyl groups are added to each terminal guanidino

nitrogen atom, symmetrically, or if two methyl groups are added to a single terminal guanidino nitrogen atom, asymmetrically.

Table 1. Histone code writers, readers, and erasers. Classification of proteins and protein families involved in deposition, removal, and recognition of histone modifications.

Writers		
Class	**Targets**	**Example proteins**
Histone acetyltransferases	lysine residues	TIP60, P300/ CREB-binding protein (CBP), MOF complex
Histone methyltransferases	lysine and arginine residues	mixed lineage leukemia (MLL), disruptor of telomeric silencing (DOT1L), G9A, EZH2, SUV39H1, protein arginine methyltransferases (PRMTs)
Histone ubiquitylase	lysine residues	RNF20, RING1B, 2A-HUB
Erasers		
Class	**Targets**	**Example proteins**
Histone deacetylases	acetylated lysine residues	Histone deacetylases (HDACs)
Histone demethylases	methylated lysine and arginine residues	Jumonji family or lysine specific demethylases (LSD1/2)
Histone deubiquitylase	ubiquitinated lysine residues	USP22, 2A-DUB
Readers		
Class	**Recognition motif**	**Example proteins**
Bromodomain containing proteins	histone acetylation	Bromodomain-containing proteins (BRD), brahma-related gene 1 (BRD1)
Tudor domain containing proteins	di and trimethylated lysine and dimethylated arginine	survival motor neuron (SMN), JMJD2, PHF20, 53, BP1
MBT domain containing proteins	mono and dimethylated lysine	Malignant brain tumor domain 1 (MBTD1), LIN-61
Chromodomain containing proteins	trimethylated lysine	Chromodomain protein 1 (Chd1), SUV29H1, MYST1, Tip60
PHD domain containing proteins	diverse substrates (methylated arginine, methylated lysine, and acetylated lysine), unmethylated lysine residues	mixed lineage leukemia (MLL), inhibitor of growth (ING2), Pygopus homolog 1 (Pygo1), DNA methyltransferase 2 (DNMT3)

Most lysine methyltransferases are Class II methyltransferases and contain a SuVar3-9, Enhancer of zeste, Trithorax (SET) domain (*10*). They are capable of adding one, two, or three methyl groups to the terminal ε-amino group of lysine residues resulting in mono, di, or trimethylation of lysine (Figure 1.1.1). Only one lysine methyltransferase has been identified that does not belong to the SET domain family of KMTs, known as

disruptor of telomeric silencing 1 like (*DOT1L*) which carries out mono, di, and trimethylation of histone H3 lysine 79 (H3K79) (*11*). All histone methyltransferase enzymes utilize the small molecule cofactor S-adenosylmethionine (SAM) as a methyl donor (Fig. 1.1.1) (*12*). Methylation of lysine residues can be carried out in either a processive mechanism, in which the methyltransferase adds methyl groups to the same lysine residue consecutively without dissociation from the substrate or by a distributive mechanism in which the methyltransferase dissociates from the substrate after each transfer of a methyl group.

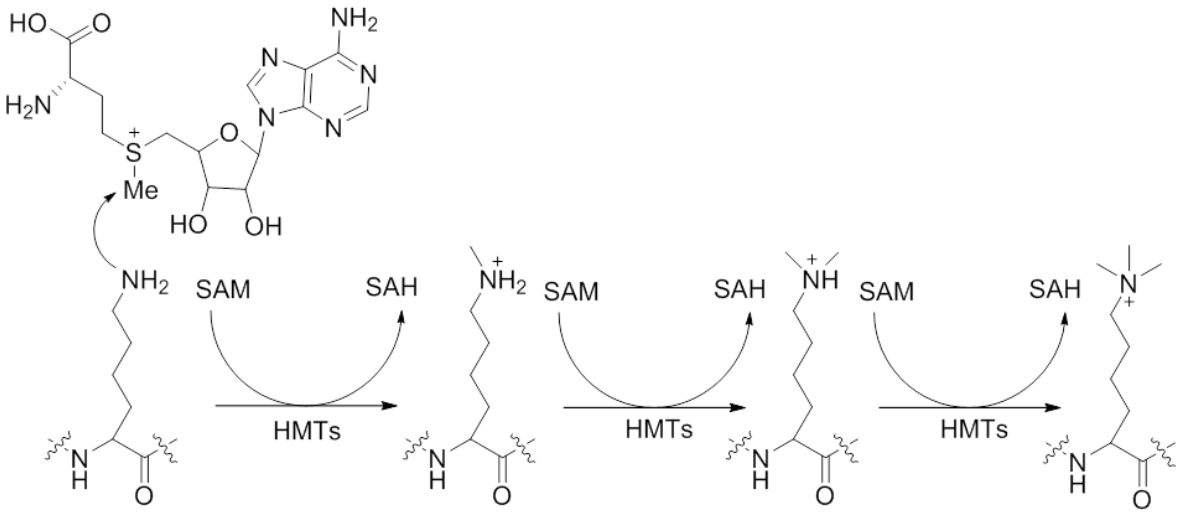

Figure 1.1.1 Mechanism of histone lysine methylation. Transfer of a methyl group from S-adenosylmethionine (SAM) to the ε-amine of histone lysine residues catalyzed by the enzymatic activity of histone methyltransferases.

Methylation of different lysine residues results in either repression or activation of associated genes. For instance, histone H3 lysine 9 (H3K9), H3 lysine 27 (H3K27), and H4 lysine 20 (H4K20) are associated with repression of gene transcription and histone H3 lysine 4 (H3K4), H3 lysine 36 (H3K36), and H3 lysine 79 (H3K79) methylation are associated with transcriptional activation (*13*).

However, methylation events on individual lysine residues are not solely responsible for establishing the transcriptional status of an individual gene. The combination of various

histone modifications and the protein complexes recruited by such modifications alter the physical chromatin structure leading to a specific transcriptional outcome. Numerous histone modifications within a portion of the genome create a multi-component context resulting in activation or repression of chromatin-mediated transcription. Furthermore, the complex pattern of histone modifications is a dynamic process involving co-regulation of adjacent marks in a process known as “histone crosstalk” (*14*). For example, methylation of histone H3K79 is enhanced in the presence of ubiquitinated histone H2B (*15, 16*). In additional to H3K79 methylation, H3K4 trimethylation is enhanced by monoubiquitination of H2B, however this methylation can be blocked if the adjacent H3 arginine 2 (H3R2) is previously methylated (*14*). As a result of the critical roles histone methyltransferases play in regulating gene transcription in normal development and tissue homeostasis, dysregulation of their functions are implicated in numerous human diseases such as cancer (*6, 13*). Therefore, the identification and biological characterization of histone methyltransferase enzymes is of significant interest.

1.2 DOT1L Histone Methyltransferase

1.2.1 Discovery of DOT1L

The disruptor of telomeric silencing 1 (*DOT1*) gene was identified in a yeast genetic screen in which overexpression of the gene reduced silencing at telomeres and other repressed genes (*17*). The function of the encoded protein, DOT1p was unknown for several years until it was demonstrated that Dot1p is a histone methyltransferase that methylates histone H3 lysine 79 (H3K79) (*11, 18, 19*). The function of DOT1 is conserved from yeast to humans thus, the human homolog DOT1L has the same histone methyltransferase enzymatic activity and carries out mono, di, and trimethylation of H3K79 (*20*). DOT1 appears to be the only enzyme responsible for methylation of H3K79 as knockout in yeast and mice results in complete loss of H3K79 methylation (*18, 21-23*).

1.2.2 Biochemical characterization of DOT1L

DOT1L is a distributive enzyme that catalyzes a S_N2 mediated transfer of a methyl group from SAM to the ε-amino group of H3K79 on the nucleosome core introducing mono, di, or trimethylation (*24*). DOT1L is a unique histone methyltransferase due to the fact that its substrate H3K79 is in the globular domain of histone H3 as opposed to the flexible N-terminal tail where most other lysine methylation is found. Interestingly, this results in exclusive substrate specificity and DOT1L only methylates H3K79 in the context of a nucleosome substrate or a milieu of core histones but is inactive against a recombinant H3 substrate, H3/H4 tetramer, or peptide substrate. This is likely due the requirement of additional interactions with the surface of the nucleosome for proper substrate recognition. It has been shown that an acidic patch of H4 is necessary for DOT1L HMTase activity (*25, 26*) and interaction with H2B lysine 120 (H2BK120) ubiquitination greatly promotes H3K79 methylation (*15, 16, 27*).

1.2.3 Biological functions of DOT1L

The initially identified function of H3K79 methylation in yeast, disrupting telomeric silencing, is attributed to the alteration of Sir protein localization along chromosomes (*18*). Loss of DOT1p was also shown to be required for “pachytene checkpoint” mitotic cell cycle arrest in yeast (*28*). To further assess the role of H3K79 methylation in higher eukaryotes, chromatin immunoprecipitation (ChIP) coupled with gene micro-array analysis of 5,000 genes in *Drosophila* demonstrated that H3K79 methylation correlates with active gene transcription (*29*). This observation was confirmed for several genes in human cells (*30, 31*) and demonstrated that H3K79 methylation is positively associated with transcriptional activation in several human cell lines over a large population of genes (*32, 33*). Recently, it has been shown that the Tudor domain contain protein survival motor neuron (SMN) recognizes H3K79 mono and dimethylation but the mechanism of how SMN regulates downstream processes remains an active area of investigation (*34*). Interestingly, no histone demethylase of H3K79 has been discovered

at this point, but it is speculated that there is an active eraser of this mark and is being sought.

DOT1L exists in numerous multi-protein complexes and is associated with transcriptional elongation as part of the ENL-associated proteins (EAP) complex (*35*). Coimmunoprecipitation of the Eleven Nineteen Leukemia (ENL) protein revealed that DOT1L interacts directly with ENL and was co-purified with p-TEFb (CDK9, CYCT, HSP70). Knockdown of ENL protein resulted in a partial loss of global H3K79 methylation indicating that DOT1L H3K79 methylation activity in cells is regulated in part by the context of multi-protein complexes. In addition, knockdown of ENL resulted in reduced levels of H3K79 methylation at the *Hoxa9* gene, which is an important homeobox transcription factor, resulting in reduced expression demonstrating that ENL is required to properly recruit DOT1L to genes in order to carry out H3K79 methylation and regulate the transcriptional activation (*35*). Further studies suggested that ENL has a dual role in regulating gene transcription by sequentially recruiting a higher order protein complex, termed AEP, containing AF5q31, AF4, and p-TEFb and forming a separate secondary complex with DOT1L (Figure 1.2.1) (*36*). This study suggested a model in which AEP is important for sustained expression of target genes whereas recruitment of DOT1L plays a role in the maintenance of transcriptional memory (*36*).

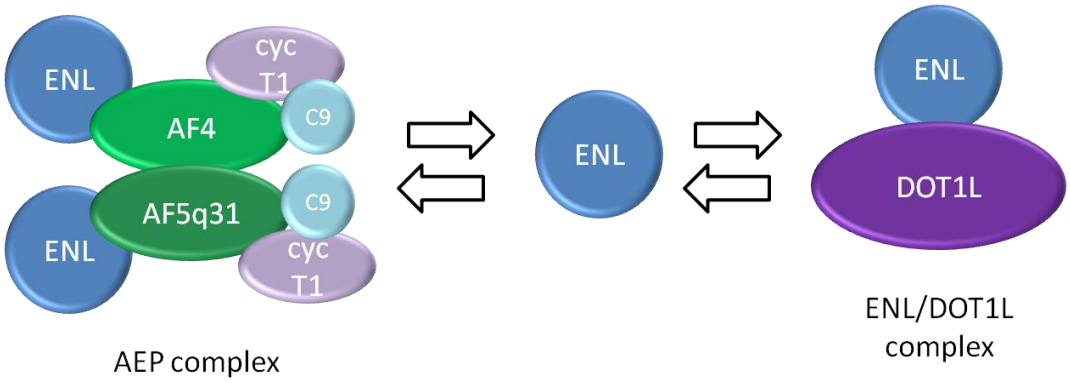

Figure 1.2.1. ENL/ DOT1L complex and alternate AEP complex. (Modified from Yokoyama, A. et al. *Cell*, 2010)

H3K79 methylation has numerous important functions under normal biological conditions. DOT1L is involved in double strand break repair in yeast to higher

eukaryotes (*37-40*). Loss of DOT1L in avian DT40 cells results in defects of DNA damage response through loss of recruitment of the tudor domain tumor suppressor protein 53BP1 to damaged chromatin (*38*). Furthermore, loss of DOT1L results in defects in cell cycle regulation and in murine model bone marrow cells, conditional loss of DOT1L leads to cell cycle arrest at G1/S phase and accumulation of G0/G1 cells with loss of S and G2/M phase cells (*21, 22, 28, 41*). In embryonic stem cells lacking DOT1L induction of differentiation results in arrest in G2/M phase, aneuploidy and proliferating arrest indicating that DOT1L is required for proper regulation of gene transcription in the early stages of embryonic stem cell differentiation (*42*). DOT1L is also involved in mediating sodium (Na^+) uptake in epithelial cells in response to aldosterone via regulation of the epithelial Na^+ channel (*ENaC*) gene via H3K79 methylation of the gene promoter (*43-47*). Additionally, DOT1L has a role in cardiac function by regulating expression of the *Dystrophin (Dmd)* gene required for stabilization of the dystrophin-glycoprotein complex important for cardiomyocyte viability. Cardiac specific loss of DOT1L results in cardiomyocyte cell death, heart chamber dilation, and systolic dysfunction phenotypes (*48*). As previously mentioned, DOT1L is associated with numerous multi-protein complexes; along with the interacting partner AF9, DOT1L methylation of H3K79 is also important for proper neuronal development through regulation of the TBR1 protein (*49*).

Due to the role of DOT1L in these numerous essential functions, it is not surprising that it is essential for embryonic development and DOT1L null mice die between 9.5-13.5 days post coitum (*21, 50*). Defects in yolk sac angiogenesis is suspected as the major cause for embryonic lethality. Cardiac dilation is thought to be a secondary effect of yolk sac defects and early lethality made it difficult to distinguish affects on erythropoiesis. Embryonic stem cells derived from DOT1L mutant blastocysts display aneuploidy, telomere elongation, and proliferation defects as a result of deficient heterochromatin establishment at centromeres and telomeres (*21*). Furthermore, defects in erythropoiesis were observed with deficient erythroid development, G0/G1 accumulation, and increased apoptosis demonstrating an important role for DOT1L in prenatal hematopoiesis (*50*).

Due to embryonic lethality and the need to understand the biological function of DOT1L in mammals, especially its role in MLL-fusion protein mediated leukemogenesis, several conditional DOT1L deletion models were generated (*22, 23*). Chang and colleagues generated mice with a Cre-excisable floxed exon 5 in the *Dot1l* gene (*Dot1l fl/fl*) generating a truncated non-functional protein (1-87 aa of the 1,543 wild type aa). Using hematopoietic progenitor cells isolated from Dot1l fl/fl mice, they demonstrated that numerous leukemogenic MLL-fusion proteins require DOT1L for their transformation capability. Jo and colleagues were the first to investigate the conditional knockout of DOT1L in a postnatal setting and demonstrated that systemic loss of DOT1L did not produce toxicity for 7-8 weeks. Mice with floxed *Dot1l at* 6-10 week old were injected with tamoxifen to induce CreER excision of DOT1L and showed complete loss of H3K79 methylation in bone marrow cells and other tissue. Mice lacking DOT1L became moribund and developed pancytopenia 8-12 weeks after tamoxifen injection. These findings and evaluation of hematopoietic stem cells (HSCs) by cell surface marker staining and flow cytometry demonstrated that DOT1L is required to maintain steady-state hematopoiesis. Furthermore, this mouse model provided a system in which the role of DOT1L in leukemia could be investigated. Bone marrow cells derived from conditional DOT1L knockout mice were used to investigate the requirement for DOT1L in MLL-fusion mediated leukemogenesis (*22*).

1.2.4 DOT1L and Mixed lineage leukemia (MLL) translocation induced leukemias

Chromosomal translocations of the mixed lineage leukemia gene located at chromosome 11q23 result in acute myeloid leukemia (AML) and acute lymphoblastic leukemias (ALL) or biphenotypic mixed lineage leukemias (MLL) (*51*). Leukemias bearing rearrangements of the MLL gene are aggressive and have poor prognosis (*52*) and are found in >70% of infant leukemias with either AML or ALL phenotypes and 10% of adult AMLs (*53*).

The MLL gene is normally expressed as a large multidomain protein with histone H3K4 trimethylation activity and is associated with transcriptional activation of target genes

(*54*). The most common result of translocations of the MLL-gene is the fusion of the N-terminal portion of the MLL protein to one of more than 60 fusion partners. However, several rearrangement partners are most common and MLL-AF4 resulting from the t(4;11)(q21;q23) rearrangement, MLL-AF9 resulting from the t(9;11)(p22;q23) rearrangement, MLL-ENL resulting from t(11;19)(q23;p13.3) rearrangement, MLL-AF10 resulting from t(10;11)(p12;q23) rearrangement, and MLL-AF6 resulting from t(6;11)(q27;q23) rearrangement account for around 80% of the MLL rearrangements observed in leukemias (Figure 1.2.2) (*53*).

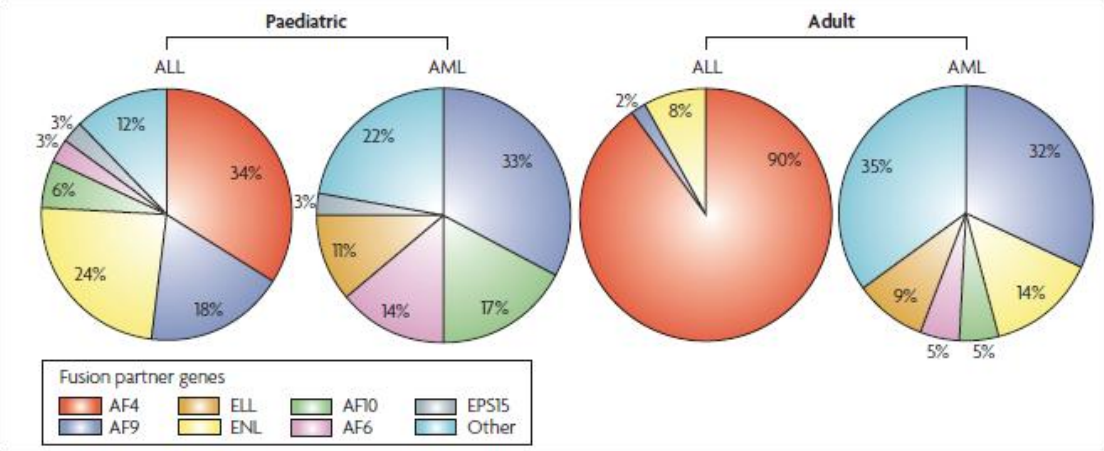

Figure 1.2.2 Distribution of MLL rearrangement partners in pediatric and adult ALL and AML. The fusion partners resulting from MLL-rearrangements are predominantly AF4, AF9, ENL, and AF10 in pediatric ALL and AML. AF4 is the primary fusion partner in adult ALL and AF9 and ENL predominate in adult AML. (Krivstsov, A.V., and Armstrong, S.A. *Nature Reviews*, 2007)

MLL typically exists in large multiprotein complexes containing WDR5, Ash2L, and RBP5 which make up the core complex (*55*). It associates with numerous other chromatin modifying proteins such as the H4K16 acetyltransferase MOF complex (*56*) and CBP/p300 (*57*) for full transcriptional activation of target genes. However these interactions are mediated by the c-terminal portion of MLL which is lost in MLL-fusion proteins. There are a number of additional interaction sites in the N-terminal portion of MLL which are maintained in MLL-fusion proteins and are key mediators of MLL-rearrangement induced leukemias. The N-terminal 40 amino acids of MLL mediate an important interaction with menin and this interaction has been shown to be necessary

for MLL induced leukemogenesis (*58, 59*). This interaction also requires a third binding partner LEDGF for optimal transformation capabilities (*60*). Additionally, interaction with the polymerase associated factor complex (PAFc) is mediated by upstream regions of MLL that are maintained in MLL-fusion proteins and is required for optimal expression of MLL target genes such as *Hoxa9* and is required for MLL-AF9 leukemogenesis (*61*). Interestingly, the wild-type allele of MLL is also recruited by menin to *Hox* genes and is required for MLL-AF9 transformation although the mechanism of cooperation between MLL-fusion proteins and wild-type MLL is not well understood (*62*).

1.2.5 Mechanism of DOT1L mediated MLL-transformation

In addition to the protein interactions that are maintained in the formation of MLL-fusion proteins, the most common MLL-fusion partners form a new interaction through the N-terminal fusion partners with the histone methyltransferase DOT1L (Figure 1.2.3). The common MLL-fusion protein AF10 first implicated DOT1L in leukemogenesis by when they were identified as interacting partners in a yeast two hybrid screening. The interaction was subsequently confirmed in mammalian cells and shown to be mediated by an octapeptide motif and leucine zipper (OM-LZ) in AF10 (*31*). The ability of the MLL-AF10 fusion protein to transform bone marrow was recapitulated by direct fusion of the N-terminal third of DOT1L to MLL and this effect was abrogated by an enzymatically inactivating mutation of DOT1L. Furthermore, MLL-AF10 was shown to increase H3K79 methylation at the MLL-target gene *Hoxa9* and to increase expression of this critical mediator of leukemogenesis (*31*). To demonstrate the requirement for DOT1L in the transformation of MLL-fusion protein mediated leukemias, hematopoietic cells from a conditional knockout model of DOT1L were transformed with several MLL-fusion protein or the non-MLL oncogenes E2a-Pbx1 and DOT1L expression was abolished by introduction of retroviral transduction of Cre recombinase. MLL-AF9 transformed bone marrow requires the presence of DOT1L for colony forming ability in methylcellulose. DOT1L excision resulted in decreased expression of *Hoxa9* and resulted in apoptosis of MLL-AF9 transformed cells but no E2a-Pbx1 transformed cells (*23*). Furthermore,

conditional knockout of DOT1L abrogated the ability of MLL-AF9 transformed murine bone marrow to induce leukemia in a lethally irradiated recipient mouse (*63, 64*).

Several other common fusion partners resulting from MLL chromosomal translocations have also been shown to exist in multi protein complexes with DOT1L MLL-AF4 (*65*) or directly interact with DOT1L such as MLL-ENL (*35*) and require the histone methyltransferase for leukemogenic transformation. The requirement for DOT1L in MLL-AF9 induced leukemogenic transformation requires both the enzymatic activity of DOT1L and maintenance of the direct interaction between DOT1L and MLL-AF9. Disruption of either the enzymatic activity by introduction of a catalytically inactive DOT1L mutant (RCR mutant) or disruption of the interaction between DOT1L and MLL-AF9 by deleting 10 amino acids (mDOT1L 863-872) prevents the transformation of murine bone marrow as assessed by methylcellulose colony forming ability (*66*). MLL-AF4 transformation of murine bone marrow cells produces a pre-B cell ALL phenotype and contains elevated levels of H3K79 methylation at *Hoxa9* and increased expression of *Hoxa9* compared with normal B-cell precursor cells (*67*). MLL-ENL transformed murine bone marrow cells were shown to depend specifically on the interaction of MLL-ENL with DOT1L. Loss of DOT1L interaction by a three amino acid deletion in the C-terminus of ENL prevented the expression of the MLL-target genes *Hoxa7, Hoxa9, and Meis1 (35)*.

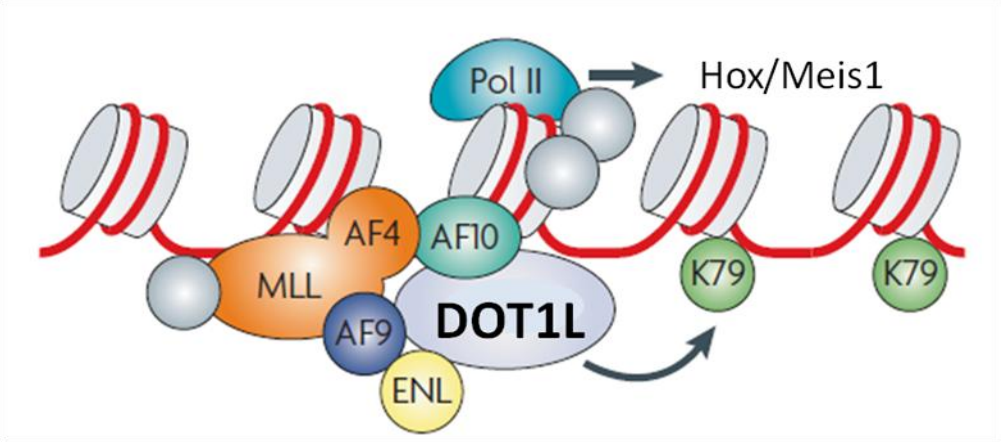

Figure 1.2.3 Schematic of MLL-fusion protein recruitment of DOT1L. (Modified from Krivstsov, A.V., and Armstrong, S.A. *Nature Reviews*, 2007)

Interestingly, other MLL-fusion proteins that have not been shown to directly interact with DOT1L, MLL-GAS7 and MLL-AFX, were hindered by loss of DOT1L but not E2a-Pbx1 (*23*). The MLL- fusion protein MLL-AF6 was also shown to depend on DOT1L for transformation despite, lack of evidence for a direct interaction between MLL-AF6 and DOT1L. However MLL-AF6 transformed hematopoietic cells demonstrate high levels of H3K79 methylation at MLL-target genes. Upon conditional deletion of DOT1L the level of H3K79 methylation and expression of several MLL-target genes are reduced for *Hoxa7, Hoxa9,* and *Hoxa10 (68).*

In addition to the numerous findings demonstrating the importance of DOT1L in MLL-fusion protein mediated leukemogenesis, these findings are also relevant in human patient populations demonstrated in human patient samples of MLL-rearranged ALLs where there exists a distinct H3K79 methylation profile from normal hematopoietic progenitor cells or other ALLs with germline MLL. The aberrant H3K79 methylation profile in MLL-rearranged ALLs also correlated with increased gene expression, especially for the *Hoxa* cluster of genes. (*69*)

In summary these studies demonstrate that MLL-fusion proteins recruit DOT1L to MLL-target genes where it carries out its enzymatic function of H3K79 methylation. Aberrant methylation leads to increased expression of genes such as *Hoxa9* and *Meis1* which are critical transcription factors driving leukemogenic transformation(*70*). Loss of DOT1L results in decreased H3K79 methylation and reduced expression of MLL-target genes inhibiting leukemogenic transformation (*23, 31, 63, 64, 68, 71*). Several MLL-fusion proteins that have not been shown to directly interact with DOT1L also appear to depend on the histone methyltransferase for leukemogenic transformation although the mechanism is not understood (*23*). Based on this model, DOT1L is an attractive therapeutic target for the treatment of leukemias bearing translocations of *MLL*.

1.2.6 Inhibiting DOT1L as a therapeutic approach in MLL

DOT1L is a well validated therapeutic target in MLL based on numerous studies demonstrating that several of the most common MLL-fusion proteins require DOT1L for leukemogenic transformation potential. Due to the nature of DOT1L's mechanistic role in MLL, there are several possible approaches for targeting DOT1L. First, as an enzyme, DOT1L has the classically exploited features of successful drug development strategies such as the well defined small molecule binding pocket for the cofactor SAM. DOT1L also has a defined substrate lysine binding channel which leaves open the possibility of substrate competitive inhibitors or even allosteric inhibitors. Besides enzymatic function, the requirement for DOT1L recruitment by MLL-fusion proteins allows for targeting the protein-protein interactions between DOT1L and the multi-protein complex binding partners.

Before the development of selective inhibitors of DOT1L, it was known that S-adenosylhomocysteine (SAH; Figure 1.2.4), the demethylated reaction product of DOT1L enzymatic activity, could non-specifically inhibit DOT1L. However many enzymes utilize the SAM cofactor and are similarly inhibited by SAH, furthermore, this compound is quickly metabolized and does not off any potential for examining the biological effects of DOT1L inhibition. The first specific inhibitor of DOT1L, EPZ004777 (Figure 1.2.4), was reported by Epizyme in 2011 and demonstrated exquisite potency and selectivity with IC_{50} = 0.4 $\pm$ 0.1 nM and >1,000 fold selectivity for DOT1L over other HMTs (*72*). EPZ004777 is an analog of SAM and binds to the SAM binding site. It contains an initially unexpected chemical feature, a large tert-butyl phenyl group at the end of the molecule occupied by the amino acid tail portion of SAM (Figure 1.2.4). The binding of this unexpected feature was shown to induce a large conformational change of DOT1L and opened a large hydrophobic portion of DOT1L that is not exploited by SAM (*73, 74*).

Subsequently, several mechanism based inhibitors which covalently bind to DOT1L were reported, the most potent of which having IC_{50} = 38 nM (Song-1; Figure 1.2.4) (*75*). These structures are also SAM analogs and maintain the amino acid moiety of the

molecule and demonstrate that substitution of the N^6 of the adenine can induce selective binding to DOT1L over other methyltransferases (*75*). The same group followed up this report with an eloquent structure activity relationship (SAR) study of reversible SAM analog inhibitors that revealed a number of less potent DOT1L inhibitors and resulted in the most potent compound being very similar to EPZ004777 with one carbon to nitrogen substitution at position 7 of the adenosine ring with equivalent potency Ki = 0.46 nM (Song-2; Figure 1.2.4) (*76*).

A modified version of this compound was then reported with a cyclopentane replacement of the ribose portion of the molecule which resulted in decreased potency Ki = 1.1 nM (Song-3; Figure 1.2.4) but improved metabolic stability in a liver microsome assay(*77*). Additional efforts to improve cellular stability and activity resulted in an additional EPZ004777 analog that was brominated at the 7 position of the adenine ring, SGC0946 (Figure 1.2.4), resulting in similar in vitro potency IC_{50} = 0.3 $\pm$ 0.1 nM but a 10-fold improvement in the IC_{50} of cellular H3K79Me2 (*73*). The demonstration that a single halogen substitution can improve potency and selectivity was further confirmed in a report demonstrating the addition of bromine to the 7 position of adenine of SAH resulted in 10-fold increase in potency resulting in a bromo-deaza-SAH compounds with IC_{50} = 77 nM (*78*). Lastly, structure guided optimization of EPZ004777 resulted in the most developed DOT1L inhibitor to date, EPZ-5676 with Ki = 0.08 $\pm$ 0.03 nM (*79*).

1.2.7 Biological characterization of SAM competitive DOT1L inhibitors

The potential of DOT1L as a therapeutic target in MLL has been verified by utilizing these potent and selective inhibitors as chemical tools to demonstrate selective killing of MLL-AF6 (*68*), MLL-AF9 (*72*), and MLL-AF10 (*71*) transformed bone marrow cells by EPZ004777. In MLL-AF6 transformed murine bone marrow cells EPZ004777 inhibition of H3K79 methylation results in decreased expression of MLL-target genes *Hoxa9, Hoxa10,* and *Meis1* and reduces proliferation by inducing apoptosis and cell cycle arrest in G0/G1 (*68*). Similar results were observed in MLL-AF9 and MLL-AF10 transformed bone marrow cells with the additional characterization of differentiation induction (*71,*

72). It is interesting to note that the cellular activity of EPZ004777 requires a long time course for treatment and no changes in cellular proliferation were observed until after day 7 (*72*). A survival advantage was demonstrated by EPZ004777 treatment administered by continuous IV infusion in an *in vivo* model of MLL, however the modest affect was attributed to low levels of circulating EPZ004777 (*72*).

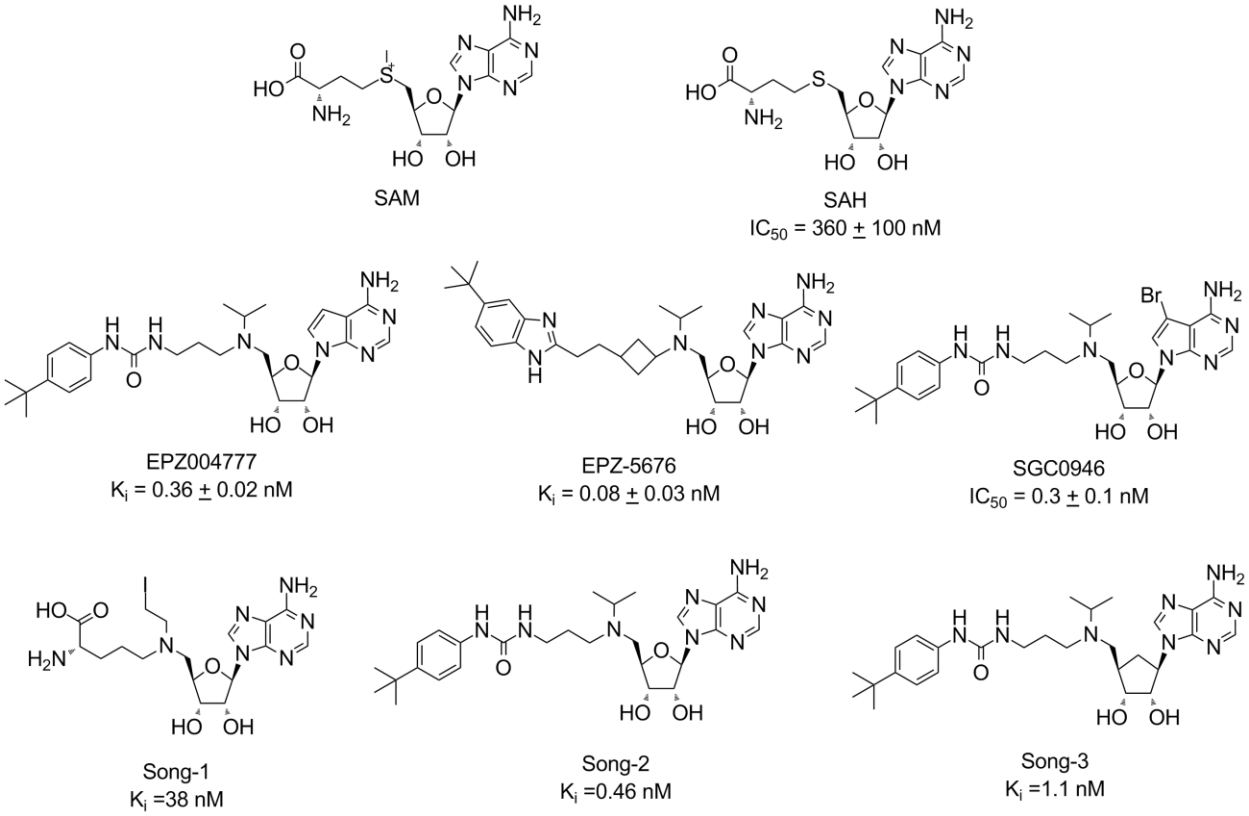

Figure 1.2.4 Chemical structures and *in vitro* inhibition potency of DOT1L inhibitors.

The second generation Epizyme DOT1L inhibitor, EPZ-5676, demonstrated improved biochemical and cellular characteristics with Ki = 0.08 nM compared with 0.3 nM for EPZ004777 (*79*). This also resulted in significant improvement in cellular assays compared to EPZ004777, giving a 43 fold improvement in IC_{50} for inhibition of MV4-11 human leukemia cell line harboring an MLL-AF4 fusion protein (*79*). Therefore, the therapeutic potential of EPZ-5676 was tested *in vivo* using a xenograft model of MV4-11. Based on low bioavailability of EPZ-5676 and rapid clearance of compound upon

intraperitoneal (IP) injection, a continuous intravenous (IV) injection regimen was used for administration of EPZ-5676 to maintain plasma levels of the compound above the concentration required to block in vitro proliferation of MV4-11 cells. A dose of 70 mg/kg showed complete regression of established subcutaneous MV4-11 tumors and a medium dose of 35 mg/kg caused tumor stasis upon 21 days of treatment with eventual resumption of growth after 7 days of ending the treatment. These doses were well tolerated over the 21 day treatment period and no weight loss was observed. Mechanistically, the effects of EPZ-5676 were confirmed by reduced H3K79 methylation in the bone marrow of rats in the treatment groups and reduced *Hoxa9* and *Meis1* expression in the tumors of EPZ-5676 treated mice (*79*). Furthermore, a panel of human leukemia cell lines was tested to measure the efficacy of cellular proliferation inhibition by EPZ-5676. Human leukemia cell lines containing MLL-AF4 translocations (RS4;11, SEM, and MV4-11), MLL-AF9 translocations (MOLM-13 and NOMO-1), and MLL-ENL translocations (KOPN-8) were more sensitive to DOT1L inhibition, giving IC_{50} values three fold lower, than non-MLL rearrangement cell lines (HL60, JURKAT, 697, KASUMI-1, and REH) (*79*). These studies indicate that DOT1L inhibition is an effective therapeutic strategy for MLL-rearranged leukemias *in vivo* and that there is no overt toxicity observed upon DOT1L inhibition over several weeks.

Based on the efficacy and safety observed in rodents, human Phase I clinical trials of EPZ-5676 were initiated in September 2012 and as of December 2013 the dose escalation stage of the trial was completed and is now in an expansion phase enrolling patients with leukemias involving MLL-translocations. It is noteworthy that despite improvement of pharmacokinetic properties compared to EPZ004777, EPZ-5676 is being administered by continuous IV infusion, indicating there is still a need to improve the properties of this compound.

1.2.8 Targeting the recruitment of DOT1L in MLL-translocation leukemias

DOT1L is a component of several multiprotein complexes ENL associated protein (EAP) (*35*), and AF4 and ENL family proteins (AEP) (*36*), and DOT1L complex (DotCom) (*80*).

The primary mediators of DOT1L recruitment to these complexes are several proteins that are predominant MLL-fusion protein partners, AF9, AF10, and ENL.

DOT1L mediated leukemogenic transformation by MLL-fusion proteins is not only dependent on the enzymatic activity of DOT1L but also upon the recruitment of DOT1L to MLL target genes. A defined region of 10 amino acids in DOT1L (amino acids 863-872 in mouse DOT1L) has been identified in the Nikolovska-Coleska laboratory to be essential for the interaction with AF9 and ENL (*66*). The colony forming ability of murine bone marrow cells from the DOT1L conditional knockout mice (*22*), transformed with MLL-AF9, is inhibited upon tamoxifen inducible Cre excision of DOT1L. Reintroduction of wild type DOT1L restores the colony formation ability of the MLL-AF9 oncogene confirms previous studies that MLL-AF9 requires DOT1L for leukemogenic transformation. Importantly, deletion of the 10 amino acids from the c-terminus of DOT1L (mDOT1L 863-872 aa), which abrogates the interaction with MLL-AF9, failed to rescue the transformation potential of MLL-AF9, similar to the enzymatically inactive DOT1L mutant (RCR mutation) (*66*). This study demonstrates that the direct interaction of DOT1L with MLL-AF9 is required for the leukemogenic transformation capabilities of MLL-AF9 and therefore targeting this interaction may be a viable therapeutic strategy for treatment of MLL-rearrangement leukemias bearing MLL-fusion proteins that recruit DOT1L.

In a reciprocal approach, it was shown that the MLL-ENL fusion protein also depended on the specific interaction with DOT1L for the transformation capability of this MLL-fusion protein. Rather than disrupting the interaction between MLL-ENL by deleting portions of DOT1L, Mueller and colleagues performed triplet alanine scanning mutagenesis on the c-terminus of ENL which was known to mediate the interaction with DOT1L. In two mutants with three alanine mutations in the c-terminus of MLL-ENL, one specifically disrupted the ability of MLL-ENL to bind to DOT1L as demonstrated by yeast two-hybrid assay. This MLL-ENL fusion protein lacking DOT1L binding was not able to transform murine bone marrow cells in comparison to wild type MLL-ENL or a triple alanine MLL-ENL mutant that maintained binding to DOT1L. Furthermore the transformation capability was directly correlated with the extent of MLL-target gene

expression. The MLL-ENL mutant that does not bind to DOT1L failed to upregulate the critical MLL-target genes *Hoxa7, Hoxa9,* and *Meis1* (*35*). Together, these studies confirm that DOT1L mediates the leukemogenic potential of certain MLL-fusion proteins by direct interaction of the c-terminal portion of AF9/ENL with a small specific amino acid sequence of DOT1L. It is highly likely that additional MLL-fusion proteins that have been shown to interact with DOT1L and require the histone methyltransferase for transformation are also dependent on the recruitment of DOT1L to MLL-target genes such as MLL-AF4, MLL-AF6, and MLL-AF10.

The protein-protein interaction between DOT1L and MLL-fusion proteins is an attractive therapeutic target due to the small size of the interaction domain of DOT1L and the potential for very specific targeting. Previously protein-protein interactions were viewed as undruggable due to the large surface area and hydrophobic nature of the interaction between some proteins. However, several examples exist for the successful targeting of protein-protein interactions that involve the binding of a small peptide segment of one protein to a definable peptide binding cleft of an interacting partner such as the pro-apoptotic protein MCL-1 interaction with BH3 proteins (*81*) and the SMAC/XIAP interaction (*82*). Therefore, the identification of a 10 amino acid fragment of DOT1L which mediates the interaction with AF9 supports the possibility for identifying small molecules which may be able to inhibit this interaction. Further structural studies of the interaction between DOT1L and the AF9 or ENL c-terminus will greatly aid in this undertaking.

As a therapeutic approach, targeting the protein-protein interaction of DOT1L and MLL-fusion proteins as opposed to the enzymatic activity of DOT1L may offer greater cellular specificity. Due to the role of DOT1L in normal development and maintenance of proper hematopoiesis (*22, 50*), targeting enzymatic activity of DOT1L H3K79 methylation may have potential side effects. Specifically targeting the interaction of DOTL1 with MLL-fusion proteins may produce fewer side effects since it will only effect H3K79 methylation at the MLL-target genes influencing only the cell population reliant on DOT1L for transformation, the leukemic cell population, while leaving H3K79 methylation in tact in other tissues and cell populations. Although overt toxicity has not

been observed with current DOT1L HMTase inhibitors and they are well tolerated in mice for several months, the long term effects remain unknown. Thus, there is a need to investigate the normal physiological role of DOT1L in numerous multiprotein complexes outside the context of MLL-fusion proteins. Therefore, the development of small molecule inhibitors of the protein-protein interaction between DOT1L and MLL-fusion proteins is highly desirable for its potential therapeutic value and as a chemical probe to further investigate the role of DOT1L in normal physiology.

1.3 Epigenetics and Wnt signaling

1.3.1 Wnt signaling functions and cancer

Wnt signaling is an essential mediator of development, proliferation, and tissue homeostasis (*83*). Misregulation of this pathway occurs frequently in human cancers especially colon cancer(*84*). Canonical Wnt signaling is regulated by constitutive degradation of the key mediator of the Wnt signaling pathway β-catenin. The destruction complex consisting of adenomatous polyposis coli (APC), Axin, and the kinases CKI and GSK3 phosphorylate newly synthesized β-catenin leading to subsequent ubiquitination and degradation. Upon induction of Wnt signaling by binding of a Wnt ligand to its cognate receptors LRP5/6 and Frizzled, components of the destruction complex are sequestered and β-catenin accumulates. The stabilization of β-catenin leads to binding with the TCF/LEF transcription factors at Wnt pathway target genes. This complex recruits other factors such as chromatin modifying and chromatin remodeling enzymes as well as transcriptional machinery to induce transcription of Wnt pathway target genes (Figure 1.3.1) (*84*).

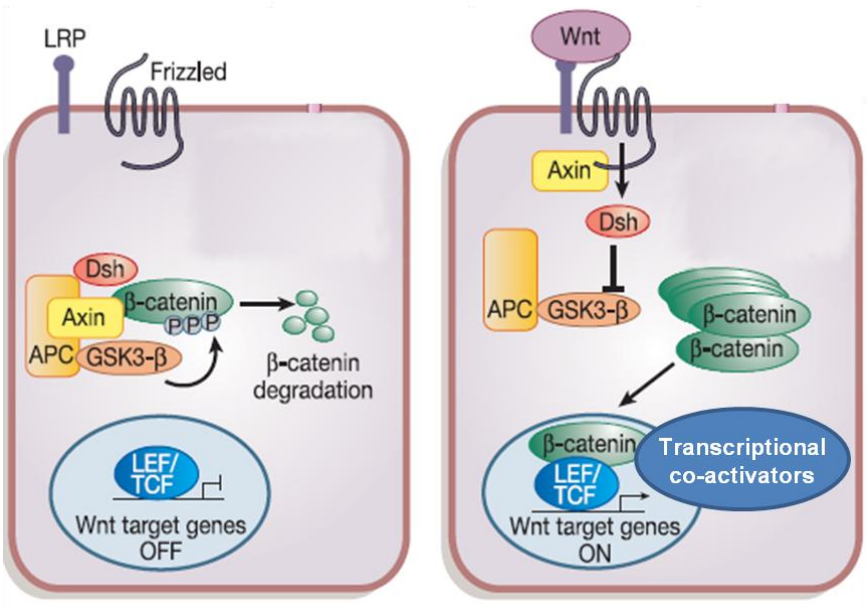

Figure 1.3.1 Schematic of canonical Wnt signaling pathway. Modified from Reya, T., and Clevers, H. *Nature*, 2005.

The Wnt signaling pathway regulates numerous processes involved in the progression of cancer such as tumor growth, senescence, cell death, differentiation, and metastasis. Inactivating mutations of the APC protein dysregulate the destruction complex function and lead to aberrant stabilization of β-catenin. Alternatively, mutations of β-catenin which truncate or mutate the protein such that phosphorylation can no longer occur also result in stabilization and accumulation of β-catenin resulting in loss of regulation of the signaling pathway and constitutive activation of Wnt pathway target genes. These process are well characterized in adenomatous polyposis of the colon which can progress to colorectal carcinomas upon KRAS activating mutations or P53 inactivating mutations(*84*) (*85*). Furthermore mutations of proteins in the Wnt signaling pathway are associated with many other forms of cancer including breast, lung, prostate, skin, and ovarian.(*85*)

Wnt signaling also plays a role in various types of leukemia(*84*). It is well established that Wnt signaling is involved in the normal physiological process of regulating hematopoietic stem cell self renewal (*86*). The Wnt pathway has been shown to be

required for stem cell maintenance in AML (*87*) and is predictive of poor prognosis (*88*). Interestingly, β-catenin was shown to be required for AML development induced by the oncogenes MLL-AF9, which also requires DOT1L, but not the Hoxa9/Meis1 transcription factors (*87*). MLL-AF9 induces the activation of β-catenin signaling however it was not investigated whether the interaction with DOT1L is involved in the activation of β-catenin. Alternatively, it appears that coordinating signaling pathways are responsible for the upregulation of β-catenin observed in MLL-AF9 induced leukemia. The G-protein coupled receptor Lgr4, a component of the R-spondin (Rspo) signaling pathway (*89*) and GPR84 (Dietrich, P. et al ASH 2013) are implicated as key mediators of MLL-AF9 induced β-catenin activation in AML.

1.3.2 Wnt signaling and chromatin modifications

Nuclear β-catenin requires a number of collaborator proteins to carry out its transcriptional activation of Wnt pathway target genes in the nucleus. Modification of chromatin through recruitment of chromatin modifying enzymes is one important mechanism β-catenin uses to regulate gene transcription. The histone acetyltransferase, CBP, and the histone H3 lysine 4 (H3K4) tri-methylation MLL1 and MLL2 chromatin-modifying complexes are recruited to Wnt pathway target genes by β-catenin (*90*). Recruitment of MLL1 and MLL2 leads to increased H3K4 trimethylation at the Wnt pathway target gene *c-MYC* (*91*). In addition to interaction and recruitment of histone methyltransferases, β-catenin has also been shown to interact with the histone acetyltransferase complex, TRRAP/TIP60 (*91*). These findings are significant because they allude to the possibility that many different chromatin modifying enzymes may be involved in the regulation of Wnt signaling and could serve as potential new therapeutic targets for Wnt signaling in cancer.

1.3.3 DOT1L as a potential transcriptional co-activator of Wnt signaling

In addition to other chromatin modifying enzymes, DOT1L was recently implicated in Wnt signaling when a campaign to identify DOT1L interacting proteins identified

components of the Wnt signaling pathway in the DOT1L complex (DotCom) (*80*). The central mediator of Wnt signaling, β-catenin, as well as TRRAP, a component of chromatin modifying multiprotein complexes, and Skp1, a component of the SCF E3 ubiquitin ligase complex, were identified as novel interacting proteins with DOT1L. To investigate the role of DOT1L in Wnt signaling in living organisms, Drosophila was used as a model organism with the homologs Wingless (Wg) signaling pathway. Tissue specific knockdown of DOT1L in wing imaginal discs of Drosophila using RNAi resulted in decreased expression of the high threshold Wg target gene *Senseless* but not *Distalless (Dll)* or *Vestigial (Vg)* Wg target genes. Several other Wg target genes *frizzled 3 (dfz3), CG5895, CG6234, Notum,* and *Homothorax (hth)* were downregulated in flies with a hypomorphic *dDot1l* allele and in RNAi line with DOT1L knockdown in wing discs. Furthermore, these affects were linked to H3K79 trimethylation which was selectively reduced compared to mono and dimethylation in the absence of H2BK120 ubiquitination in *Bre1* flies by reduction of *CG6234* and *Notum* in the absence of H2B ubiquitination and reduced H3K79 trimethylation (*80*).

These findings were extended by Mahmoudi and colleagues who demonstrated that DOT1L is recruited to the Wnt target genes *AXIN2* and *ZCCHC12* in a β-catenin dependent manner in human cells (*92*). The interaction between DOT1L and β-catenin was shown to be mediated by the known DOT1L interacting partner AF10/MLLT10. It was also demonstrated in a zebrafish Wnt-responsive GFP reporter system (TOPflash) that morpholino depletion of DOT1L reduced the expression of GFP. In zebrafish with a model of Wnt overstimulation by disrupting the function of the Wnt signaling mediator, APC, there is failure to express the differentiation marker intestinal fatty acid binding protein (i-*fabp)*. Consistent with a role in Wnt signaling, morpholino depletion of DOT1L rescued the phenotype and restored *i-fabp* expression. In the intestinal epithelium of zebrafish, morpholino depletion of DOT1L resulted in reduced proliferation, disrupted villi formation, and reduced the expression of the Wnt target gene *Axin2 (92)*.

In human cells, knockdown of DOT1L in articular chondrocytes reduced chondrogenesis which depends on Wnt signaling and a DOT1L polymorphism was identified that is associated with joint space width and reduced risk for osteoarthritis (*93*).

Although these studies implicated DOT1L in Wnt signaling, none of these studies were carried out in native mammalian tissue, thus Ho and colleagues sought to further probe the role of DOT1L in Wnt signaling and its role in intestinal homeostasis (*94*). In the intestinal epithelium, one subset of intestinal stem cells (ISCs) that depend on Wnt signaling are the crypt basal columnar cells (CBCs) which express the cell surface marker protein LGR5. They function to repopulate the adjacent villi and are the origin cells of colorectal cancer. Using this population of $LGR5^{+}$ cells compared with adjacent villi enterocytes, it was observed the H3K79 dimethylation (H3K79Me2) levels correlated with levels of gene expression, thus highly expressed genes had greater H3K79Me2 which was consistent with previous findings in mammalian cells (*29, 41*). For some specific Wnt target genes, such as *Lgr5* and *Ephb3* their expression is higher in Wnt stimulated tissue, CBCs, than in villi and there is greater H3K79Me2 at these genes. However, the well characterized Wnt target gene *Axin2* is more highly expressed in CBCs than in villi but has equivalent H3K79Me2 across the gene in both cell populations indicating that the relationship between expression levels and H3K79 methylation is not strict (*94*). This result is reminiscent of the observations in Drosophila that RNAi knockdown of DOT1L in the wing imaginal disc affected the expression of certain Wg target genes but not all (*80*).

To understand whether H3K79Me2 was specifically associated with Wnt pathway gene expression or more broadly coupled to transcriptional activation, H3K79Me2 levels were compared across 207 Wnt pathway target genes and 10 sets of 207 non-Wnt responsive genes with similar expression levels based on microarray data. It was observed that H3K79Me2 was consistently distributed across all sets of 207 genes with similar expression levels and not specifically associated with the Wnt target genes, suggesting that H3K79Me2 is associated with gene expression levels and is not Wnt-pathway specific. Furthermore, among 55 Wnt pathway target genes that are highly

expressed in LGR5+ cells relative to villi cells some were more highly marked with H3K79Me2 but others were not. This analysis provided a broader view of Wnt pathway target gene expression and H3K79Me2 in mammalian cells and suggested that H3K79Me2 is not required for regulating the expression levels of Wnt responsive genes. In addition a number of well characterized Wnt target genes were shown to have increased expression in the intestinal epithelium of mice with a conditional knockout of DOT1L specifically in the epithelium. It was also shown that other histone lysine methylation marks are not altered and it is unlikely that there is upregulation of any compensatory epigenetic mechanism (*94*).

Upon investigation of the affect of ISC specific knockout and full intestinal epithelium knockout of DOT1L, it was revealed that despite increased levels of apoptosis, there were no gross morphological or functional defects of intestinal epithelium with up to 4 months of complete absence of H3K79 methylation (*94*). This was consistent with the observation that the murine conditional knockout of DOT1L throughout the whole animal displayed no defects in the intestinal epithelium upon substantial time in the absence of H3K79 methylation (*22*). Taken together the *in vivo* findings in mammalian intestinal epithelium, where the role of Wnt signaling is well established, contradict the apparent role of DOT1L in Wnt signaling from data in mammalian cell lines, flies, and zebrafish. Each of these approaches has advantages and limitations; however they all consistently utilizing genetic approaches to reduce the expression of the full length DOT1L protein. Despite this, each study focuses on the function of H3K79 methylation but does not address the possibility of other functions of DOT1L in these contexts although it is well established that DOT1L exists in several multi-protein complexes. Further studies are required to decouple the reduction of DOT1L protein expression and loss of H3K79 methylation activity. Chemical biology approaches using small molecules to specifically inhibit the H3K79 methyltransferase activity of DOT1L are a valuable tool to address this issue and probe the role of H3K79 methylation specifically.

1.4 Summary and goals

Based on this evidence reported in the literature, it is clear that DOT1L is an important biological molecule, playing critical roles in normal development, homeostasis, and disease. Numerous MLL-translocation leukemias rely on recruitment of DOT1L and H3K79 methylation activity. Therefore, we endeavored to discover novel small molecule inhibitors of DOT1L histone methyltransferase activity. In the following chapters we present several approaches to achieve this goal and the identification of DOT1L inhibitors. Furthermore, we utilized a potent and selective small molecule inhibitor of DOT1L to probe the biological function of H3K79 methylation in Wnt signaling to address the potential of DOT1L as a therapeutic target in colon cancer.

1.5 References

1. Kornberg, R. D. (1974) Chromatin Structure - Repeating Unit of Histones and DNA, *Science 184*, 868-871.
2. Luger, K., Mader, A. W., Richmond, R. K., Sargent, D. F., and Richmond, T. J. (1997) Crystal structure of the nucleosome core particle at 2.8 angstrom resolution, *Nature 389*, 251-260.
3. Li, G. H., and Reinberg, D. (2011) Chromatin higher-order structures and gene regulation, *Curr Opin Genet Dev 21*, 175-186.
4. Kouzarides, T. (2007) Chromatin modifications and their function, *Cell 128*, 693-705.
5. Jenuwein, T., and Allis, C. D. (2001) Translating the histone code, *Science 293*, 1074-1080.
6. Arrowsmith, C. H., Bountra, C., Fish, P. V., Lee, K., and Schapira, M. (2012) Epigenetic protein families: a new frontier for drug discovery, *Nat Rev Drug Discov 11*, 384-400.
7. Bannister, A. J., and Kouzarides, T. (2011) Regulation of chromatin by histone modifications, *Cell Res 21*, 381-395.
8. Zentner, G. E., and Henikoff, S. (2013) Regulation of nucleosome dynamics by histone modifications, *Nat Struct Mol Biol 20*, 259-266.
9. Bedford, M. T. (2007) Arginine methylation at a glance, *J Cell Sci 120*, 4243-4246.
10. Dillon, S. C., Zhang, X., Trievel, R. C., and Cheng, X. D. (2005) The SET-domain protein superfamily: protein lysine methyltransferases, *Genome Biol 6*.
11. Ng, H. H., Feng, Q., Wang, H. B., Erdjument-Bromage, H., Tempst, P., Zhang, Y., and Struhl, K. (2002) Lysine methylation within the globular domain of histone H3 by Dot1 is important for telomeric silencing and Sir protein association, *Gene Dev 16*, 1518-1527.

12. Guo, H. B., and Guo, H. (2007) Mechanism of histone methylation catalyzed by protein lysine methyltransferase SET7/9 and origin of product specificity, *P Natl Acad Sci USA 104*, 8797-8802.
13. Albert, M., and Helin, K. (2010) Histone methyltransferases in cancer, *Semin Cell Dev Biol 21*, 209-220.
14. Lee, J. S., Smith, E., and Shilatifard, A. (2010) The Language of Histone Crosstalk, *Cell 142*, 682-685.
15. Ng, H. H., Xu, R. M., Zhang, Y., and Struhl, K. (2002) Ubiquitination of histone H2B by Rad6 is required for efficient Dot1-mediated methylation of histone H3 lysine 79, *J Biol Chem 277*, 34655-34657.
16. Nakanishi, S., Lee, J. S., Gardner, K. E., Gardner, J. M., Takahashi, Y., Chandrasekharan, M. B., Sun, Z. W., Osley, M. A., Strahl, B. D., Jaspersen, S. L., and Shilatifard, A. (2009) Histone H2BK123 monoubiquitination is the critical determinant for H3K4 and H3K79 trimethylation by COMPASS and Dot1, *J Cell Biol 186*, 371-377.
17. Singer, M. S., Kahana, A., Wolf, A. J., Meisinger, L. L., Peterson, S. E., Goggin, C., Mahowald, M., and Gottschling, D. E. (1998) Identification of high-copy disruptors of telomeric silencing in Saccharomyces cerevisiae, *Genetics 150*, 613-632.
18. van Leeuwen, F., Gafken, P. R., and Gottschling, D. E. (2002) Dot1p modulates silencing in yeast by methylation of the nucleosome core, *Cell 109*, 745-756.
19. Lacoste, N., Utley, R. T., Hunter, J. M., Poirier, G. G., and Cote, J. (2002) Disruptor of telomeric silencing-1 is a chromatin-specific histone H3 methyltransferase, *J Biol Chem 277*, 30421-30424.
20. Feng, Q., Wang, H. B., Ng, H. H., Erdjument-Bromage, H., Tempst, P., Struhl, K., and Zhang, Y. (2002) Methylation of H3-lysine 79 is mediated by a new family of HMTases without a SET domain, *Curr Biol 12*, 1052-1058.
21. Jones, B., Su, H., Bhat, A., Lei, H., Bajko, J., Hevi, S., Baltus, G. A., Kadam, S., Zhai, H. L., Valdez, R., Gonzalo, S., Zhang, Y., Li, E., and Chen, T. P. (2008) The Histone H3K79 Methyltransferase Dot1L Is Essential for Mammalian Development and Heterochromatin Structure, *Plos Genet 4*.
22. Jo, S. Y., Granowicz, E. M., Maillard, I., Thomas, D., and Hess, J. L. (2011) Requirement for Dot1l in murine postnatal hematopoiesis and leukemogenesis by MLL translocation, *Blood 117*, 4759-4768.
23. Chang, M. J., Wu, H. Y., Achille, N. J., Reisenauer, M. R., Chou, C. W., Zeleznik-Le, N. J., Hemenway, C. S., and Zhang, W. Z. (2010) Histone H3 Lysine 79 Methyltransferase Dot1 Is Required for Immortalization by MLL Oncogenes, *Cancer Res 70*, 10234-10242.
24. Frederiks, F., Tzouros, M., Oudgenoeg, G., van Welsem, T., Fornerod, M., Krijgsveld, J., and van Leeuwen, F. (2008) Nonprocessive methylation by Dot1 leads to functional redundancy of histone H3K79 methylation states, *Nat Struct Mol Biol 15*, 550-557.
25. Altaf, M., Utley, R. T., Lacoste, N., Tan, S., Briggs, S. D., and Cote, J. (2007) Interplay of chromatin modifiers on a short basic patch of histone H4 tail defines the boundary of telomeric heterochromatin, *Mol Cell 28*, 1002-1014.

26. Fingerman, I. M., Li, H. C., and Briggs, S. D. (2007) A charge-based interaction between histone H4 and Dot1 is required for H3K79 methylation and telomere silencing: identification of a new trans-histone pathway, *Gene Dev 21*, 2018-2029.
27. McGinty, R. K., Kim, J., Chatterjee, C., Roeder, R. G., and Muir, T. W. (2008) Chemically ubiquitylated histone H2B stimulates hDot1L-mediated intranucleosomal methylation, *Nature 453*, 812-U812.
28. San-Segundo, P. A., and Roeder, G. S. (2000) Role for the silencing protein Dot1 in meiotic checkpoint control, *Mol Biol Cell 11*, 3601-3615.
29. Schubeler, D., MacAlpine, D. M., Scalzo, D., Wirbelauer, C., Kooperberg, C., van Leeuwen, F., Gottschling, D. E., O'Neill, L. P., Turner, B. M., Delrow, J., Bell, S. P., and Groudine, M. (2004) The histone modification pattern of active genes revealed through genome-wide chromatin analysis of a higher eukaryote, *Gene Dev 18*, 1263-1271.
30. Vakoc, C. R., Sachdeva, M. M., Wang, H. X., and Blobel, G. A. (2006) Profile of histone lysine methylation across transcribed mammalian chromatin, *Mol Cell Biol 26*, 9185-9195.
31. Okada, Y., Feng, Q., Lin, Y., Jiang, Q., Li, Y., Coffield, V. M., Su, L., Xu, G., and Zhang, Y. (2005) hDOT1L links histone methylation to leukemogenesis, *Cell 121*, 167-178.
32. Steger, D. J., Lefterova, M. I., Ying, L., Stonestrom, A. J., Schupp, M., Zhuo, D., Vakoc, A. L., Kim, J. E., Chen, J. J., Lazar, M. A., Blobel, G. A., and Vakoc, C. R. (2008) DOT1L/KMT4 recruitment and H3K79 methylation are ubiquitously coupled with gene transcription in mammalian cells, *Mol Cell Biol 28*, 2825-2839.
33. Wang, Z. B., Zang, C. Z., Rosenfeld, J. A., Schones, D. E., Barski, A., Cuddapah, S., Cui, K. R., Roh, T. Y., Peng, W. Q., Zhang, M. Q., and Zhao, K. J. (2008) Combinatorial patterns of histone acetylations and methylations in the human genome, *Nat Genet 40*, 897-903.
34. Sabra, M., Texier, P., El Maalouf, J., and Lomonte, P. (2013) The Tudor protein survival motor neuron (SMN) is a chromatin-binding protein that interacts with methylated lysine 79 of histone H3, *J Cell Sci 126*, 3664-3677.
35. Mueller, D., Bach, C., Zeisig, D., Garcia-Cuellar, M. P., Monroe, S., Sreekumar, A., Zhou, R., Nesvizhskii, A., Chinnaiyan, A., Hess, J. L., and Slany, R. K. (2007) A role for the MLL fusion partner ENL in transcriptional elongation and chromatin modification, *Blood 110*, 4445-4454.
36. Yokoyama, A., Lin, M., Naresh, A., Kitabayashi, I., and Cleary, M. L. (2010) A higher-order complex containing AF4 and ENL family proteins with P-TEFb facilitates oncogenic and physiologic MLL-dependent transcription, *Cancer Cell 17*, 198-212.
37. Conde, F., Refolio, E., Cordon-Preciado, V., Cortes-Ledesma, F., Aragon, L., Aguilera, A., and San-Segundo, P. A. (2009) The Dot1 histone methyltransferase and the Rad9 checkpoint adaptor contribute to cohesin-dependent double-strand break repair by sister chromatid recombination in Saccharomyces cerevisiae, *Genetics 182*, 437-446.
38. FitzGerald, J., Moureau, S., Drogaris, P., O'Connell, E., Abshiru, N., Verreault, A., Thibault, P., Grenon, M., and Lowndes, N. F. (2011) Regulation of the DNA

Damage Response and Gene Expression by the Dot1L Histone Methyltransferase and the 53Bp1 Tumour Suppressor, *Plos One 6*.

39. Huyen, Y., Zgheib, O., DiTullio, R. A., Gorgoulis, V. G., Zacharatos, P., Petty, T. J., Sheston, E. A., Mellert, H. S., Stavridi, E. S., and Halazonetis, T. D. (2004) Methylated lysine 79 of histone H3 targets 53BP1 to DNA double-strand breaks, *Nature 432*, 406-411.
40. Levesque, N., Leung, G. P., Fok, A. K., Schmidt, T. I., and Kobor, M. S. (2010) Loss of H3 K79 trimethylation leads to suppression of Rtt107-dependent DNA damage sensitivity through the translesion synthesis pathway, *J Biol Chem 285*, 35113-35122.
41. Schulze, J. M., Jackson, J., Nakanishi, S., Gardner, J. M., Hentrich, T., Haug, J., Johnston, M., Jaspersen, S. L., Kobor, M. S., and Shilatifard, A. (2009) Linking Cell Cycle to Histone Modifications: SBF and H2B Monoubiquitination Machinery and Cell-Cycle Regulation of H3K79 Dimethylation, *Mol Cell 35*, 626-641.
42. Barry, E. R., Krueger, W., Jakuba, C. M., Veilleux, E., Ambrosi, D. J., Nelson, C. E., and Rasmussen, T. P. (2009) ES Cell Cycle Progression and Differentiation Require the Action of the Histone Methyltransferase Dot1L, *Stem Cells 27*, 1538-1547.
43. Reisenauer, M. R., Wang, S. W., Xia, Y., and Zhang, W. (2010) Dot1a contains three nuclear localization signals and regulates the epithelial Na+ channel (ENaC) at multiple levels, *Am J Physiol Renal Physiol 299*, F63-76.
44. Zhang, W., Hayashizaki, Y., and Kone, B. C. (2004) Structure and regulation of the mDot1 gene, a mouse histone H3 methyltransferase, *Biochem J 377*, 641-651.
45. Zhang, W., Xia, X., Jalal, D. I., Kuncewicz, T., Xu, W., Lesage, G. D., and Kone, B. C. (2006) Aldosterone-sensitive repression of ENaCalpha transcription by a histone H3 lysine-79 methyltransferase, *Am J Physiol Cell Physiol 290*, C936-946.
46. Zhang, W., Xia, X., Reisenauer, M. R., Hemenway, C. S., and Kone, B. C. (2006) Dot1a-AF9 complex mediates histone H3 Lys-79 hypermethylation and repression of ENaCalpha in an aldosterone-sensitive manner, *J Biol Chem 281*, 18059-18068.
47. Zhang, W., Xia, X., Reisenauer, M. R., Rieg, T., Lang, F., Kuhl, D., Vallon, V., and Kone, B. C. (2007) Aldosterone-induced Sgk1 relieves Dot1a-Af9-mediated transcriptional repression of epithelial Na+ channel alpha, *J Clin Invest 117*, 773-783.
48. Nguyen, A. T., Xiao, B., Neppl, R. L., Kallin, E. M., Li, J. A., Chen, T. P., Wang, D. Z., Xiao, X. A., and Zhang, Y. (2011) DOT1L regulates dystrophin expression and is critical for cardiac function, *Gene Dev 25*, 263-274.
49. Buttner, N., Johnsen, S. A., Kugler, S., and Vogel, T. (2010) Af9/Mllt3 interferes with Tbr1 expression through epigenetic modification of histone H3K79 during development of the cerebral cortex, *P Natl Acad Sci USA 107*, 7042-7047.
50. Feng, Y., Yang, Y. P., Ortega, M. M., Copeland, J. N., Zhang, M. C., Jacob, J. B., Fields, T. A., Vivian, J. L., and Fields, P. E. (2010) Early mammalian erythropoiesis requires the Dot1L methyltransferase, *Blood 116*, 4483-4491.

51. Hess, J. L. (2004) MLL: a histone methyltransferase disrupted in leukemia, *Trends Mol Med 10*, 500-507.
52. Marschalek, R. (2010) Mixed lineage leukemia: roles in human malignancies and potential therapy, *Febs J 277*, 1822-1831.
53. Krivtsov, A. V., and Armstrong, S. A. (2007) MLL translocations, histone modifications and leukaemia stem-cell development, *Nat Rev Cancer 7*, 823-833.
54. Milne, T. A., Briggs, S. D., Brock, H. W., Martin, M. E., Gibbs, D., Allis, C. D., and Hess, J. L. (2002) MLL targets SET domain methyltransferase activity to Hox gene promoters, *Mol Cell 10*, 1107-1117.
55. Dou, Y. L., Milne, T. A., Ruthenburg, A. J., Lee, S., Lee, J. W., Verdine, G. L., Allis, C. D., and Roeder, R. G. (2006) Regulation of MLL1 H3K4 methyltransferase activity by its core components, *Nat Struct Mol Biol 13*, 713-719.
56. Dou, Y. L., Milne, T. A., Tackett, A. J., Smith, E. R., Fukuda, A., Wysocka, J., Allis, C. D., Chait, B. T., Hess, J. L., and Roeder, R. G. (2005) Physical association and coordinate function of the H3K4 methyltransferase MLL1 and the H4K16 acetyltransferase MOF, *Cell 121*, 873-885.
57. Ernst, P., Wang, J., Huang, M., Goodman, R. H., and Korsmeyer, S. J. (2001) MLL and CREB bind cooperatively to the nuclear coactivator CREB-binding protein, *Mol Cell Biol 21*, 2249-2258.
58. Caslini, C., Yang, Z., El-Osta, M., Milne, T. A., Slany, R. K., and Hess, J. L. (2007) Interaction of MLL amino terminal sequences with menin is required for transformation, *Cancer Res 67*, 7275-7283.
59. Grembecka, J., Belcher, A. M., Hartley, T., and Cierpicki, T. (2010) Molecular Basis of the Mixed Lineage Leukemia-Menin Interaction IMPLICATIONS FOR TARGETING MIXED LINEAGE LEUKEMIAS, *J Biol Chem 285*, 40690-40698.
60. Yokoyama, A., and Cleary, M. L. (2008) Menin critically links MLL proteins with LEDGE on cancer-associated target genes, *Cancer Cell 14*, 36-46.
61. Muntean, A. G., Tan, J. Y., Sitwala, K., Huang, Y. S., Bronstein, J., Connelly, J. A., Basrur, V., Elenitoba-Johnson, K. S. J., and Hess, J. L. (2010) The PAF Complex Synergizes with MLL Fusion Proteins at HOX Loci to Promote Leukemogenesis, *Cancer Cell 17*, 609-621.
62. Thiel, A. T., Blessington, P., Zou, T., Feather, D., Wu, X. J., Yan, J. Z., Zhang, H., Liu, Z. G., Ernst, P., Koretzky, G. A., and Hua, X. X. (2010) MLL-AF9-Induced Leukemogenesis Requires Coexpression of the Wild-Type Mll Allele, *Cancer Cell 17*, 148-159.
63. Nguyen, A. T., Taranova, O., He, J., and Zhang, Y. (2011) DOT1L, the H3K79 methyltransferase, is required for MLL-AF9-mediated leukemogenesis, *Blood 117*, 6912-6922.
64. Bernt, K. M., Zhu, N., Sinha, A. U., Vempati, S., Faber, J., Krivtsov, A. V., Feng, Z. H., Punt, N., Daigle, A., Bullinger, L., Pollock, R. M., Richon, V. M., Kung, A. L., and Armstrong, S. A. (2011) MLL-Rearranged Leukemia Is Dependent on Aberrant H3K79 Methylation by DOT1L, *Cancer Cell 20*, 66-78.
65. Bitoun, E., Oliver, P. L., and Davies, K. E. (2007) The mixed-lineage leukemia fusion partner AF4 stimulates RNA polymerase II transcriptional elongation and mediates coordinated chromatin remodeling, *Hum Mol Genet 16*, 92-106.

66. Shen, C. X., Jo, S. Y., Liao, C. Z., Hess, J. L., and Nikolovska-Coleska, Z. (2013) Targeting Recruitment of Disruptor of Telomeric Silencing 1-like (DOT1L) CHARACTERIZING THE INTERACTIONS BETWEEN DOT1L AND MIXED LINEAGE LEUKEMIA (MLL) FUSION PROTEINS, *J Biol Chem 288*, 30585-30596.
67. Krivtsov, A. V., Feng, Z., Lemieux, M. E., Faber, J., Vempati, S., Sinha, A. U., Xia, X., Jesneck, J., Bracken, A. P., Silverman, L. B., Kutok, J. L., Kung, A. L., and Armstrong, S. A. (2008) H3K79 methylation profiles define murine and human MLL-AF4 leukemias, *Cancer Cell 14*, 355-368.
68. Deshpande, A. J., Chen, L. Y., Fazio, M., Sinha, A. U., Bernt, K. M., Banka, D., Dias, S., Chang, J., Olhava, E. J., Daigle, S. R., Richon, V. M., Pollock, R. M., and Armstrong, S. A. (2013) Leukemic transformation by the MLL-AF6 fusion oncogene requires the H3K79 methyltransferase Dot1l, *Blood 121*, 2533-2541.
69. Krivtsov, A. V., Feng, Z., Lemieux, M. E., Faber, J., Vempati, S., Sinha, A. U., Xia, X., Jesneck, J., Bracken, A. P., Silverman, L. B., Kutok, J. L., Kung, A. L., and Armstrong, S. A. (2008) H3K79 Methylation Profiles Define Murine and Human MLL-AF4 Leukemias, *Cancer Cell 14*, 355-368.
70. Sitwala, K. V., Dandekar, M. N., and Hess, J. L. (2008) HOX Proteins and Leukemia, *Int J Clin Exp Patho 1*, 461-474.
71. Chen, L., Deshpande, A. J., Banka, D., Bernt, K. M., Dias, S., Buske, C., Olhava, E. J., Daigle, S. R., Richon, V. M., Pollock, R. M., and Armstrong, S. A. (2013) Abrogation of MLL-AF10 and CALM-AF10-mediated transformation through genetic inactivation or pharmacological inhibition of the H3K79 methyltransferase Dot1l, *Leukemia 27*, 813-822.
72. Daigle, S. R., Olhava, E. J., Therkelsen, C. A., Majer, C. R., Sneeringer, C. J., Song, J., Johnston, L. D., Scott, M. P., Smith, J. J., Xiao, Y. H., Jin, L., Kuntz, K. W., Chesworth, R., Moyer, M. P., Bernt, K. M., Tseng, J. C., Kung, A. L., Armstrong, S. A., Copeland, R. A., Richon, V. M., and Pollock, R. M. (2011) Selective Killing of Mixed Lineage Leukemia Cells by a Potent Small-Molecule DOT1L Inhibitor, *Cancer Cell 20*, 53-65.
73. Yu, W. Y., Chory, E. J., Wernimont, A. K., Tempel, W., Scopton, A., Federation, A., Marineau, J. J., Qi, J., Barsyte-Lovejoy, D., Yi, J. N., Marcellus, R., Iacob, R. E., Engen, J. R., Griffin, C., Aman, A., Wienholds, E., Li, F. L., Pineda, J., Estiu, G., Shatseva, T., Hajian, T., Al-awar, R., Dick, J. E., Vedadi, M., Brown, P. J., Arrowsmith, C. H., Bradner, J. E., and Schapira, M. (2012) Catalytic site remodelling of the DOT1L methyltransferase by selective inhibitors, *Nat Commun 3*.
74. Basavapathruni, A., Jin, L., Daigle, S. R., Majer, C. R. A., Therkelsen, C. A., Wigle, T. J., Kuntz, K. W., Chesworth, R., Pollock, R. M., Scott, M. P., Moyer, M. P., Richon, V. M., Copeland, R. A., and Olhava, E. J. (2012) Conformational Adaptation Drives Potent, Selective and Durable Inhibition of the Human Protein Methyltransferase DOT1L, *Chem Biol Drug Des 80*, 971-980.
75. Yao, Y., Chen, P. H., Diao, J. S., Cheng, G., Deng, L. S., Anglin, J. L., Prasad, B. V. V., and Song, Y. C. (2012) Selective Inhibitors of Histone Methyltransferase DOT1L: Design, Synthesis, and Crystallographic Studies, *J Am Chem Soc 134*, 17834-17834.

76. Anglin, J. L., Deng, L. S., Yao, Y., Cai, G. B., Liu, Z., Jiang, H., Cheng, G., Chen, P. H., Dong, S., and Song, Y. C. (2012) Synthesis and Structure-Activity Relationship Investigation of Adenosine-Containing Inhibitors of Histone Methyltransferase DOT1L, *J Med Chem 55*, 8066-8074.
77. Deng, L. S., Zhang, L., Yao, Y., Wang, C., Redell, M. S., Dong, S., and Song, Y. C. (2013) Synthesis, activity and metabolic stability of non-ribose containing inhibitors of histone methyltransferase DOT1L, *Medchemcomm 4*, 822-826.
78. Yu, W. Y., Smil, D., Li, F. L., Tempel, W., Fedorov, O., Nguyen, K. T., Bolshan, Y., Al-Awar, R., Knapp, S., Arrowsmith, C. H., Vedadi, M., Brown, P. J., and Schapira, M. (2013) Bromo-deaza-SAH: A potent and selective DOT1L inhibitor, *Bioorgan Med Chem 21*, 1787-1794.
79. Daigle, S. R., Olhava, E. J., Therkelsen, C. A., Basavapathruni, A., Jin, L., Boriack-Sjodin, P. A., Allain, C. J., Klaus, C. R., Raimondi, A., Scott, M. P., Waters, N. J., Chesworth, R., Moyer, M. P., Copeland, R. A., Richon, V. M., and Pollock, R. M. (2013) Potent inhibition of DOT1L as treatment of MLL-fusion leukemia, *Blood 122*, 1017-1025.
80. Mohan, M., Herz, H. M., Takahashi, Y. H., Lin, C. Q., Lai, K. C., Zhang, Y., Washburn, M. P., Florens, L., and Shilatifard, A. (2010) Linking H3K79 trimethylation to Wnt signaling through a novel Dot1-containing complex (DotCom), *Gene Dev 24*, 574-589.
81. Abulwerdi, F. A., Liao, C. Z., Mady, A. S., Gavin, J., Shen, C. X., Cierpicki, T., Stuckey, J. A., Showalter, H. D. H., and Nikoovska-Coleska, Z. (2014) 3-Substituted-N-(4-Hydroxynaphthalen-1-yl)arylsulfonamides as a Novel Class of Selective Mcl-1 Inhibitors: Structure-Based Design, Synthesis, SAR, and Biological Evaluation, *J Med Chem 57*, 4111-4133.
82. Nikolovska-Coleska, Z., Sun, H., Lu, J., Qiu, S., Meagher, J., Stuckey, J., Yi, H., Jiang, S., Roller, P., and Wang, S. (2006) Characterization of novel Smac mimetics as highly potent and effective antagonists of X-linked inhibitor of apoptosis protein, *Ejc Suppl 4*, 52-52.
83. Logan, C. Y., and Nusse, R. (2004) The Wnt signaling pathway in development and disease, *Annu Rev Cell Dev Bi 20*, 781-810.
84. Reya, T., and Clevers, H. (2005) Wnt signalling in stem cells and cancer, *Nature 434*, 843-850.
85. Anastas, J. N., and Moon, R. T. (2013) WNT signalling pathways as therapeutic targets in cancer, *Nat Rev Cancer 13*, 11-26.
86. Zhao, C., Blum, J., Chen, A., Kwon, H. Y., Jung, S. H., Cook, J. M., Lagoo, A., and Reyal, T. (2007) Loss of beta-catenin impairs the renewal of normal and CML stem cells in vivo, *Cancer Cell 12*, 528-541.
87. Wang, Y. Z., Krivtsov, A. V., Sinha, A. U., North, T. E., Goessling, W., Feng, Z. H., Zon, L. I., and Armstrong, S. A. (2010) The Wnt/beta-Catenin Pathway Is Required for the Development of Leukemia Stem Cells in AML, *Science 327*, 1650-1653.
88. Ysebaert, L., Chicanne, G., Demur, C., De Toni, F., Prade-Houdellier, N., Ruidavets, J. B., Mansat-De Mas, V., Rigal-Huguet, F., Laurent, G., Payrastre, B., Manenti, S., and Racaud-Sultan, C. (2006) Expression of beta-catenin by

acute myeloid leukemia cells predicts enhanced clonogenic capacities and poor prognosis, *Leukemia 20*, 1211-1216.
89. Yi, H. Y., Wang, J. L., Kavallaris, M., and Wang, J. Y. (2013) Lgr4-Mediated Potentiation Of Wnt/beta-Catenin Signaling Promotes MLL Leukemogenesis Via An Rspo3/Wnt3a-Gnaq Pathway In Leukemic Stem Cells, *Blood 122*.
90. Mosimann, C., Hausmann, G., and Basler, K. (2009) beta-Catenin hits chromatin: regulation of Wnt target gene activation, *Nat Rev Mol Cell Bio 10*, 276-U257.
91. Sierra, J., Yoshida, T., Joazeiro, C. A., and Jones, K. A. (2006) The APC tumor suppressor counteracts beta-catenin activation and H3K4 methylation at Wnt target genes, *Gene Dev 20*, 586-600.
92. Mahmoudi, T., Boj, S. F., Hatzis, P., Li, V. S., Taouatas, N., Vries, R. G., Teunissen, H., Begthel, H., Korving, J., Mohammed, S., Heck, A. J., and Clevers, H. (2010) The leukemia-associated Mllt10/Af10-Dot1l are Tcf4/beta-catenin coactivators essential for intestinal homeostasis, *PLoS Biol 8*, e1000539.
93. Castano Betancourt, M. C., Cailotto, F., Kerkhof, H. J., Cornelis, F. M., Doherty, S. A., Hart, D. J., Hofman, A., Luyten, F. P., Maciewicz, R. A., Mangino, M., Metrustry, S., Muir, K., Peters, M. J., Rivadeneira, F., Wheeler, M., Zhang, W., Arden, N., Spector, T. D., Uitterlinden, A. G., Doherty, M., Lories, R. J., Valdes, A. M., and van Meurs, J. B. (2012) Genome-wide association and functional studies identify the DOT1L gene to be involved in cartilage thickness and hip osteoarthritis, *Proc Natl Acad Sci U S A 109*, 8218-8223.
94. Ho, L. L., Sinha, A., Verzi, M., Bernt, K. M., Armstrong, S. A., and Shivdasani, R. A. (2013) DOT1L-mediated H3K79 methylation in chromatin is dispensable for Wnt pathway-specific and other intestinal epithelial functions, *Mol Cell Biol 33*, 1735-1745.

CHAPTER 2

Identification and biological characterization of DOT1L inhibitors

2.1 Introduction

Based on the important role for DOT1L in MLL-rearranged leukemias, there is significant interest in the development of small molecule inhibitors of DOT1L histone methyltransferase (HMTase) activity. Numerous methods have been employed for the successful identification of small molecule inhibitors of enzymes including biochemical screening, virtual screening, *de novo* design, and combinations of these approaches.

2.1.1 Biochemical screening

In order to maximize our chances of identifying small molecule inhibitors of DOT1L we employed a biochemical approach for the screening of chemical libraries. The advantage of this approach is that it is not mechanism biased and allows for the potential identification of SAM competitive, substrate competitive or allosteric inhibitors. Additionally, we explore a variety of chemical space in order to identify novel scaffolds that are not based on adenosine structures as are current DOT1L inhibitors.

There are many types of biochemical assays to measure enzyme functions and some of the most highly utilized are fluorescence polarization (FP), enzyme linked immunosorbent assays (ELISA), or fluorescence resonance energy transfer assays (FRET). All of these platforms were considered for the development of DOT1L HMTase assay. However, DOT1L poses a challenging target due to the fact that it does not a methylate a peptide substrate mimicking H3K79 region of H3 as many other HMTases are able to methylate peptide substrates mimicking the region of histone around their respective target. DOT1L also does not methylate recombinant H3 or H3/H4 tetramer

alone but requires all core histones H2A, H2B, H3, and H4 and has maximal activity against nucleosomes (*1-3*).

We also considered utilizing a general methyltransferase activity assays that measure the production of SAH from the turnover of SAM in methyltransferase reactions. However, these assays have serious drawbacks for the purpose of screening campaigns. In particular they utilize several additional enzyme coupled reactions in the assay to produce a colormetric, luminescent, or fluorescent signal. Therefore compounds that may inhibit these enzymes as opposed to the target methyltransferase can be identified in the screening leading to many false positive hits. Furthermore, colormetric, luminescent, and fluorescent assay readouts can be influenced by compounds that are colored, autofluorescent, or fluorescent quenchers.

Based on these considerations, we sought to develop a DOT1L HMTase assay with minimal reaction components, which is amenable to core histone or nucleosome substrate, and has a readout that is not influenced by colored or fluorescent compounds. Therefore we chose a gold standard, tritium radiolabeling assay format. This assay is based on the mechanism of DOT1L activity and utilizes a ^{3}H-methyl-S-adenosylmethionine (^{3}H-SAM) as the source of radioisotope. In the presence of DOT1L enzymatic activity the ^{3}H-methyl group is transferred from ^{3}H-SAM to the amine of lysine 79 on histone H3 in the context of either core histones or nucleosomes. The reaction mixture is transferred to P81 filter paper which binds histones based on ionic interactions and unreacted ^{3}H-SAM is washed away, leaving only radioactivity transferred to H3K79 by DOT1L on the filter paper which is measured by liquid scintillation counting. DOT1L is responsible for mono, di, and tri methylation of H3K79, therefore this assay does not distinguish between different methylation states but measures the total amount of ^{3}H-Methyl group transferred to H3K79.

For the purposes of screening chemical libraries, the DOT1L 3H-methyltransferase assay was modified to a 96-well plate format. The HMTase reaction is the same however there difference is that it is carried out in the wells of a 96-well filter plate with a permeable glass frit filter at the bottom of each well. Upon completion of the HMTase reaction the core histone substrate is precipitated with 50% cold trichlroroacetic acid

(TCA). The liquid reaction mixture is then removed by vacuum filtration through the glass filter at the bottom of the wells and the precipitated histones remain in the well, captured by the filter. Unreacted ^{3}H-SAM is washed away with 25% cold TCA and the remaining radioactivity results from ^{3}H-methyl groups transferred to H3K79 of the core histones (Figure 2.1.1). Radioactivity is then measure directly in the plate by scintillation counting.

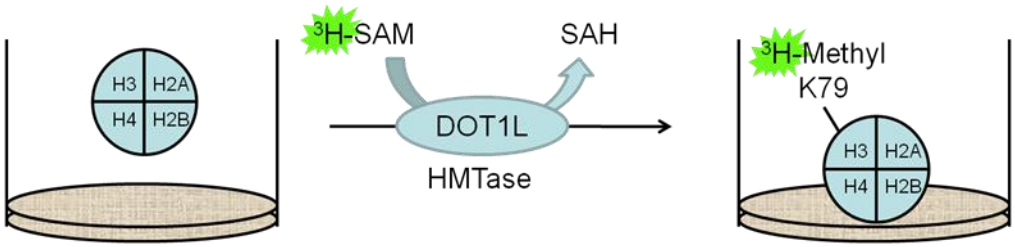

Figure 2.1.1 Schematic of 96-well plate DOT1L HMTase assay. In each well of the 96-well plate, core histones were combined with DOT1L and ^{3}H-SAM. The Histones were precipitated and captured on the glass filter at the bottom of the well by vacuum filtration. After washing to remove unreacted ^{3}H-SAM, only radioactivity transferred to core histones remains in the well and is measured by scintillation counting directly in the 96-well plate.

2.1.2 Virtual screening

Although biochemical screening has many advantages and allows us to directly assess the inhibition potential of compounds, there are limitations for the number of compounds that can be tested due to availability of libraries and cost. Therefore, we applied virtual screening, a computational technique used in drug discovery for identifying novel compounds with structural diversity that bind to a particular biological target. It involves *in silico* assessment of large libraries of chemical structures mainly using two different methods: ligand based (LBVS) and structure-based virtual screening (SBVS). There have been a mounting number of success stories reported by use of SBVS among which docking-based virtual screening (DBVS) is arguably the most widely applied one in practice.(*4-6*)

To take advantage of the available crystal structure of DOT1L (1-416) in complex with SAM (PDB 1NW3) (*7*) which offered in-depth structural details of the SAM binding site as well as the interactions between SAM and DOT1L, we applied DBVS for identifying

novel chemical scaffolds as potential DOT1L inhibitors. In 2011, the first DOT1L inhibitor, EPZ004777, and its selective activity against MLL-rearranged leukemia was reported.(*8*) To understand the interactions of this ligand on a structural level and incorporate those findings in our screening strategy, we modeled the complex structure between EPZ004777 and DOT1L and used it in the virtual screening together with the SAM-bound structure. Beside the experimentally solved or computationally modeled target structure, the compound library used for screening is the second important input of virtual screening.(*9*) To maximize the chance of discovering hits, libraries with structural diversity may be desired. However, focused libraries may be designed that contain chemical motifs known to interact with an individual target or a family of related targets, such as ATP analogues to target kinases (*10*). Thus, in our study we interrogated a focused small molecule library containing 1,200 nucleoside analogues that were designed as a nucleoside antibiotic-like library wherein the 5'-position was substituted to block normal nucleoside phosphorylation and metabolic incorporation. In fact, a subset of this library contained specific 5'-amine linkages that are ideal for mimicking SAM. Each compound in the library was virtually docked into both the experimental crystal structure and the modeled DOT1L:EPZ004777 complex structure and computationally models of the ligand–target interaction were obtained based on the optimal complementarity, steric, and physicochemical properties. Using different scoring functions the fitness between the docked compound and the target was evaluated, and after visual inspection the top-ranked compounds were selected for further biochemical and biological characterization.

2.1.3 Biochemical, biophysical, and biological characterization of identified hit compounds

Screening of compounds leads to numerous false positive hits, many of which are aggregators or promiscuous inhibitors (*11*). In order to identify and validate true hits and select potential lead compounds for future development, rigorous evaluation by secondary assays is essential for any successful screening campaign (*12*). We employ a traditional enzymatic kinetics analysis of inhibitors to assess the mechanism of action for each compound. We next subject potential inhibitors to several biophysical methods

to analyze and confirm direct binding to the target protein DOT1L. Each method has advantages and drawbacks, therefore it is important to be aware of the extent that each assay can be applied to compounds with different intrinsic chemical properties. A thermal stability shift (ThermoFluor) assay is used to assess ligand dependent thermal stabilization of DOT1L, indicative of binding. The advantages of this method are that it does not require labeling of investigated protein and represents a mix and measure assay format. However the disadvantage of this method is that fluorescent compounds can interfere with the assay readout and cannot be assessed by this method (*13*). Saturation transfer difference nuclear magnetic resonance (STD NMR) experiments are also used to assess direct binding of small-molecules to protein targets. One advantage of this method is that it can be used in a competitive format allowing interrogation of the binding site of an inhibitor. For example, if the compounds bind to the same site as co-factor SAM, upon addition of excess SAM or its analogue SAH, displacement of a SAM competitive small molecule results in loss of STD NMR signal and provides evidence that the compound binds to the SAM binding site. However, not all compounds are soluble enough to provide quality ^{1}H NMR spectra in buffer and cannot be assessed by this method. Biolayer interferometry assays can also be applied using the ForteBio OctetRED system in which biosensors are immobilized with a protein that is being tested, for example DOT1L, and immersed in solutions of potential inhibitors to determine direct binding (*14*). The benefit of this method is that it can provide quantitative measurements of binding constants. Some compounds are not amenable to this assay due to solubility issues and non-specific binding to control biosensors. Additionally, compounds with color that absorb visible light can be assessed by measurement of the absorbance spectrum of the compound in the presence of a binding partner (*15*). This method provides a rapid and simple qualitative assessment of binding but is only amenable to compounds that absorb light in the visible spectrum.

After biochemical and biophysical assessment of compounds, the cellular activity of potential DOT1L inhibitors is characterized to determine the suitability of compounds as potential chemical tools as well as leads for further development. One of the most important readouts of cellular activity is the selective inhibition of H3K79 methylation in cells. Histones are extracted from treated cells and analyzed for H3K79 methylation and

additional histone methylation marks by western blot to determine if compounds are able to penetrate cells and inhibit DOT1L function. Assessment of selectivity is important to ensure that the compounds are specific and not disrupting histone methylation by a non-specific mechanism. Cell growth inhibition is also important to assess the selectivity of DOT1L inhibition by compounds and to ensure they are not generally toxic. For this purpose, we measure cell growth in a panel of human leukemia cell lines that harbor either MLL-translocation oncogenes, and should be sensitive to DOT1L inhibition (KOPN-8, THP-1, MV4-11, and U937), or other oncogenes that do not depend on DOT1L for growth (Kasumi-1 and K562). However, cultured human cancer cell lines have many dysregulated pathways; therefore several murine model cell lines are employed. Established cell lines from murine bone marrow transformed with either MLL-AF9, and depend on DOT1L, or E2A-HLF, and do not depend on DOT1L are used to measure the selectivity of cell growth inhibition by potential DOT1L inhibitors (*16*). Additional cellular effects on cell cycle, apoptosis, differentiation, and gene expression are assessed to examine the influence of compounds on cells in order to determine if the phenotypes are consistent with genetic loss of DOT1L, and to further confirm that compound inhibits endogenous cellular DOT1L.

2.2 Results

2.2.1 Development of a DOT1L ^{3}H-methyltransferase assay

Each of the approaches for identification of DOT1L inhibitors requires a robust *in vitro* biochemical assay to validate and characterize inhibitors identified through the various screening approaches. Therefore, our first goal was to establish and optimize an HMTase assay for DOT1L. Based on the unique requirement of a nucleosome or core histone substrate for DOT1L HMTase activity many of the fluorescence based assays using peptide substrates could not be applied to this system. Additional enzyme coupled assays have numerous shortcomings discussed previously; therefore we developed a radiolabeling ^{3}H-methyltransferase assay that is a gold standard utilized by others for similar purposes (*8*). Recombinant DOT1L with N-terminal six histidine repeat (His-6) and GST tag was expressed in *E. coli* and purified by nickel affinity chromatography. Upon purification of DOT1L solely by nickel column, DNA fragments were also co-

purified, as detected by a high 260/280 absorbance ratio. Further purification by size exclusion and cation exchange chromatography resulted in pure DOT1L protein. Core histones extracted from calf thymus were ultimately chosen as the assay substrate because DOT1L demonstrated good enzymatic activity towards the substrate and it was available commercially at low cost. The assay conditions were optimized by determining the Km for the substrate, 0.09 $\pm$ 0.02 ug/uL, and SAM, 110.7 $\pm$ 29.4 nM. The conditions chosen for compound screening were near or below the Km for both the substrate (0.037 ug/uL) and SAM (125 nM) to unbias the assay towards the mechanism of inhibitors identified in screening. The buffer conditions were briefly optimized starting from a commonly used reported HMTase buffer (*2*) with the addition of 0.01% Triton x-100 to limit the number of false positive aggregator compounds identified in chemical library screening. The assay was initially carried out in microcentrifuge tubes and 3H-methyltransfer was measured by filter binding and liquid scintillation counting in vials. In order to make the assay amenable for screening compound libraries we adapted it to a 96-well plate format using MultiScreen filter plates (MilliPore) which allowed us to carry out the HMTase reaction and measure radioactivity transferred directly in the plate (*17*). The DOT1L HMTase assay was validated using the non-specific methyltransferase inhibitor SAH and provided IC_{50} = 1.6 $\pm$ 0.4 µM in a similar range with other reports (*18*). Upon optimization and validation of the DOT1L HMTase assay it was utilized to verify the *in vitro* DOT1L inhibition potency of compounds identified by virtual screening and *de novo* design approaches and for biochemical screening of chemical libraries.

2.2.2 Virtual screening of a nucleoside focused library

To take advantage of the available crystal structure of the DOT1L catalytic domain (1-416) in complex with SAM which offered in-depth structural details of the SAM binding site as well as the interactions between SAM and DOT1L, we applied DBVS for identifying novel chemical scaffolds as potential DOT1L inhibitors. In 2011, the first DOT1L inhibitor, EPZ004777, was reported demonstrating selective activity against MLL-rearranged leukemia (*8*). To understand the interactions of this ligand on a structural level and incorporate those findings in our screening strategy, we modeled the complex structure between EPZ004777 and DOT1L and used it in the virtual screening

together with the SAM-bound structure. The compound library used for screening is the other important input together with the experimentally solved or computationally modeled target structure (*9*). To maximize the chance of discovering hits, libraries with structural diversity are desired. However, focused libraries may be designed that contain chemical motifs known to interact with an individual target or a family of related targets, such as ATP analogues to target kinases (*10*). Thus, in our study we interrogated a focused small molecule library containing 1,200 nucleoside analogues that were designed as a nucleoside antibiotic-like library wherein the 5'-position was substituted to block normal nucleoside phosphorylation and metabolic incorporation. Importantly, a subset of this library contained specific 5'-amine linkages that are ideal for mimicking SAM. Each compound in the library was virtually docked into both the experimental crystal structure and the modeled DOT1L:EPZ004777 complex structure and computationally models of the ligand–target interaction were obtained based on the optimal complementarity, steric, and physicochemical properties. Using different scoring functions the fitness between the docked compound and the target was evaluated, and after visual inspection the top-ranked compounds were selected for further biochemical and biological characterization as DOT1L inhibitors. Here is presented an implementation of DBVS workflow strategy to analyze a focused nucleoside library, followed by biological validation of identified and selected hits. Several adenosine analogues with novel scaffolds were successfully identified for further development as DOT1L inhibitors. The process for virtual screening in this study is shown in Figure 2.2.1.

Towards our goal of identifying novel inhibitors of DOT1L we first utilized the only available X-ray crystal structure of DOT1L in complex with SAM (PDB ID: 1NW3) (*19*). While our work was in progress, a potent and selective DOT1L inhibitor, EPZ004777, was reported (*8*). This compound is a SAM analogue containing a structurally unexpected urea-linked para-tert-butylphenyl hydrophobic tail, showing high potency (K_i value of 0.3 nM) (*8*). Structural data of EPZ004777 binding to DOT1L was not available at the time of our study and we performed modeling studies to predict the binding model of EPZ004777 to the SAM-binding pocket of DOT1L (PDB:1NW3).

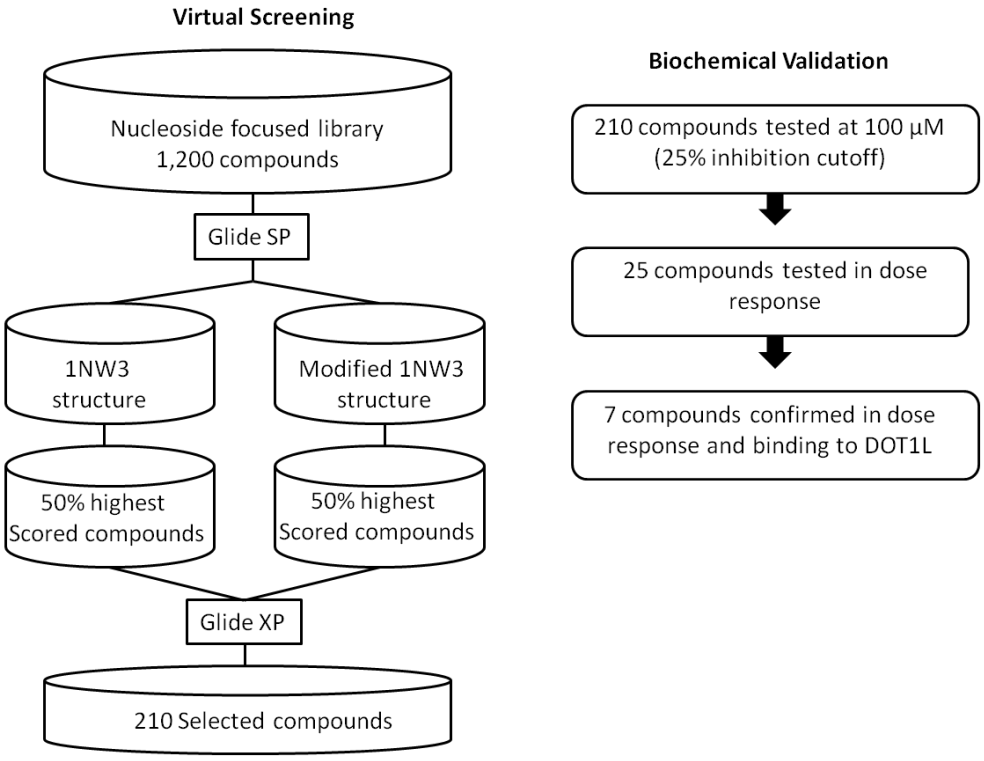

Figure 2.2.1 Schematic of the virtual and biochemical screening strategy for the identification of DOT1L inhibitors. A focused library of 1,200 nucleoside derived compounds was virtually screened by docking compounds into the structure of DOT1L with SAM (1NW3) or a modified structure of DOT1L derived from modeling of EPZ004777 into the SAM binding site of DOT1L (modified 1NW3). 210 (199 from DOT1L:SAM, 95 from DOT1L:EPZ004777 simulated complex, among them, 84 overlap) selected compounds were screened for *in vitro* inhibition of DOT1L and hits were tested for binding to DOT1L and cellular inhibition of H3K79 methylation.

However, using DOT1L/SAM complex structure failed to identify a ligand confirmation that could accommodate the bulky hydrophobic substituent within the enclosed amino-acid binding pocket.After analyzing the binding site, we inferred that the bulky hydrophobic tert-butylphenyl group may occupy an unopened sub-pocket towards the substrate-binding site while the remaining part interacts with DOT1L similar to SAM. Based on this idea, first a compound derived from EPZ004777 without the tert-butylphenyl group was docked into the active site and the best scored docking pose was very similar to the binding pose of SAM. We then manually built in the tert-butylphenyl group into the docked molecule, and identified several hydrophobic residues with strong van der Waals conflicts with the hydrophobic group, in particular Thr 139, Val 144, Met 147, Val 169 and Phe 239 (Figure 2.2.2a). After a minimization

and 2ns molecular dynamics simulation using AMBER (version 11.0), van der Waals conflicts between the para-tert-butylphenyl group and the surrounding residues were resolved. Redocking of EPZ004777 into this simulated complex, the result showed that the docking pose is very reasonable: the adenosine part has same interactions as SAM; the urea group has three hydrogen bonds with Asp 161 and Thr 139; and the para-tert-butylphenyl group inserts an open cavity and has strong hydrophobic interactions with the surrounding residues Leu 143, Val 144, Met 147, Phe 239, Val 267 and Tyr 312. Based on the simulation results, we predicted that the bulky hydrophobic group para-tert-butylphenyl group can induce conformational changes and the opening of the hydrophobic cavity which is not present in the DOT1L:SAM complex and probably is the major factor for having high binding affinity and inhibition of DOT1L enzyme activity. Thus, this model DOT1L:EPZ004777 complex structure was also used for the virtual screening along with the DOT1L:SAM complex in order to identify compounds with diverse chemical scaffold and binding interactions. After the virtual screening was performed, the three-dimensional structure of the DOT1L bound to EPZ004777 was reported (*20*). This structure reveals remodeling of the catalytic site and uncovered novel and unexpected conformational variability of the cofactor-binding site that can accommodate compounds significantly larger and more hydrophobic than SAM. Importantly, after the superimposing of the reported crystal structure (PDB: ID 4EKI) and our modeled and simulated DOT1L:EPZ004777 complex (Figure 2.2.2b), the RMSD of the α carbon of the two proteins is 1.741 Å and the RMSD of the heavy atoms of the two ligands is 1.188 Å, indicating similar confirmation and accuracy of our predicted model, used for the virtual screening approach.

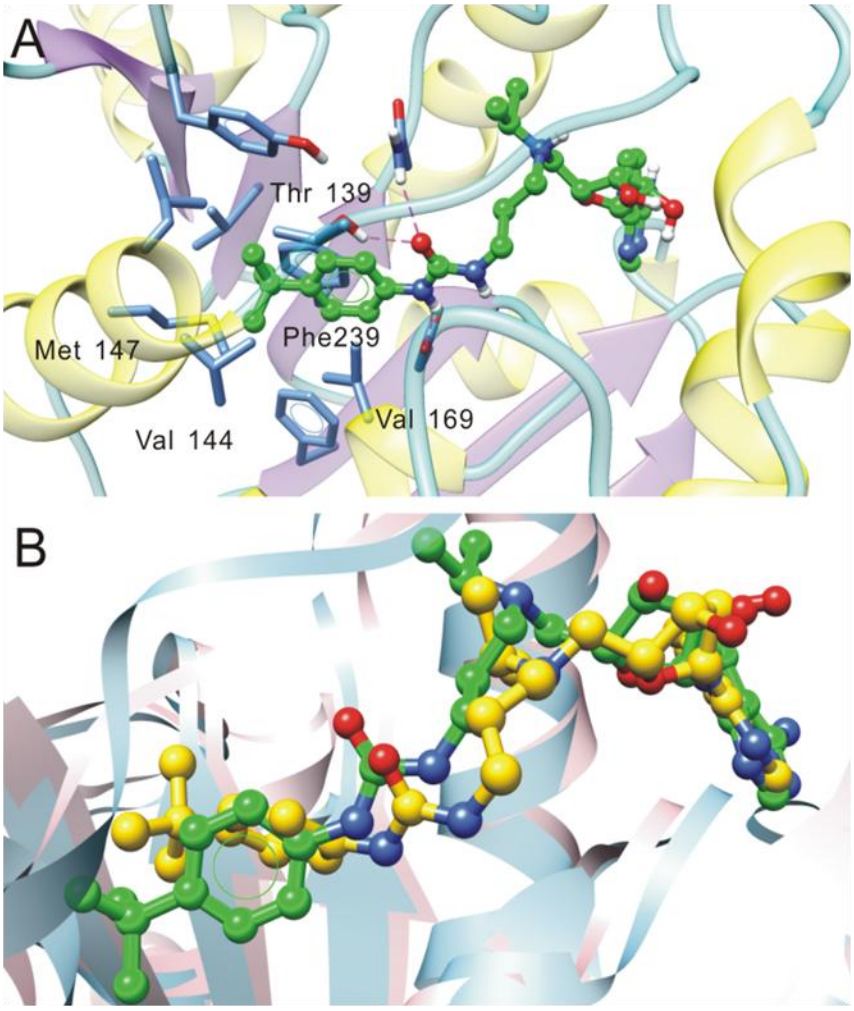

Figure 2.2.2 DOT1L:EPZ004777 model complex. (a) A molecule which does not have the tert-butylphenyl group of EPZ004777 was docked into the active site of 1NW3. The tert-butylphenyl group was manually incorporated to the docking pose, indicating there are very sharp Van der Waals conflictions between this group and the surrounding residues of Thr 139, Val 144, Met 147, Val 169 and Phe 239. (b) Superimposing of the crystal structure of 4EKI (gold) and the simulated DOT1L:EPZ004777 complex (green).

The compounds contained in a focused library of 1,200 nucleoside analogues, were prepared for docking using LigPrep 2.5 module of Schrodinger and then docked to the active sites of both used complex structures od DOT1L, the crystal structure with SAM and modeled structure with EPZ004777 inhibitor, using Glide 5.9. In the first step standard precision (SP) docking was used, where an extensive sampling using Monte Carlo procedure was carried out. From here, only top 50% (600 compounds from each used complex structure) of all the good scoring state was retained and passed on to the

next stage in which extra precision (XP) docking was performed. XP docking does a more extensive sampling and uses anchor-and-grow strategy to weed out false positives. XP docking employs a more stringent scoring function than the SP Glidescore, which includes terms for hydrophobic enclosure and desolvation penalties (*21*). Top 50% having good XP Gscore values were selected for visual inspection of binding pattern and the final subset of compounds for biological characterization were selected.

The selection criterion were that at least one docking pose of each compound has similar interactions as SAM or EPZ004777 with the protein, i.e., the nucleoside part of each compound should form hydrogen bonds and π-π stack interactions as the adenosine portion of SAM. The compounds which contained a hydrophobic tail that could insert into the induced open hydrophobic cavity of DOT1L were given priority since the binding affinity of EPZ004777 is much higher than SAM. In this way, 199 compounds were selected from the DOT1L:SAM complex (1NW3) and 95 compounds were selected from the modeled DOT1L:EPZ004777 complex. 84 compounds overlapped from the two complexes resulting in total 210 compounds that were selected for biochemical validation of DOT1L inhibition activity.

To verify the *in vitro* DOT1L inhibition potency of *in silico* virtual screening hits we tested compounds for inhibition of DOT1L HMTase activity using a radio-isotope labeling histone methyltransferase assay. The assay utilizes ^{3}H-methyl-SAM as the methyl donor in the HMTase reaction of GST-DOT1L incubated with core histone substrate. Of the 210 compounds initially screened at a single concentration of 100 μM with core histone substrate of the HMTase reaction, we identified 25 compounds that provided inhibition of 25% or greater. The relatively high concentration of compound and low inhibition cutoff were selected in order to identify compounds with even weak inhibition of DOT1L in order to improve the likelihood of developing a preliminary SAR from the small library and to identify inhibitors with novel chemical scaffolds for development as future lead compounds. A follow up dose response screening of compounds using a more physiologically relevant nucleosome substrate resulted in the identification of

seven compounds with DOT1L inhibition potency of IC_{50} = 32-168 μM (Figure 2.2.3). All these seven compounds have a hydrophobic tail and were come from the virtual screening employing the DOT1L:EPZ004777 complex, demonstrating the advantage of utilizing the generated model of DOT1L:EPZ004777 as opposed to using the only available structural information of DOT1L:SAM. Identification of this class of compounds is consistent with EPZ004777, demonstrating the importance of utilizing the available interactions in the predicted hydrophobic pocket generated in this model.

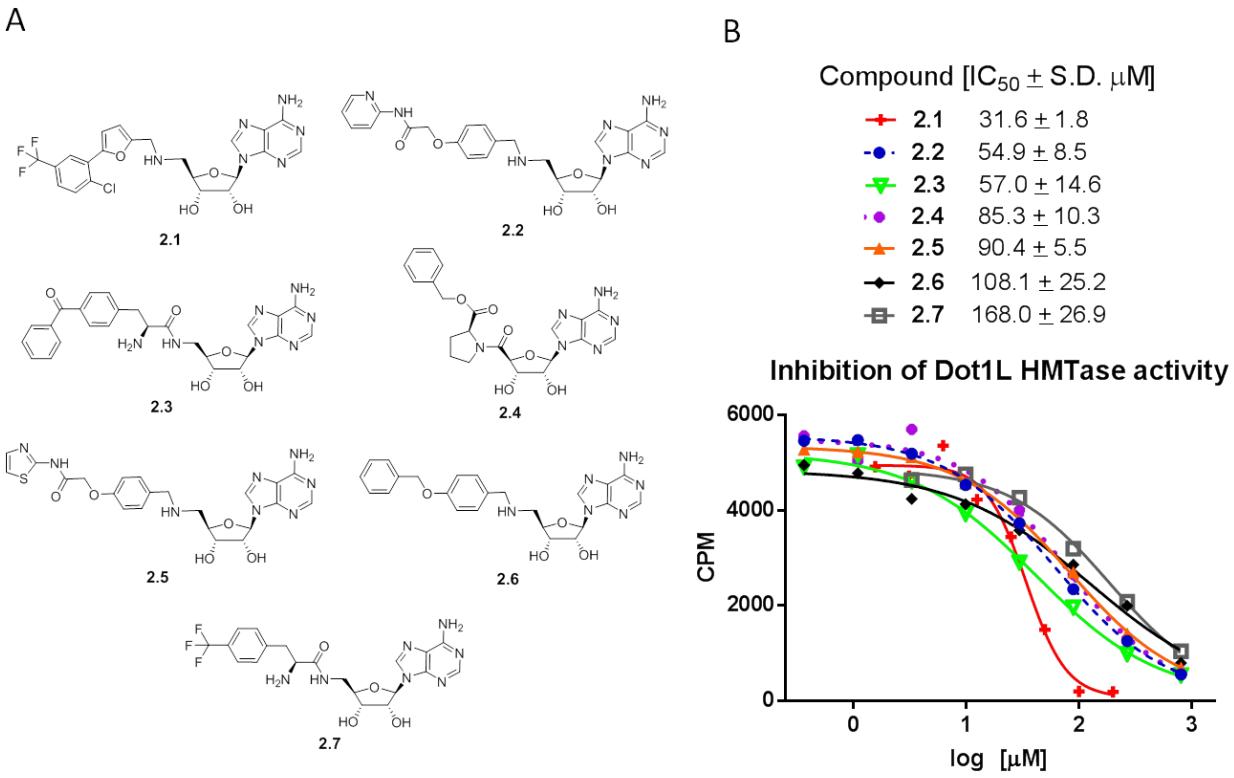

Figure 2.2.3 DOT1L inhibitors and *in vitro* inhibition of DOT1L HMTase activity. (a) Chemical structures of DOT1L inhibitors identified by virtual screening that were confirmed inhibitors of DOT1L HMTase activity *in vitro.* (b) Inhibition curves and IC_{50} values of DOT1L inhibitors determined with 3H-methyl radiolabeling HMTase assay.

The putative binding modes of the most potent DOT1L inhibitors identified **2.1** and **2.2** (Figure 2.2.4). The adenosine parts of **2.1** and **2.2** have exact same interaction modes as SAM and EPZ004777: three hydrogen bonds and π-π stack interactions can be observed. The hydrophobic tails of the two compounds insert into the induced hydrophobic cavity. The difference is that these two compounds do not have hydrogen

bonds with Asp 161. Hydrogen bonding with this residue can be observed for both of SAM and EPZ004777. We may induce that this hydrogen bonding with Asp 161 is important for receiving high potency to inhibit DOT1L, so in the future to modify our hits identified here to get more potent DOT1L inhibitors, we may add groups containing hydrogen bond donors into the scaffolds or modify the scaffolds to make the new designed compounds having hydrogen bonds with this residue. Additionally, to increase our compounds affinity, we may connect isopropyl or similar groups to the amine of compounds **2.1** and **2.2** since SAR study has indicated that such groups are favorable to the binding to DOT1L. Compounds **2.3 – 2.7** have similar interactions as compounds **2.1** and **2.2** having to the target of DOT1L. Since all the seven hits identified from this study have a hydrophobic segment in the tail parts, they could not be docked into the active site of the DOT1L:SAM complex, demonstrating the utility of our strategy to employ a simulated binding mode of EPZ004777 to increase the likelihood of identifying novel DOT1L inhibitors.

In order to verify that the identified DOT1L inhibitors bind to DOT1L as predicted, saturation transfer difference (STD) NMR and thermal stability shift assays were used to assess binding. All seven compounds that inhibit DOT1L activity showed binding to GST-DOT1L by STD NMR. The proton signals in the ^{1}H NMR spectra of **2.2** were assigned (Figure 2.2.5a) and observed in the STD NMR spectra (Figure 2.2.5b) which demonstrates that **2.2** binds to DOT1L. SAH was added to the mixture of **2.2** and DOT1L in five-fold molar excess and additional peaks were observed in the ^{1}H NMR from SAH protons (Figure 2.2.5c). In the presence of SAH, only STD NMR signal for SAH was observed and the STD NMR signal from **2.2** was diminished, indicating that **2.2** was competed off by SAH (Figure 2.2.5). This result demonstrates that **2.2** binds to the SAM binding site as predicted by the computational modeling.

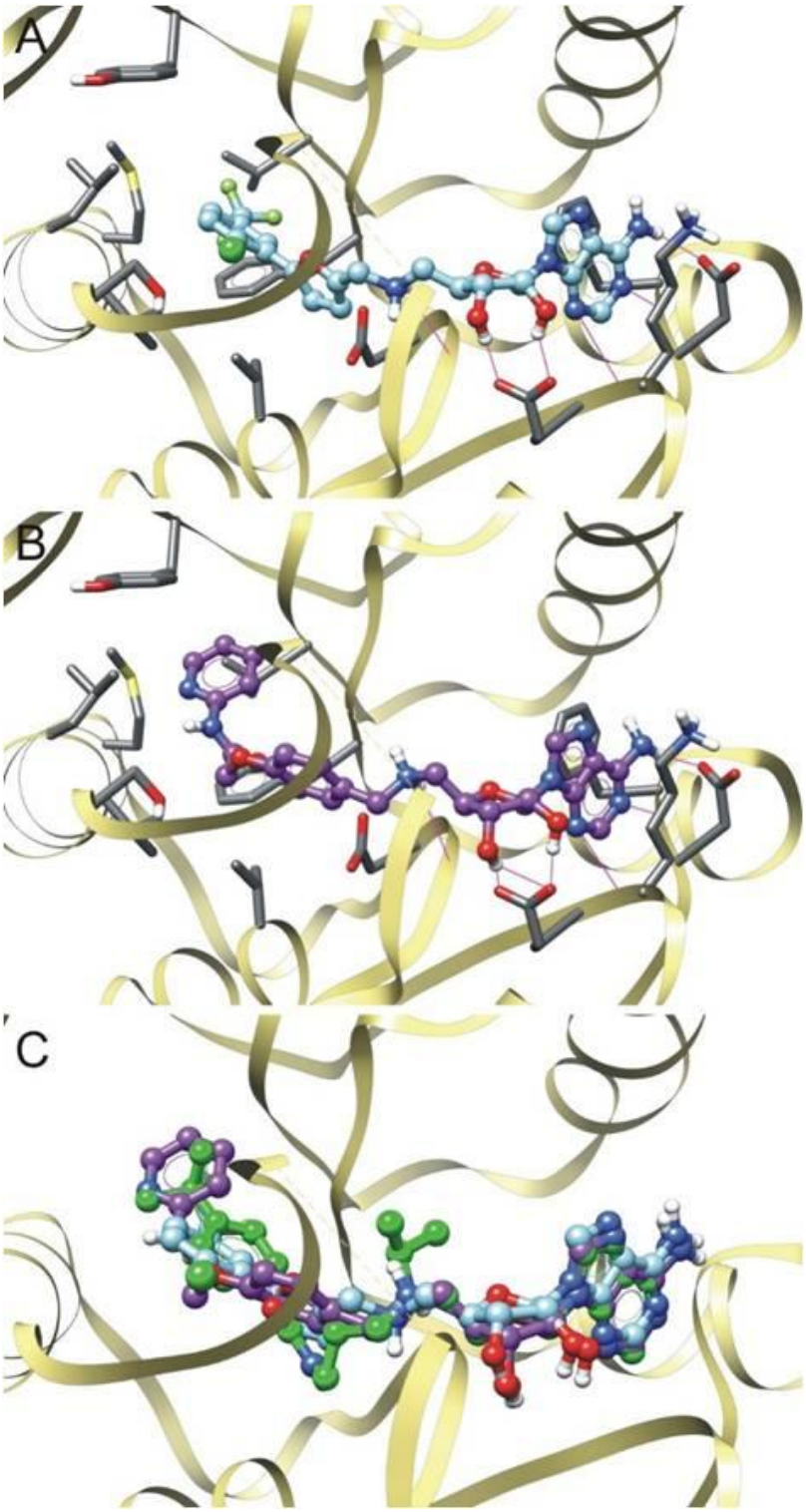

Figure 2.2.4 Putative binding modes of compounds 2.1 and 2.2 to DOT1L. Glide XP binding pose of (a) **2.1** and (b) **2.2** to the DOT1L:EPZ004777 simulated complex. (c) Superimposition of docking poses of **2.1** (cyan), **2.2** (purple) to EPZ004777 (green).

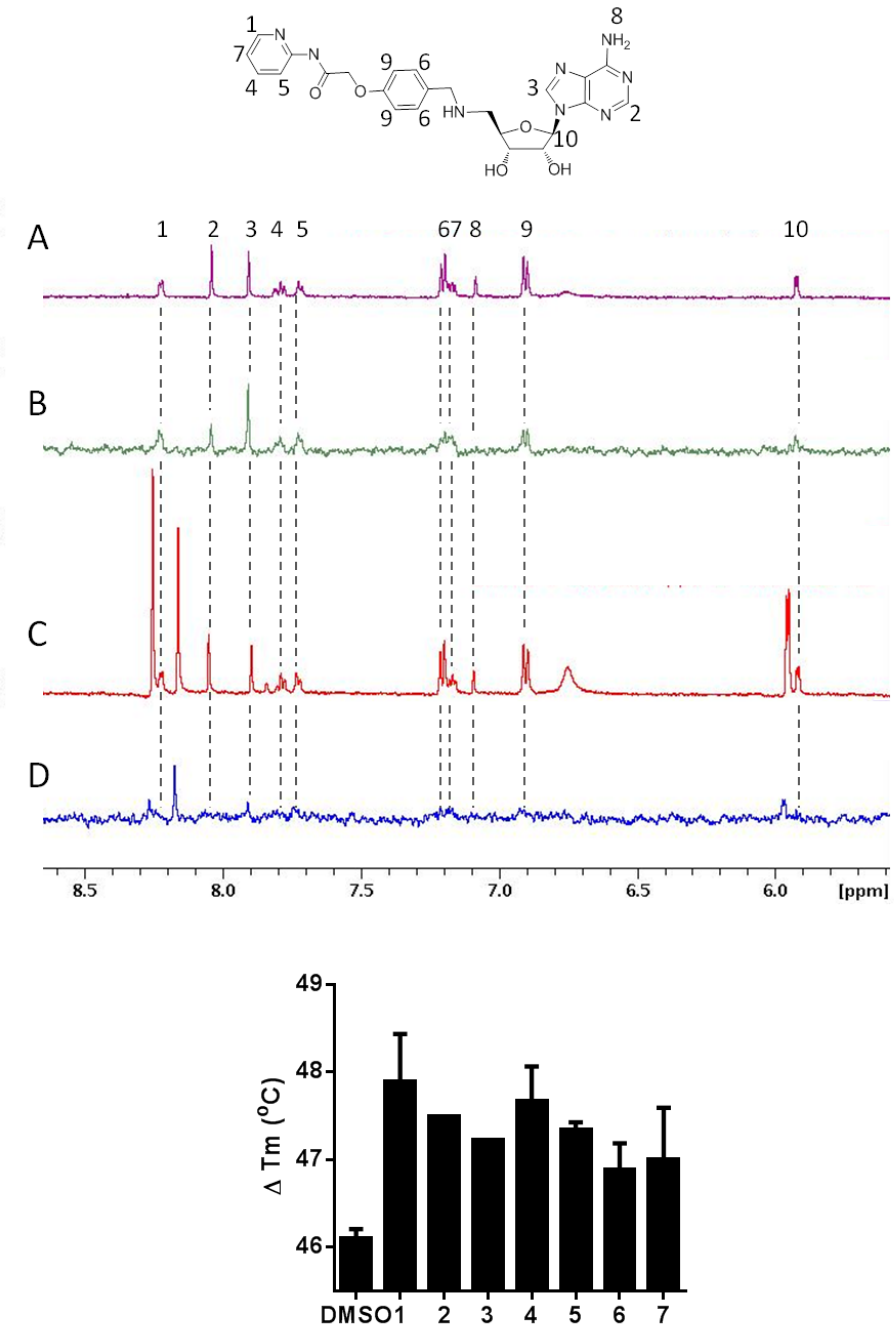

Figure 2.2.5. DOT1L inhibitors bind to the SAM binding site. (a) Structure of **2.2** and ^{1}H NMR of 200 µM **2.2** in the presence of 5 µM GST-DOT1L. Compound protons numbered according to corresponding ^{1}H NMR signal. (b) STD NMR of 200 µM **2.2** in the presence of 5 µM GST-DOT1L demonstrates binding of **2.2** to DOT1L. (c) ^{1}H NMR of 2 mM SAH with 200 µM **2.2** in the presence of 5 µM GST-DOT1L. Additional peaks in spectra that do not correspond to **2.2** are from SAH. (d) STD NMR 2 mM SAH with 200 µM **2.2** in the presence of 5 µM GST-DOT1L. Loss of STD NMR signal from **2.2** indicates that SAH competes with **2.2** for binding to the SAM binding site. (e) Thermal stability shift assay of 1µM GST-DOT1L in the presence of DMSO or 100 µM DOT1L inhibitors showing increased melting temperature in the presence of compounds, indicating binding to DOT1L.

Binding of inhibitors to DOT1L was further verified by ligand dependent thermal stability shift assay (ThermoFluor). This assay is based on the principle that ligand binding stabilizes the protein resulting in increase thermal stability. All of the identified inhibitors bind to GST-DOT1L as indicated by strong stabilization of the protein which increases the melting temperature of GST-DOT1L in the presence of compounds compared with DMSO (Figure 2.2.5e). Together, these results indicate that the compounds identified as DOT1L inhibitors through virtual screening and *in vitro* inhibition of DOT1L HMTase activity indeed bind to DOT1L and are SAM competitive as predicted based on virtual screening.

In order to determine if the identified *in vitro* inhibitors of DOT1L inhibit DOT1L in cells, MLL-AF9 transformed murine bone marrow cells were treated with **2.2** for 3 days and H3K79 methylation was analyzed by Western blot (Figure 2.2.6a). The toxicity of compound **2.1** prohibited the evaluation of H3K79 methylation inhibition in cells. Methylation of H3K79 was reduced in the presence of the DOT1L inhibitor, **2.2**. H3K4, H3K27, and H3K36 trimethylation states were not changed in the presence of **2.2** indicating that inhibition of HMTase activity is selective for DOT1L (Figure 2.2.6b). A slight decrease of H3K9 trimethylation was observed but not to the extent as H3K79 trimethylation suggesting that there may be limited non-selective inhibition of other histone methyltransferases which is reasonable due to the similarity of **2.3** to SAM. However the overall affect observed was most dramatic for H3K79, indicating the DOT1L is the primary cellular target of **2.3**. Furthermore, the affect of prolonged DOT1L inhibition was measured of the course of 6 and 9 days (Figure 2.2.6a). During the time course, H3K79 dimethylation was continually decreased consistent with the notion that cellular turnover is required to observe the affect of DOT1L inhibition by small molecule inhibitors due the lack of any known H3K79 demethylases.

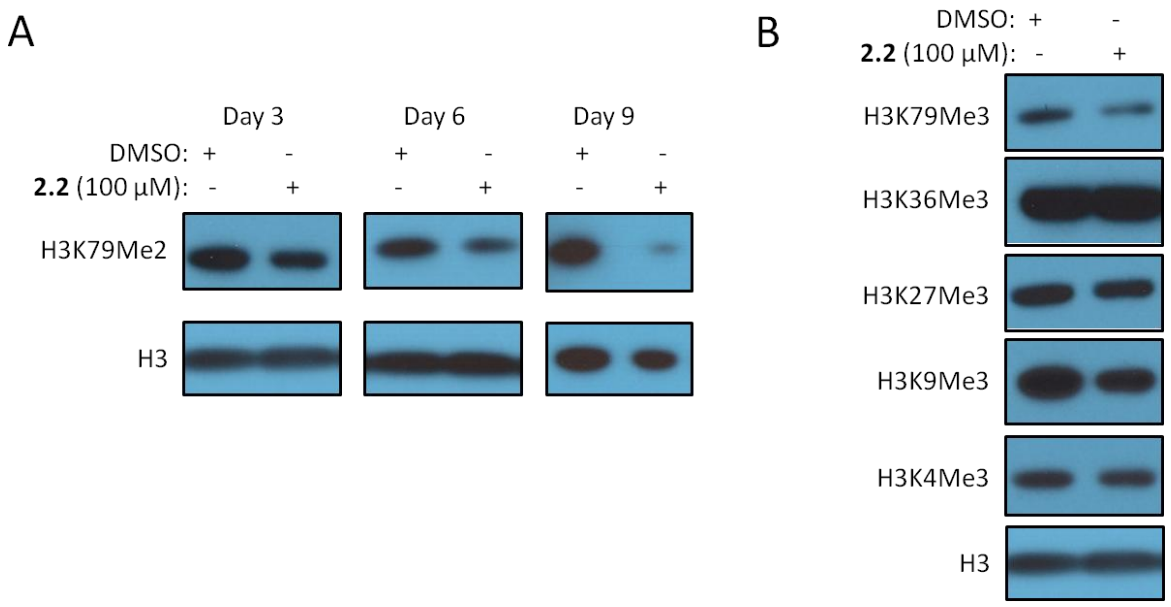

Figure 2.2.6 DOT1L inhibitors reduce cellular H3K79 methylation in a MLL-AF9 murine model cell line. (a) H3K79 dimethyaltion inhibition by100 µM **2.2** in MLL-AF9 murine model cells over the time course of 3, 6, and 9 days (b) Western blot analysis of the selectivity of H3K79 inhibition with H3K4, H3K9, H3K27, and H3K36 trimethylation in MLL-AF9 cells upon 3 days of DOT1L inhibition with by100 µM **2.2**.

Here, we demonstrate the utility of applying structure-based virtual screening using a nucleoside focused library followed by biochemical validation to identify novel inhibitors of the histone methyltransferase DOT1L. Virtual screening techniques which have not been applied to this target resulted in identification of, 210 SAM analogues as potential hits. Upon their biochemical testing using tritium based assay, seven compounds demonstrated inhibition of DOT1L HMTase activity with IC_{50} values from 32-168 µM. All of the compounds which inhibited DOT1L HMTase activity were assessed for binding to DOT1L by STD NMR and ThermoFluor assays and demonstrated that directly bindand interact with DOT1L.. Furthermore, SAH competes with **2.2** for binding to the SAM binding site, confirming the predicted binding mode of these compounds.

For applying a structure-based virtual screening, in this work we utilized two different complex structures, crystal structure of DOT1L with SAM and modeled structure of the DOT1L-EPZ004777 complex. It should be pointed out that the model structure with EPZ004777 inhibitor leads to a considerable protein conformational changes. In

particular, the 4-tert-butylphenyl-substituted urea group is located in a newly formed pocket, which includes the amino acid binding pocket of SAM and an additional adjacent hydrophobic cavity. Importantly, our model structure was later confirmed with the solved crystal structure of the DOT1L-EPZ004777 complex was reported (*20*). Using these two structures allowed us to perform virtual screening and simultaneously docked the compounds from the focused library to different protein conformations and to identify the best combination of compound binding pose and protein conformer. Indeed, all validated DOT1L inhibitors were identified by using the model structure, which probably would be missed if only DOT1L-SAM structure was used, proving that the generated model structure served as an important tool for virtual screening of the nucleoside analog library. Thus, we demonstrate the importance of using complex structure of target proteins including a predicted one for which only apo-structure is available which will allow introducing multiple protein conformations in virtual screening strategy.

Although the inhibitors of DOT1L identified in this study are less potent than those reported in the meantime, these compounds provide novel chemical moieties for further development of DOT1L inhibitors. Future work towards improving the potency of these compounds will involve utilizing the novel portions of these molecules in combination with the components of current potent inhibitors to derive new analogues with the prospect of improved potency and pharmacokinetic properties.

Included in the 210 compounds selected for biochemical validation from the nucleoside focused library were several compounds that did not contain an adenosine scaffold. In the initial screening for HMTase inhibition most of these compounds provided no inhibition or very weak inhibition. In order to improve our chances of identifying novel scaffold, we probed even the weak inhibitors for starting scaffolds for future modification. Therefore, we modified our selection criteria to identify compounds that bind to DOT1L. Using this strategy, we screened 68 non-adenosine compounds from the SRI nucleoside focused library using the ligand induced thermal stability shift (ThermoFluor) assay. This resulted in the identification of four classes of compounds

that demonstrate binding to DOT1L by increasing the melting temperature in the ThermoFluor assay (Figure 2.2.7).

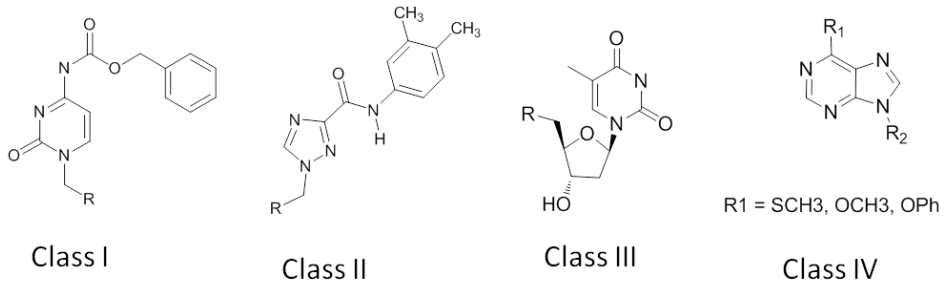

Figure 2.2.7 Chemical structures of SRI non-adenosine compounds identified by ThermoFluor screening.

The most potent compound of class I, SRI-26103, inhibited DOT1L with IC_{50} = 316 µM. (Fig 2.2.8). SRI-26103 demonstrated binding to DOT1L by inducing a dose dependent increase in thermal stability of DOT1L (Figure 2.2.9a). The binding of SI-26103 to DOT1L was also demonstrated by a strong STD NMR signal. Interestingly, the binding of SRI-26103 was not competed off by the presence of 10 fold molar excess of SAH (Figure 2.2.9b). This indicates that SRI-26103 may not bind at the SAM binding site which is contrary to the predicted binding model by which it was identified. SRI-26103 was also shown to bind to DOT1L by OctetRED, demonstrating a Kd = 123 µM (Figure 2.2.9c).

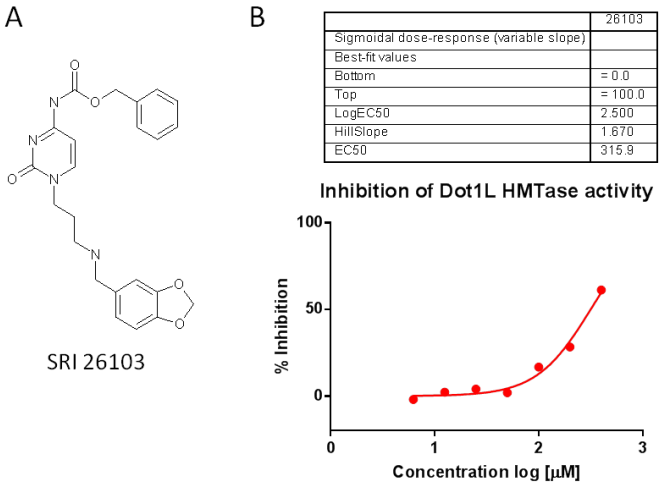

Figure 2.2.8 Non-adenosine DOT1L inhibitor SRI-26103. (a) Chemical structure of SRI-26103. (b) DOT1L *in vitro* inhibition with core histone substrate.

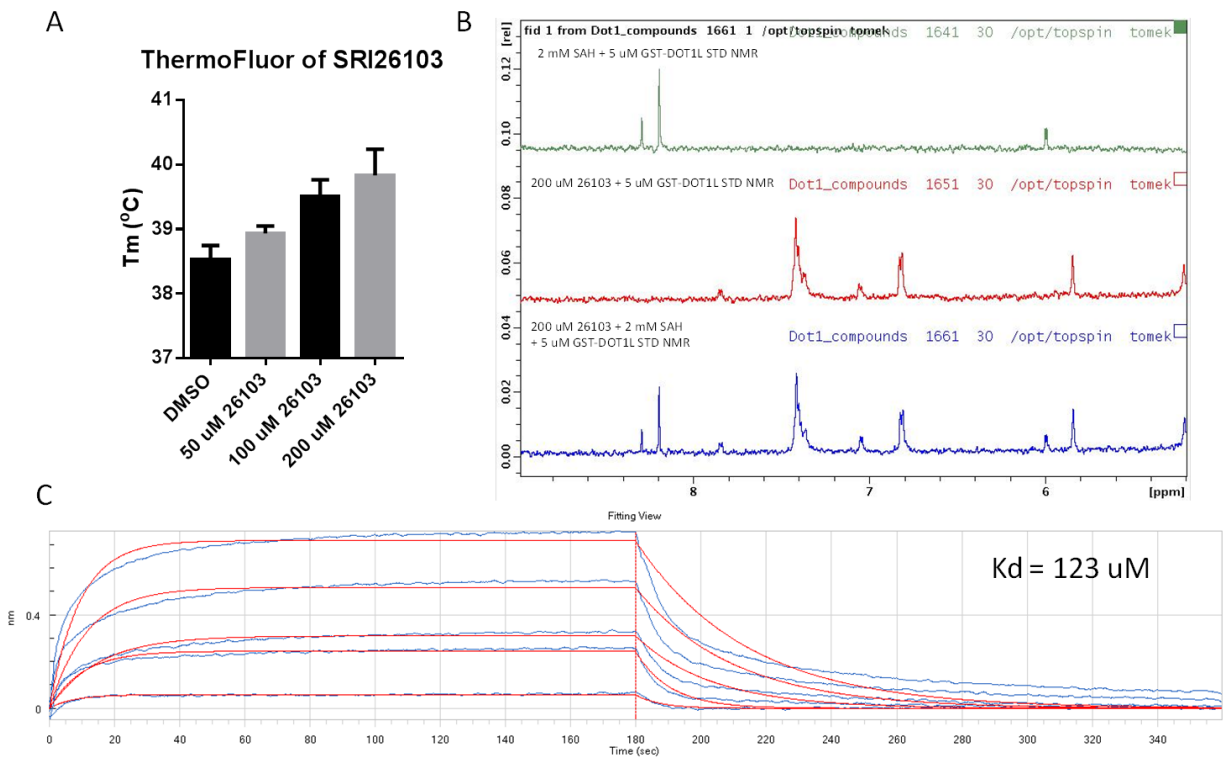

Figure 2.2.9. SRI-26103 binds to DOT1L. (a) ThermoFluor assay (b) STD NMR of 5 µM GST-DOT1L with 2 mM SAH (green/top), 200 uM SRI-26103 (red/middle), or 2 mM SAH and 200 uM SRI-26103 (blue/bottom). (c) OctetRED binding of SRI-26103 to DOT1L.

From SRI inhibitor Class II, the most potent compound SRI-26124 (Figure 2.2.10a) inhibits DOT1L with IC_{50} = 330 µM (Figure 2.2.10b). SRI-26124 provides a 2^{o}C stabilization of DOT1L in the ThermoFluor assay indicating that it binds to DOT1L (Figure 2.2.10c). Class III and class IV compounds failed to demonstrate inhibition of DOT1L HMTase activity *in vitro* despite evidence of binding by ThermoFluor. Due to the weak inhibition of DOT1L with IC_{50} > 300 µM (Figure 2.2.8b and 2.2.10b) non-adenosine compounds class I and II were not pursued as lead compounds.

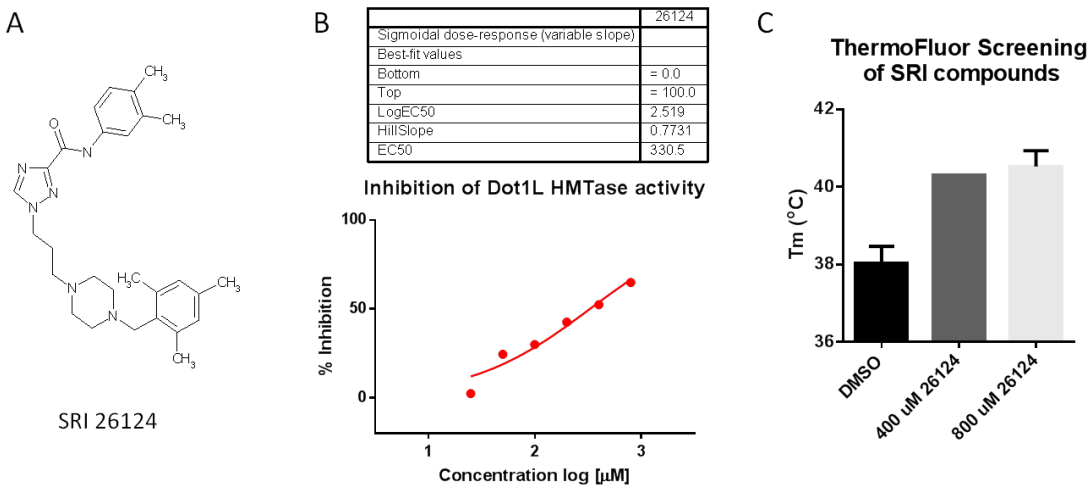

Figure 2.2.10 SRI-26124 inhibits DOT1L HMTase activity and binds to DOT1L. (a) Chemical structure of SRI-26124. (b) DOT1L *in vitro* inhibition with core histone substrate. (c) ThermoFluor assay.

2.2.3 Biochemical screening identification of H3K79 methylation inhibitors

Utilizing the previously described 96-well plate DOT1L HMTase assay, we screened a total of 5,500 compounds from the Diversity Set I and Mechanistic Set compound libraries from the National Cancer Institute (NCI) chemical repository (2,864 compounds), Boston University (1,920 compounds), and University of Southern California (760 compounds). These libraries contain structural diversity to cover a variety of chemical space. We identified 61 compounds that demonstrated dose dependent inhibition of H3K79 methylation in a secondary dose response experiment. Based on the chemical structure and commercial availability of these compounds, 48 hits and analogues were purchased from commercial sources (Figure 2.2.11). Eleven compounds were confirmed as inhibitors of DOT1L H3K79 methylation activity with IC_{50} = 0.85- 28.1 µM, belonging in two distinct chemical classes: naphthosulfonyl class A (Figure 2.2.12) and naphthoquinone class B (Figure 2.2.21).

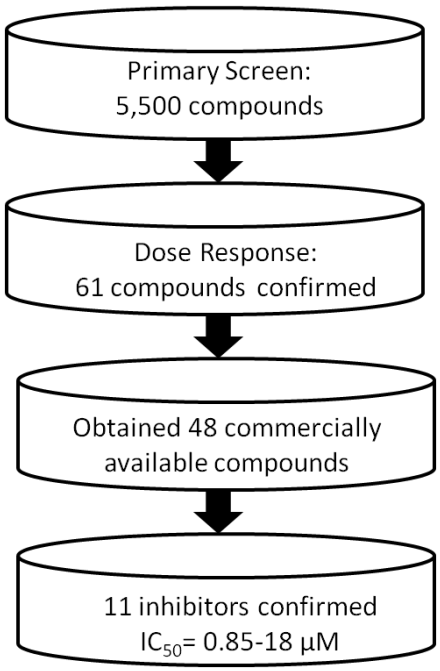

Figure 2.2.11 Schematic of biochemical screening of compound libraries.

Here we present the *in vitro* and cellular characterization of the most potent compound in class A, University of Michigan Disruptor of H3K79 methylation inhibitor-7 (UMD-7). Additionally, UMD-1 was identified as an inactive analog with a comparable chemical scaffold (Figure 2.2.12) and was utilized as a control compound in subsequent experiments. Based on the *in* vitro biochemical activity of UMD-7 and the importance of H3K79 methylation in MLL-translocation leukemias, we sought to investigate the impact that chemical modulation of H3K79 methylation could have on human leukemias. In order to investigate whether UMD-7 could inhibit the growth of human leukemia cells, a panel of leukemia cell lines was treated with UMD-7 and cell viability measured by WST-assay. UMD-7 selectively inhibited the growth of H3K79 methylation dependent cell lines, KOPN-8, MV4-11, THP-1 and U937 with IC_{50} = 3.5 - 9.7 µM. As expected, the cell lines that do not rely on DOT1L, KASUMI-1 and K562, were much less sensitive to UMD-7 and had IC_{50} = 27.2 and 25.6 µM respectively. In addition, UMD-1, a close analog of UMD-7 that does not inhibit DOT1L failed to effect the growth of the most sensitive cell line, KOPN-8 at concentrations up to 100 µM (Figure 2.2.13a). These results demonstrate that UMD-7 treatment leads to selective cell growth inhibition of human leukemia cell lines that contain fusion proteins that require H3K79 methylation to

mediate their leukemogenic properties. Cell growth inhibition is specific to UMD-7 and the analog with low *in vitro* potency, UMD-1, did not have the same effect on KOPN-8 cells demonstrating that cell growth inhibition correlates with H3K79 methylation inhibition potency.

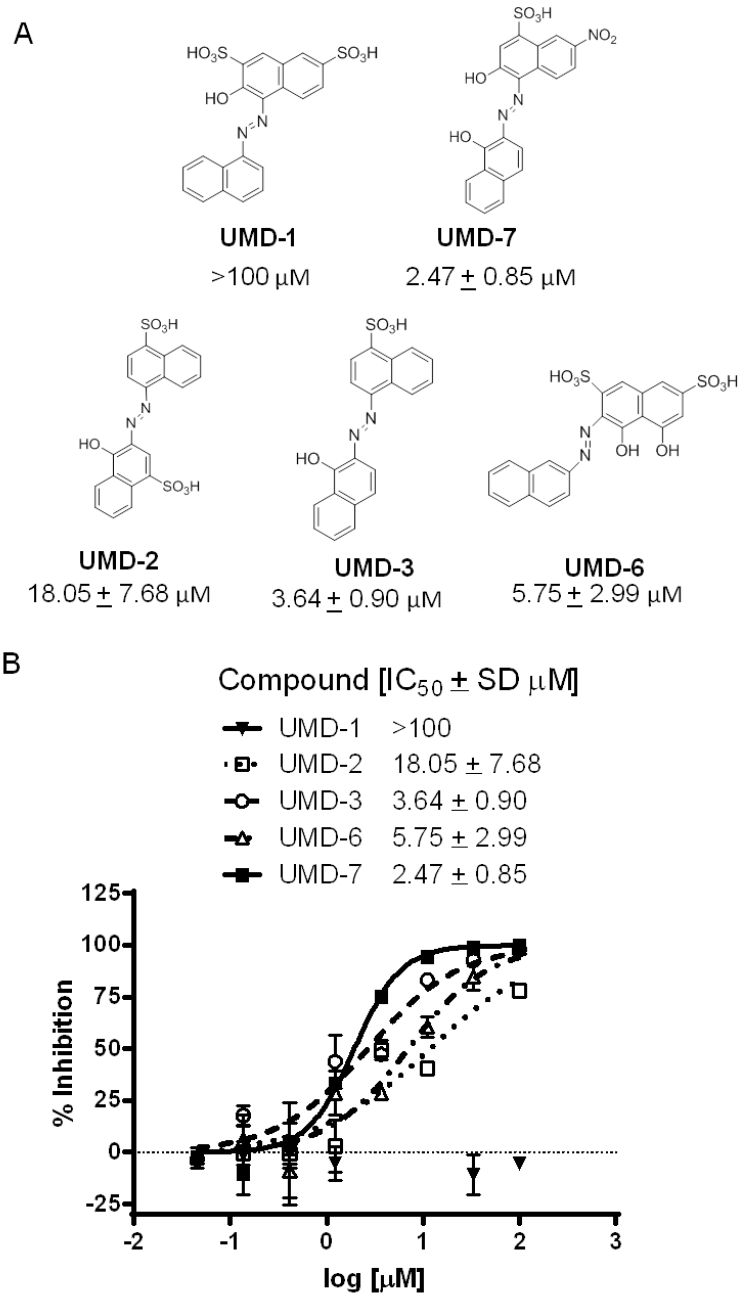

Figure 2.2.12 H3K79 methylation inhibitors identified through biochemical screening. (a) Chemical structures of H3K79 methylation inhibitors. (b) Curves for H3K79 methylation inhibition of identified UMD compounds.

In order to investigate the anti-proliferative effects of UMD-7 on MLL-rearranged cell lines, induction of apoptosis was measured by Annexin V and propidium iodide staining by flow cytometry. In MLL-ENL containing KOPN-8 cells UMD-7 potently induced apoptosis after only 24 hr treatment whereas only a slight increase of Annexin V staining was observed in the AML1-ETO fusion containing Kasumi-1 cell line with UMD-7 at concentrations up to 30 μM (Figure 2.2.13b). To investigate if H3K79 methylation inhibition by UMD-7 recapitulates the effect of genetic knockout of DOT1L on the cell cycle (*16*), DNA content was measured by propidium iodide staining and flow cytometry. UMD-7 treatment of KOPN-8 cells resulted in dose dependent G0/G1 cell cycle arrest which is consistent with genetic loss of DOT1L. This affect was show to be specific to MLL-rearranged cell lines, as no affect on cell cycle was observed in Kasumi-1 or the E2A-HLF containing K562 cells line. Furthermore, the inactive analog UMD-1 also failed to induce any changes in cell cycle in KOPN-8 cells, demonstrating that the effect was specific for UMD-7 inhibition of H3K79 methylation and not a general effect due to the chemical scaffold (Figure 2.2.13c).

To investigate whether UMD-7 inhibition of H3K79 methylation induces differentiation, the monocyte differentiation marker CD11b was analyzed by flow cytometry in the MLL-AF9 fusion protein containing promonocytic THP-1 cell line. Upon treatment with UMD-7, expression of CD11b was induced in a dose dependent manner demonstrating that UMD-7 inhibition of H3K79 methylation induces differentiation (Figure 2.2.13d).

Though the biological effects of UMD-7 on human leukemia cells lines are consistent with genetic loss of DOT1L, we investigated whether these effects were due to inhibition of H3K79 methylation. Core histone extracts were analyzed for histone H3 lysine modifications to determine the effect of UMD-7 on H3K79 methylation as well as determine the selectivity for this lysine methylation in comparison with H3K4, K9, K27, and K36 trimethylation. UMD-7 induced a dose and time dependent reduction in H3K79 mono and trimethylation at 24 and 48 hr. However, H3K79Me2 was reduced at 24 hr but there was no effect observed at 48 hr while mono and trimethyl H3K79 were significantly decreased. UMD-7 displayed selective inhibition of H3K79 methylation with limited affect on other H3 lysine methylation levels (Figure 2.2.14a).

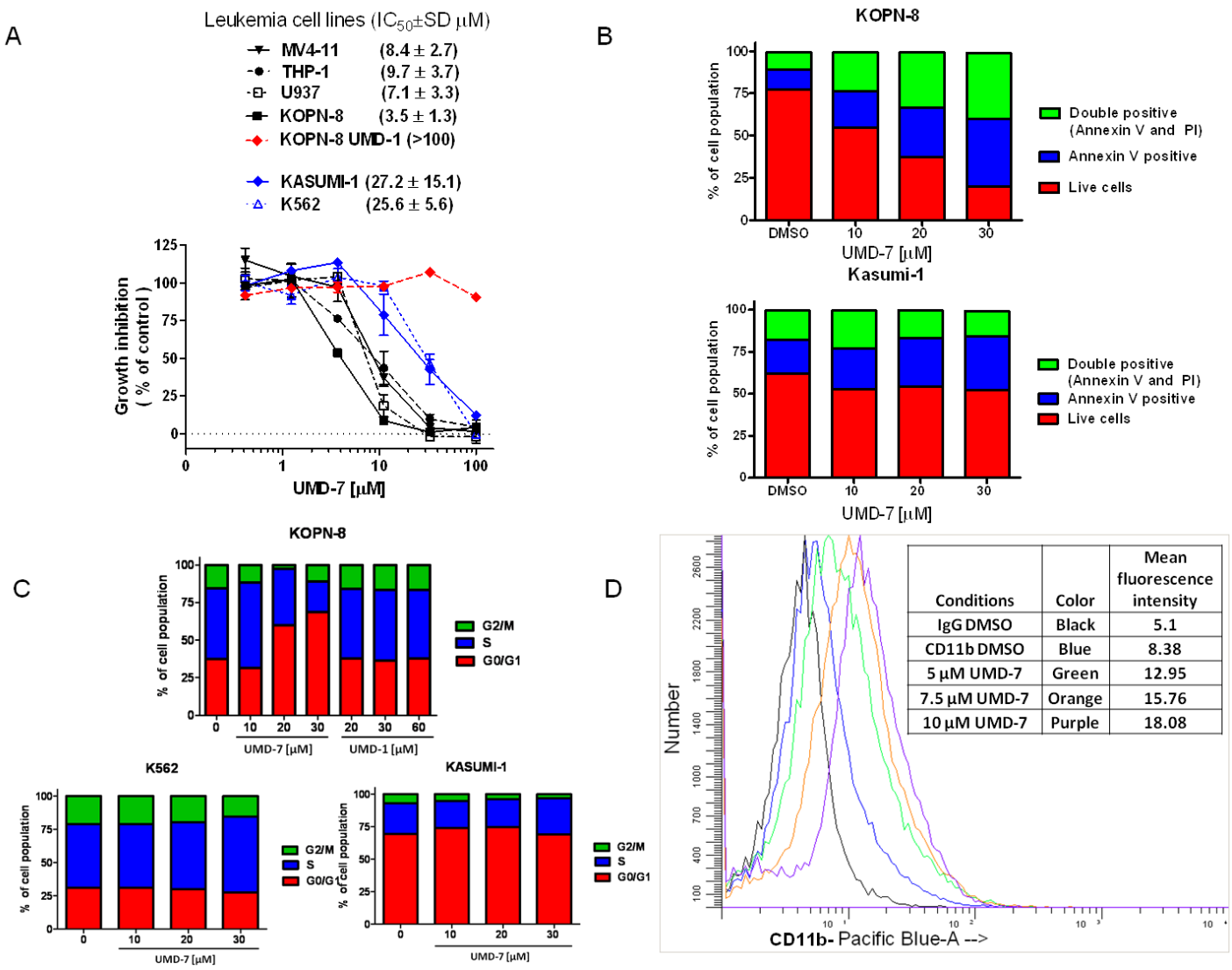

Figure 2.2.13 UMD-7 selectively induces cell growth inhibition by apoptosis, cell cycle arrest and differentiation in MLL-rearranged human leukemia cell lines. (a) Cell growth inhibition of a panel of human leukemia cell lines shows selective inhibition of MLL-rearranged cell lines MV4-11 (MLL-AF4), THP-1 (MLL-AF9), U937 (CALM-AF10), and KOPN-8 (MLL-ENL) compared with non-MLL rearranged leukemia cell lines, KASUMI-1 (E2A-HLF), and K562 (BCR-ABL) measured by WST-assay. (b) Apoptosis induction by UMD-7 treatment in representative cell lines KOPN-8 and KASUMI-1 measured by Annexin V and PI staining. (c) Cell cycle analysis of KOPN-8 cells upon treatment with UMD-7 and the inactive analog UMD-1 and UMD-7 treatment of non-MLL rearranged cell lines KASUMI-1 and K562 measured by PI incorporation. (d) Differentiation induction by UMD-7 treatment of the human acute monocytic leukemia cell line THP-1 monitored by CD11b/Mac-1 cell surface marker expression measured by flow cytometry.

H3K36 trimethylation was also slightly decreased at the highest concentration of 30 μM but not to the same extent as with H3K79 trimethylation which is nearly absent. We next evaluated whether the observed global reduction of H3K79 methylation lead to changes in MLL-target gene expression. *Hoxa9* and *Meis1* are two critical mediators of MLL-fusion mediated leukemogenesis (*22*) and are hypermethylated at H3K79 in MLL-fusion containing leukemias (*23*). Expression of these MLL-fusion target genes were evaluated in KOPN-8 cells by qRT-PCR upon treatment with UMD-7 and a dose dependent decrease of both target genes was observed after only 24 hr treatment (Figure 2.2.14b). Furthermore, this affect was specific to these MLL-target genes as no change was observed in the housekeeping gene β-actin. These results suggest that the cell growth inhibition of human leukemia cell lines induced by UMD-7 is due to selective inhibition of H3K79 methylation and decreased MLL-target gene expression.

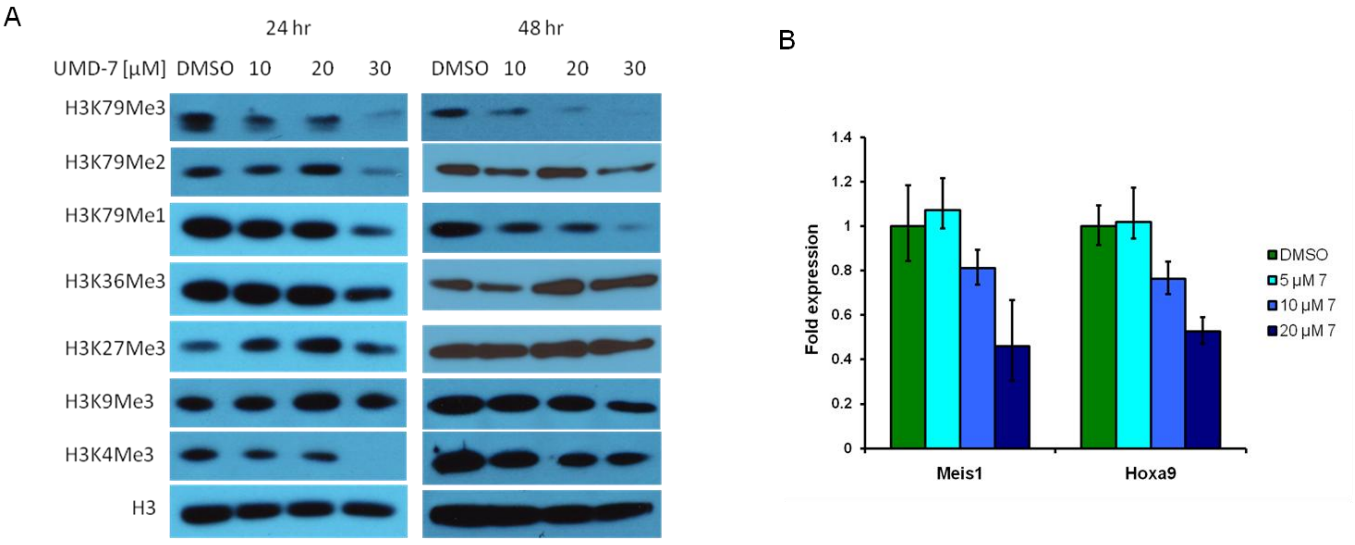

Figure 2.2.14 UMD-7 selectively inhibits H3K79 methylation and downstream MLL-target gene expression in cells. (a) Western blot analysis of H3K79 mono, di, and trimethylation and off target H3 lysine methylation demonstrating selective cellular inhibition by UMD-7 in KOPN-8 cells after 24 and 48 hr treatment. (b) mRNA levels of HoxA9 and Meis1 in KOPN-8 after 24 hr treatment with UMD-7 measured by qRT-PCR, RNA levels normalized to GAPDH.

Due to the variable genetic changes that accumulate in cell lines cultured over long periods of time, we wanted to utilize a clean model system in which a single oncogene is responsible for the leukemic phenotype of cells. Therefore we performed colony forming unit (CFU) assay of murine bone marrow transformed with either MLL-AF9 or

E2A-HLF. Treatment with UMD-7 resulted in a reduction of colony number in MLL-AF9 cells but not E2A-HLF (Figure 2.2.15). This is consistent with genetic studies demonstrating the requirement for DOT1L in MLL-AF9 transformed cells (*16, 24-26*). The selective influence of UMD-7 on MLL-AF9 transformed bone marrow supports a specific mechanism of cell growth inhibition as opposed to a general toxic affect. E2A-HLF cells have been shown to grow in the absence of DOT1L and H3K79 methylation, thus, inhibition of H3K79 methylation with UMD-7 does not affect the growth of E2A-HLF cells to the same extent as MLL-AF9 cells which require H3K79 methylation.

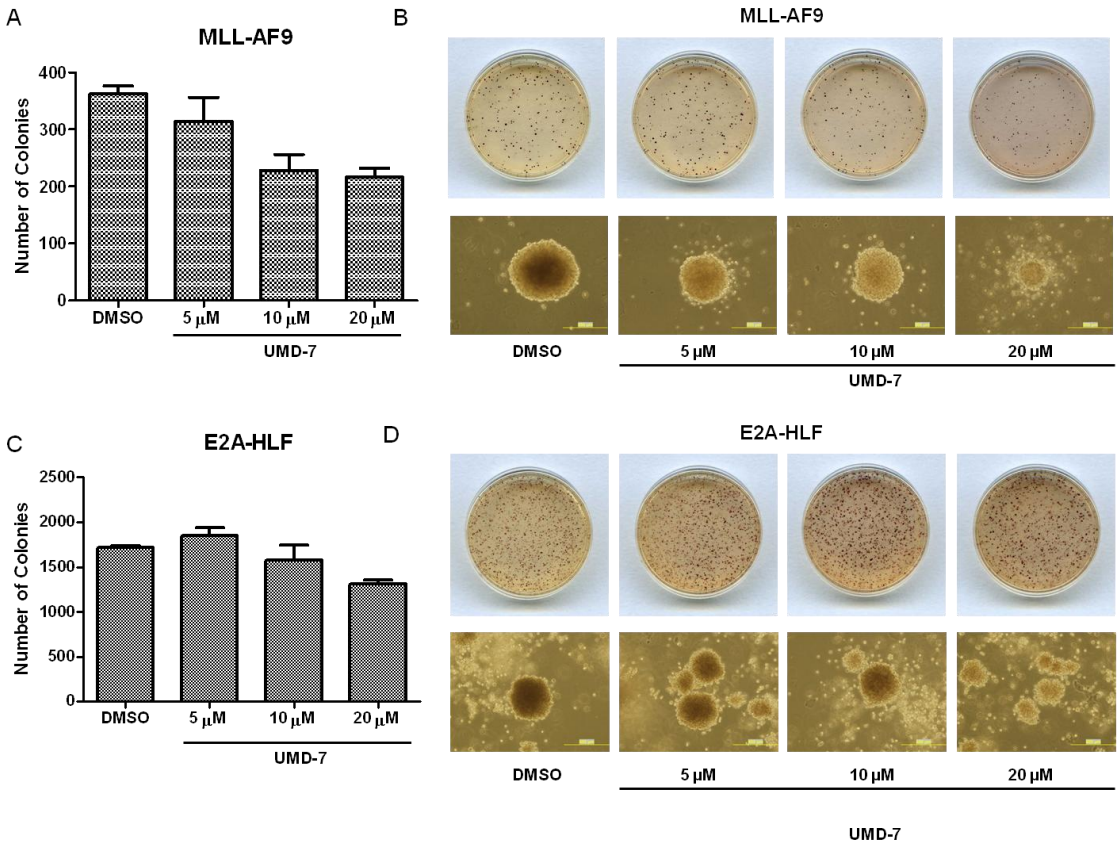

Figure 2.2.15 UMD-7 selectively inhibits colony formation ability of MLL-AF9 transformed murine model cells. (a) The number of colony formation units of MLL-AF9 and (b) the colony morphology and INT staining are shown for MLL-AF9. (c) The number of colony formation units of E2A-HLF and (d) the colony morphology and INT staining are shown for E2A-HLF.

Furthermore, to demonstrate that the cell growth inhibition induced by UMD-7 was selective for MLL-AF9 cells requirement for H3K79 methylation and to test whether UMD-7 showed non-selective toxicity, we tested the colony forming ability of normal

bone marrow cells in the presence of UMD-7. We observed that UMD-7 did not inhibit the ability of normal bone marrow cells to form colonies in methylcellulose soft agar media (Figure 2.2.16). Together, these results demonstrate that UMD-7 has low toxicity and selectively inhibits the cell colony forming capacity of the H3K79 methylation dependent MLL-AF9 oncogene.

In order to assess the mechanism of UMD-7 mediated inhibition of MLL-AF9 murine model cells, the growth of MLL-AF9 and E2A-HLF cells was measured in liquid culture over 7 days. Consistent with the CFU assay, UMD-7 selectively inhibited the growth of MLL-AF9 but not E2A-HLF transformed murine bone marrow in liquid culture (Figure 2.2.17).

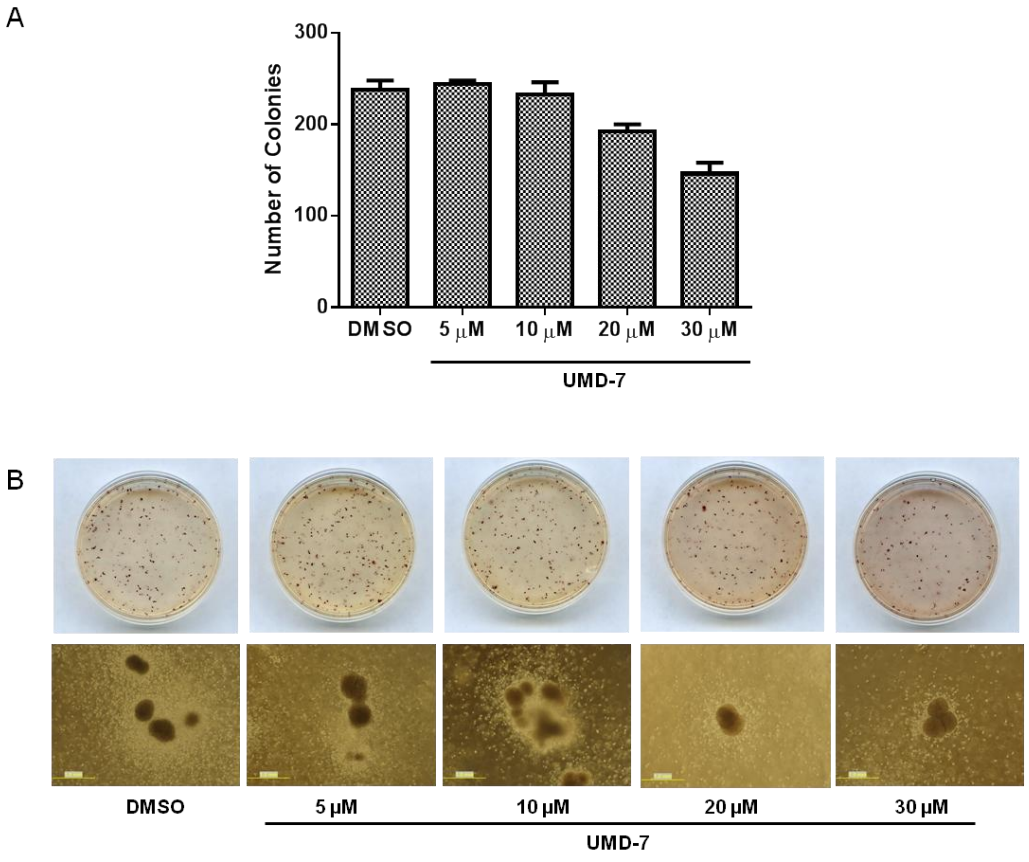

Figure 2.2.16 UMD-7 has low toxicity against normal bone marrow. (a) The number of colony formation units of normal bone marrow cells in methylcellulose media upon treatment with UMD-7. (b) Colony morphology and INT staining for normal bone marrow cells in methylcellulose media with UMD-7 treatment.

Due to the difference in methylation inhibition kinetics in cells, we sought to determine the mechanism of UMD-7 inhibition. This was achieved by measuring the initial velocity of the DOT1L H3K79 HMTase reaction in the presence or absence of UMD-7. Using Michaelis-Menten non-linear regression analysis of DOT1L kinetics, Lineweaver-Burk plots were generated and demonstrate that UMD-7 increases the Km of the reaction with respect to the substrate (Figure 2.2.18a). This is consistent with a compound which interferes with binding of the histones to DOT1L, requiring higher concentrations of substrate to achieve half the maximum reaction velocity as the concentration of the compound is increased. However, UMD-7 does not compete with SAM due to its reduction of the reaction velocity at increasing concentration but showing little affect on the Km with respect to SAM (Figure 2.2.18b). Furthermore, the mechanism of UMD-7 inhibition was investigated by analyzing how UMD-7 inhibition of H3K79 methylation changed in response to variation of the substrate and SAM concentrations (*27*). High concentrations of the substrate overcomes UMD-7 inhibition of H3K79 methylation further demonstrating that UMD-7 affects ability of substrate histones to be methylated until a sufficiently high concentration overcomes these effects (Figure 2.2.18C). Inhibition by UMD-7 is partially, but not completely, abrogated in the presence of high SAM concentrations (Figure 2.2.18D). These findings suggest that UMD-7 is acting through a non-SAM competitive mechanism.

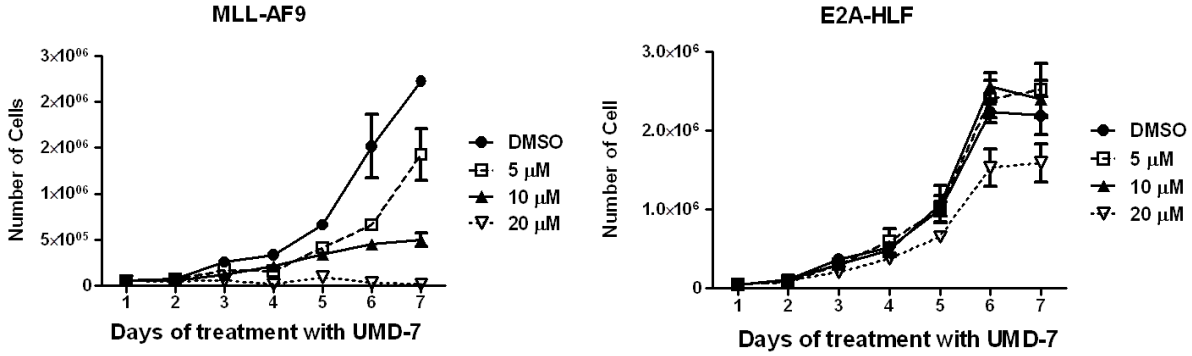

Figure 2.2.17 UMD-7 preferentially inhibits cell growth of DOT1L dependent murine model cell lines. Cell growth curves of DOT1L dependent MLL-AF9 and DOT1L independent E2A-HLF transformed murine model cell lines grown in liquid culture.

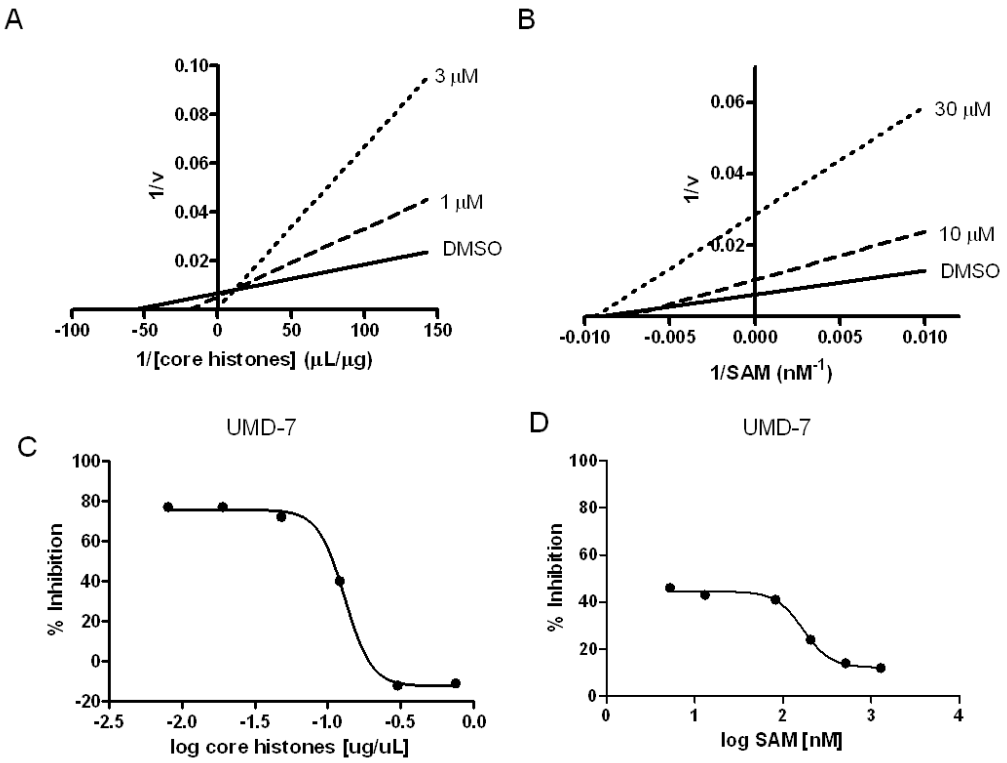

Figure 2.2.18 UMD-7 mechanism of inhibition. (a) Lineweaver-Burk plot of UMD-7 inhibition of DOT1L with respect to substrate core histones. (b) Lineweaver-Burk plot of UMD-7 inhibition of DOT1L with respect to the small molecule cofactor SAM. (c) The percent inhibition of 10 μM UMD-7 with a constant concentration of 125 nM ^{3}H-SAM and varying concentrations of core histones from 0.01 to 0.76 ug/uL. (d) The percent inhibition of 10 μM UMD-7 with a constant concentration of 0.038 ug/uL core histones and varying concentrations of 3H-SAM between 5.2 and 1,280 nM.

Based on the *in vitro* mechanism of UMD-7 H3K79 methylation inhibition and the rapid effect on cellular H3K79 methylation which is inconsistent with other published DOT1L inhibitors, we wondered if UMD-7 is acting by through a different mechanism and directly binding to the substrate histones. In order to address this question, we took advantage of the UV-Vis absorbance of UMD-7 as demonstrated in previous reports of arginine methyltransferase inhibitors that bind to histones (*15*). We first tested whether the *in vitro* substrate core histones affected UMD-7 absorbance and found that core histones indeed caused a dose dependent decrease in UMD-7 absorbance (Figure 2.2.19a). This affect was recapitulated by the presence of recombinant H3 alone (Figure 2.2.19b). To demonstrate this effect was specific, we also titrated H3 into a solution of the inactive compound UMD-1 and showed that H3 had no affect on the absorbance

spectra of UMD-1 (Figure 2.2.19c). In fact each component of the core histones had some affect on the absorbance of UMD-7 at its peak absorbance of 620 nm, however recombinant DOT1L had no affect (Figure 2.2.19d).

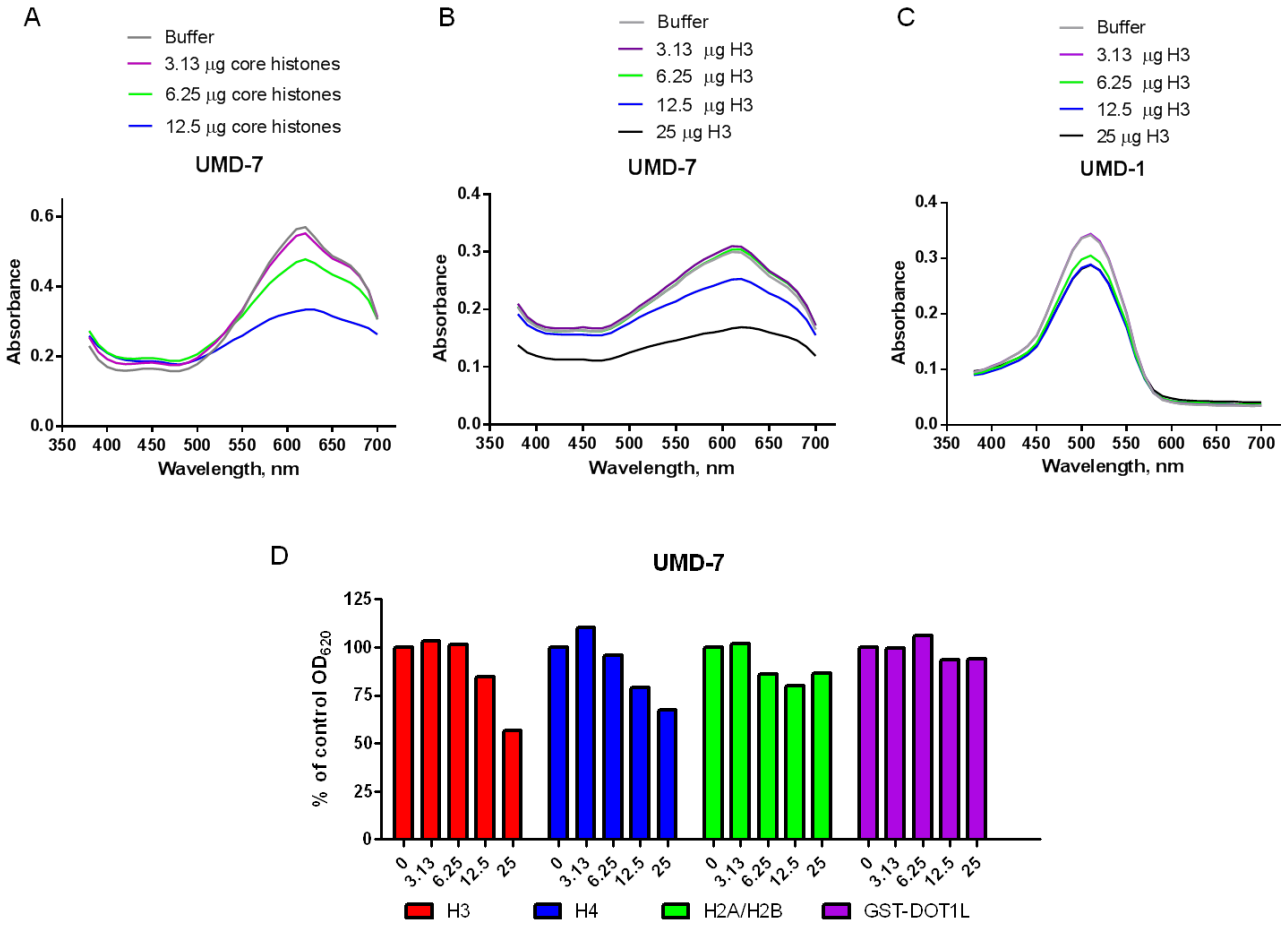

Figure 2.2.19 UMD-7 absorbance is diminished by core histone components but not DOT1L. (a) Absorbance spectra of 100 μM UMD-7 in the presence of core histones. (b) Absorbance spectra of 100 μM UMD-7 in the presence of recombinant H3. (c) Absorbance spectra of 100 μM UMD-1 in the presence of recombinant H3. (d) Quantification of 100 μM UMD-7 absorbance at 620 nm in the presence of recombinant core histone components or GST-DOT1L.

In order to assess whether UMD-7 binds to the portion of H3 around H3K79, we tested whether a peptide mimicking this region, amino acids 61-86, of H3 affected the absorbance of UMD-7. We found that indeed UMD-7 absorbance is affected by peptide portions of H3 and that residues 61-86 had more of an impact on the spectra of UMD-7 than a peptide of the first 20 amino acids of H3 (Figure 2.2.20). These results suggest

that the mechanism of UMD-7 is through binding to the core histones to prevent H3K79 methylation and is not targeting DOT1L directly. These results demonstrate the identification and biological characterization of a novel H3K79 methylation inhibitor, UMD-7. Several napthyl-sulfo compounds were identified as inhibitors of H3K79 methylation through biochemical screening.

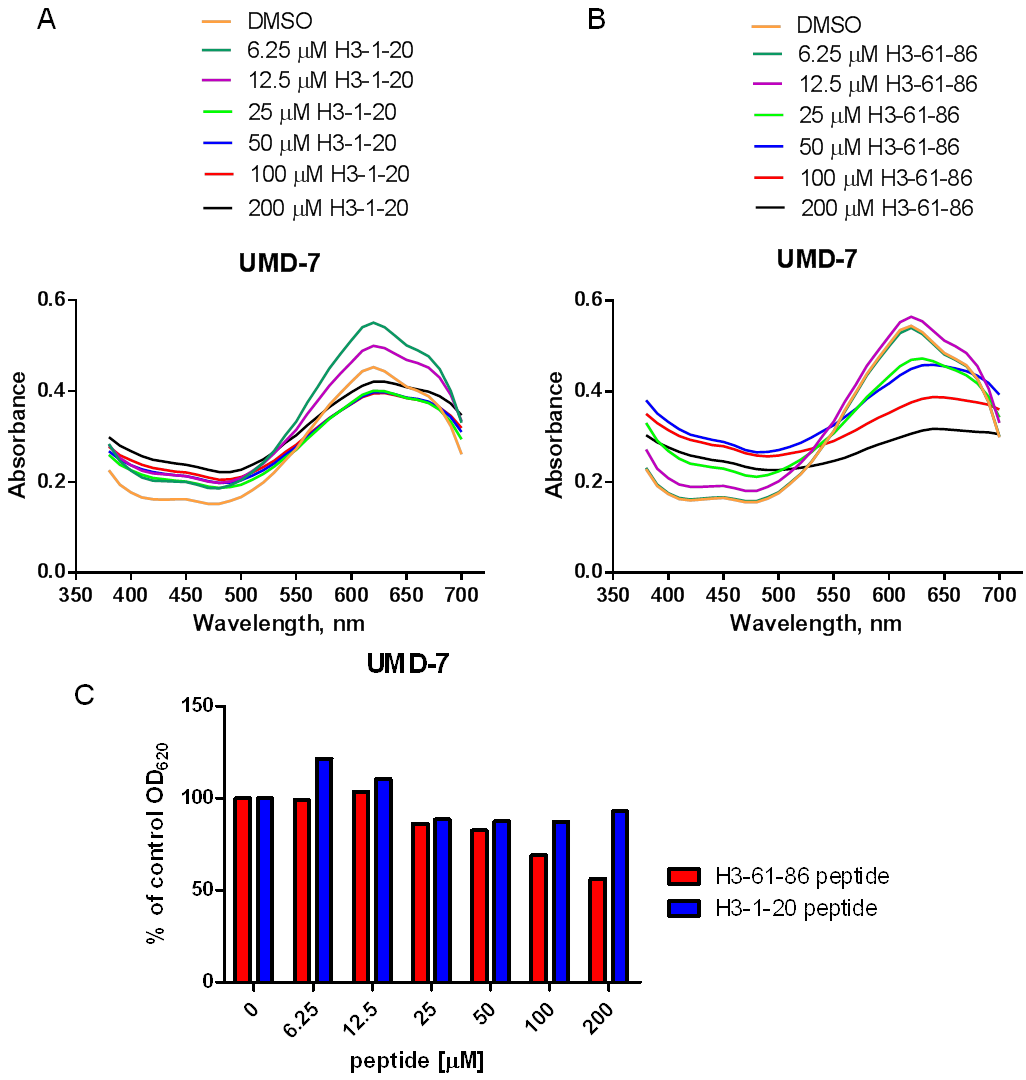

Figure 2.2.20 UMD-7 absorbance is diminished by a peptide mimic of histone H3 amino acids 61-86. (a) Absorbance spectra of 100 μM UMD-7 in the presence of a peptide consisting of the N-terminal tail of H3, amino acids 1-20. (b) Absorbance spectra of 100 μM UMD-7 in the presence of a peptide consisting of the H3 amino acids surrounding H3K79, amino acids 61-86. (c) Quantification of 100 μM UMD-7 absorbance at 620 nm in the presence of either H3 peptide.

Intriguingly, the identified compounds demonstrated substrate competitive kinetics, which is unique from other currently known SAM competitive inhibitors of H3K79 methylation which target the enzyme DOT1L. Our studies indicate that UMD-7 binds to the core histones substrate of DOT1L as opposed to the enzyme in a novel mechanism of H3K79 methylation inhibition. This mechanism is not inherent to the naphyl-sulfo core of the compound, as the inactive compound UMD-1 does not show changes in UV-vis absorbance in the presence of core histones as UMD-7.

Human leukemias with the most common chromosomal translocation of the MLL-gene, require H3K79 methylation for transformation and proliferation. Importantly, UMD-7 inhibits the growth of human leukemia cell lines with MLL-translocations but not the H3K79 methylation independent cell lines with unrelated oncogenes. The inactive analog UMD-1 does not affect the growth of the sensitive cell line KOPN-8 indicating that the mechanism of UMD-7 inhibition is due to H3K79 methylation inhibition. Furthermore, UMD-7 induces apoptosis, cell cycle arrest, and differentiation in leukemia cell lines with MLL-translocations. These results are consistent with genetic abrogation of H3K79 methylation in mouse models of conditional DOT1L deletion and other inhibitors of H3K79 methylation which target the histone methyltransferase activity of DOT1L.

Upon investigation of the mechanism of UMD-7 induced cell growth inhibition of human leukemia cell lines, we demonstrated that this small molecule selectively inhibits H3K79 methylation and has little affect on other histone lysine methylation marks. The inhibition of H3K79 methylation resulted in decreased expression of MLL-target genes *Hoxa9* and *Meis1*. These results are consistent with the mechanism of MLL-translocation mediated transformation of cells. Compared with other H3K79 methylation inhibitors, UMD-7 induces these biological responses rapidly in 24 hours, whereas EPZ004777 requires 4 days for maximal H3K79 methylation inhibition and 6 days for maximal inhibition of MLL-target genes (*28*). It is possible that the difference in targets of the small molecules may be responsible for this difference, EPZ004777 targets the histone methyltransferase DOT1L and UMD-7 binds directly to the substrate core histones. At this time, the reason for differences in time required for H3K79 methylation is not clear,

however, the end results of apoptosis, cell cycle inhibition, and differentiation are consistent.

In addition to the evidence for specific inhibition of H3K79 methylation provided by the analog compound UMD-1 and investigation of effects on a broad range of lysine methylation, murine model cell lines were used to further investigate the specificity of the biological effects of UMD-7. Selective growth inhibition of the MLL-AF9 transformed murine cell line, which requires H3K79 methylation, compared with the H3K79 methylation independent E2A-HLF cell line supports a targeted mechanism for UMD-7. We demonstrate that UMD-7 disrupts H3K79 methylation at MLL-target genes and which are required for the MLL-translocation mechanism of cellular transformation. UMD-7 shows low toxicity against normal bone marrow cells and further demonstrates that UMD-7 is to inhibit cell growth through specific targeting of H3K79 methylation and is not acting through a non-specific toxicity.

Together, these results demonstrate that inhibition of H3K79 methylation with the small molecule UMD-7 through a novel histone binding mechanism is specific and recapitulates the biological effects of genetic and chemical targeting of DOT1L. UMD-7 provides a novel chemical scaffold for inhibition of H3K79 methylation with rapid inhibition of H3K79 methylation in cells. Further studies may elucidate how and where UMD-7 binds to histones which may provide insight into the differences in timing observed for histone targeting H3K79 methylation inhibition compared with DOT1L targeted inhibition. Therefore UMD-7 provides a novel chemical scaffold and mechanism for H3K79 methylation inhibition and has promising utility as a chemical tool to further probe the biological role of H3K79 methylation.

Next, we characterized the naphthoquinone class B (DFC) compounds. We identified seven active inhibitors in class B with IC_{50} = 0.85 – 28 μM (Fig 2.2.21). Six of the compounds had similar potency of less than 7 μM, these compounds can be further subdivided into classes of acetyl or keto-phenyl substituted. These two groups display similar initial SAR with para substitution being most potent followed by meta and ortho respectively. However there is not a large difference in potency even between the most potent para substituted and the less potent ortho susbstituted. Both acetyl and keto-

phenyl substituted classes display a similar range of potency without much difference depending upon the substituent. However the one compound DFC 234 which was less potent, having IC_{50} = 28 µM, is structurally distinct and has an additional fused ring which is clearly less favorable. We then characterized the most potent representative compounds of each DFC sub-class, DFC 231 and DFC 242.

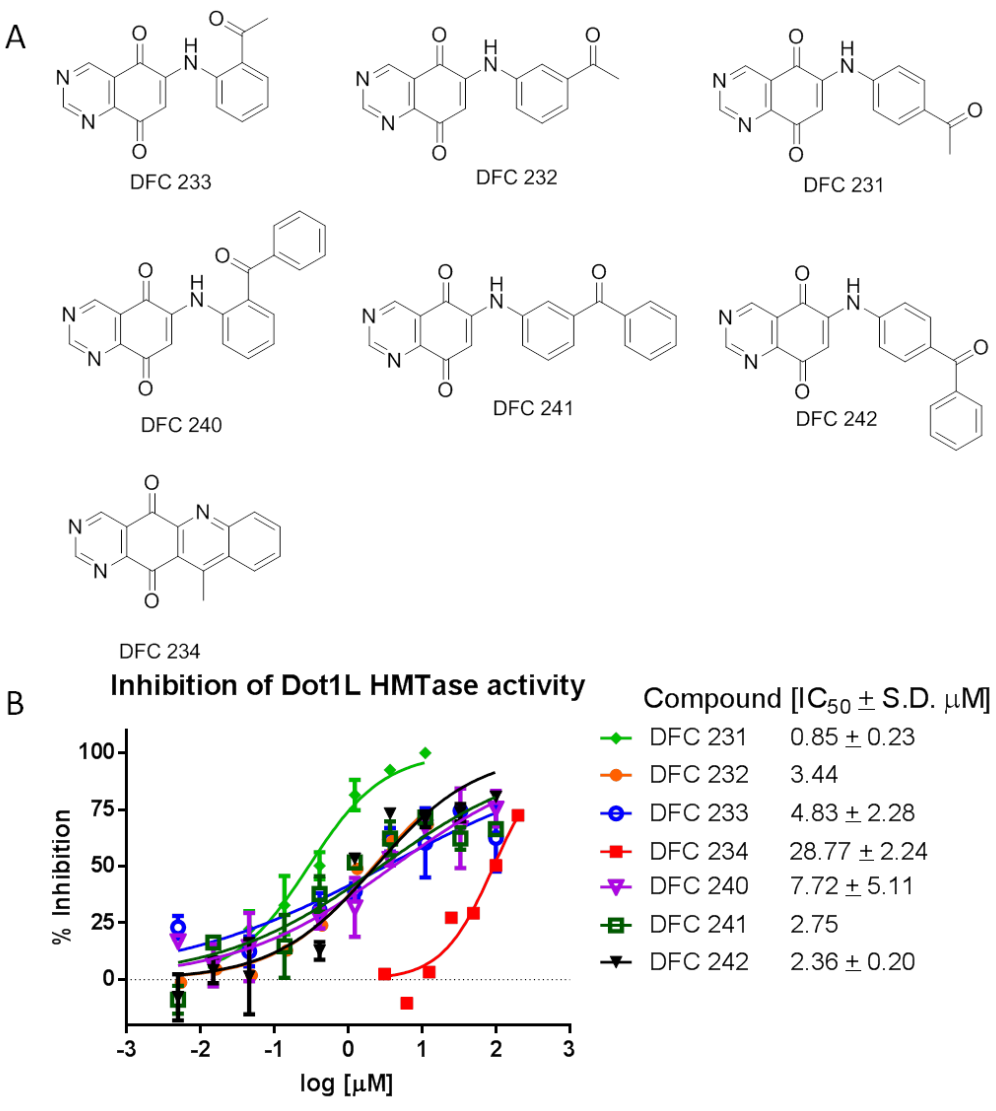

Figure 2.2.21 DFC class of DOT1L inhibitors. (a) Chemical structures of DFC compounds (b) Inhibition curves of DOT1L in an *in vitro* DOT1L HMTase activity assay.

In order to characterize the mechanism of action of these compounds, we used a traditional enzymatic kinetics approach. The initial velocity of the DOT1L HMTase reaction was measured at varying concentrations of substrate with saturating SAM

concentrations or varying concentrations of SAM at saturating substrate concentrations in the presence or absence of the DFC compounds. DFC 231and DFC 242 behaved very similarly in the characterization of their mechanisms of action. They displayed non-competitive kinetics with SAM (Fig 2.2.22a and c) by decreasing the Vmax of the reaction while not affecting the Km. DFC 231 and DFC 242 displayed substrate competitive/mixed mechanism kinetics with the substrate core histones. The Km of the reaction was increased in each case, suggesting a substrate competitive mechanism (Figure 2.2.22 b and d). However the Vmax of the reaction was not unaffected as would be expected for a purely competitive inhibitor. The Vmax of DOT1L with respect to core histones was decreased in the presence of DFC compounds demonstrating that the mechanism of DFC compounds was not strictly competitive with substrate core histones and was more likely a mixed mechanism.

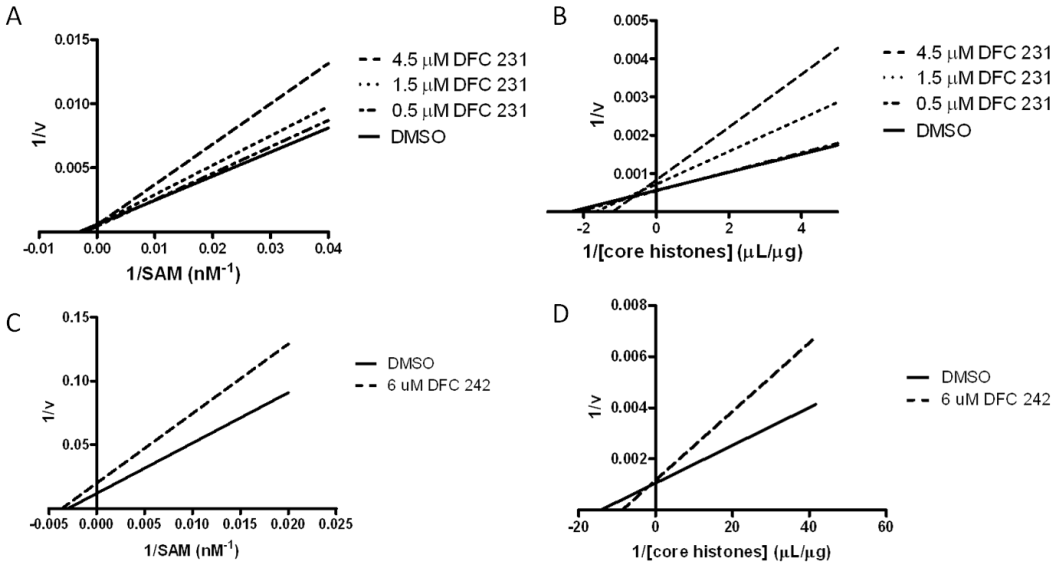

Figure 2.2.22 Mechanism of action of DFC compounds. (a) DFC 231 mechanism of action with respect to SAM and (b) substrate. (c) DFC 242 mechanism of action with respect to SAM and (d) substrate.

We next characterized the effect of DFC compounds in cells to determine if they are capable of inhibiting DOT1L in cells. Therefore we treated the human leukemia cell line, KOPN-8, bearing the MLL-ENL translocation with DFC231, 242, and 234 for 4 days and measured the IC_{50} of cell growth inhibition. We observed that the potency of cell growth inhibition in KOPN-8 cells by DFC compounds followed the same trend as inhibition of DOT1L *in vitro* (Figure 2.2.23a). However the concentrations that were effective at inhibiting the growth of KOPN-8 cells were less than the concentrations required for *in vitro* IC_{50}. We assessed whether the compounds were effectively inhibiting DOT1L in cells by measuring H3K79 methylation and saw that indeed DFC 242 inhibited H3K79 dimethylation whereas the less effective DFC 234 compound did not effectively inhibit H3K79 methylation (Figure 2.2.23b).

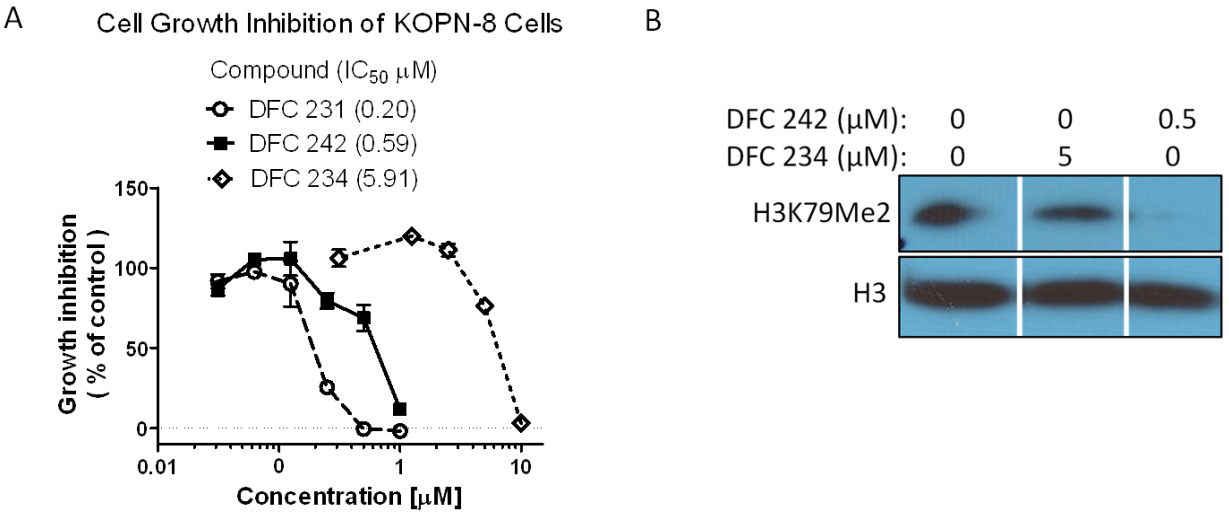

Figure 2.2.23 DFC compound inhibition of human leukemia cell line growth correlates with in vitro DOT1L HMTase activity. (a) Cell growth inhibition of KOPN-8 cells, MLL-ENL translocation bearing human leukemia cell line, measured by WST-assay after 4 days treatment with compounds. (b) Western blot analysis of H3K79 methylation in KOPN-8 cells after 4 days treatment with compounds.

Due to the nature of immortalized human cell lines grown in cell culture long term and likelihood of developing secondary mutations and multiple pathway dysregulation, we utilized a genetically clean murine model system. Murine bone marrow cells were transformed with either MLL-AF9 of E2A-HLF and selected for transformation by growth

in liquid culture for several weeks. The transformed cell lines are useful models because the MLL-AF9 cell line is dependent on DOT1L and H3K79 methylation for continued growth whereas E2A-HLF transformed cells do not depend on DOT1L for continued growth. Therefore, these cell lines are useful to determine the selectivity between generally toxic effects of compounds and the specific effects of DOT1L inhibition.

Both cell lines were treated with DFC compounds and cell growth measured over time. Similar to in human leukemia cells, we observed that DFC 231 is more potent at inhibiting cell growth than DFC 242, consistent with the *in vitro* DOT1L inhibition potency of the respective compounds (Figure 2.2.24a and c). When comparing between cell lines, DFC 231 and DFC 242 displayed similar behavior, both inhibit MLL-AF9 (Figure 2.2.24a and c) selectively while not effecting the growth of E2A-HLF (Figure 2.2.284 and d). At 1 µM DFC 231 affects can be seen on E2A-HLF cell growth and it is reasonable that most compounds will have a limited range of concentrations at which it will display selectivity before demonstrating general toxicity. At 0.5 and 0.25 µM DFC 231 clearly inhibits the growth of MLL-AF9 while not affecting the growth of E2A-HLF cells (Figure 2.2.24a and b). DFC 242 demonstrates this same behavior with 0.5 and 1 µM treatment (Figure 2.2.24c and d). Furthermore, we demonstrated that DFC 242 inhibited H3K79 methylation in a time dependent manner over the time course of the growth experiment (Figure 2.2.24e). These results demonstrate the DFC compounds induce cell growth inhibition of murine model cell lines in a DOT1L dependent manner. The selective inhibition of MLL-AF9 over E2A-HLF and the reduction of cellular H3K79 methylation strongly support that the mechanism of inhibiting cellular proliferation is based upon inhibition of DOT1L HMTase activity.

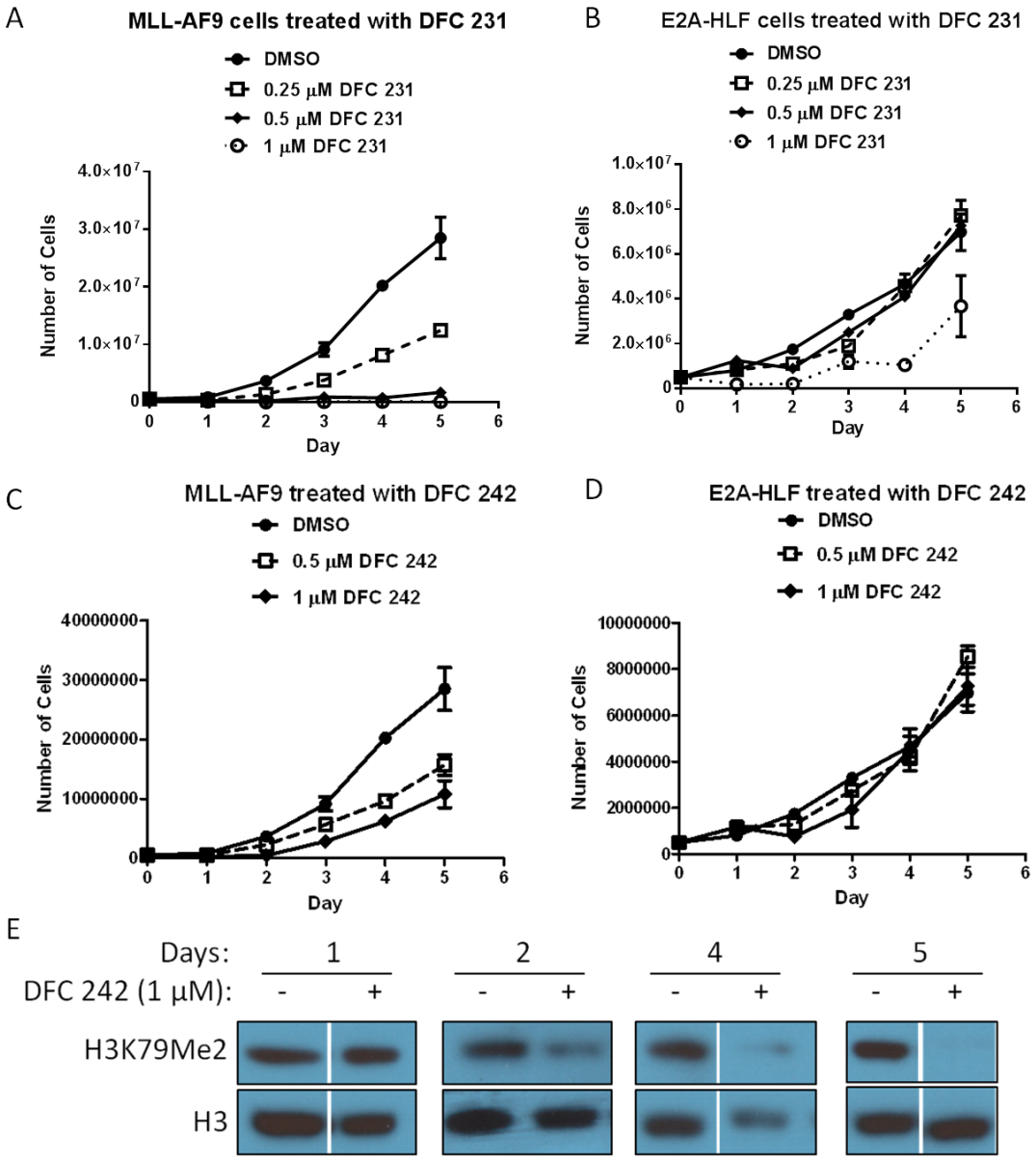

Figure 2.2.24 DFC compounds selectively inhibit the cell growth of murine models cell lines by inhibiting H3K79 methylation. (a) Cell growth of DFC 231 treated MLL-AF9 transformed cells. (b) Cell growth of DFC 231 treated E2A-HLF transformed cells. (c) Cell growth of DFC 242 treated MLL-AF9 transformed cells. (d) Cell growth of DFC 242 treated E2A-HLF transformed cells. (e) Western blot analysis of H3K79 methylation in MLL-AF9 cells upon treatment with DFC 242.

We next investigated whether DFC compounds bind directly to DOT1L using ThermoFluor and STD NMR. DFC 231 and 242 demonstrated binding to DOT1L by inducing a decrease in the thermal stability of the protein upon binding (Figure 2.2.25). Furthermore, STD NMR demonstrated a saturation transfer from DOT1L to DFC 231 indicating direct binding of the compound to DOT1L (Figure 2.2.25b). However, based on the inhibition of cellular proliferation at concentrations below the *in vitro* IC_{50}, our concerns for non-specific toxicity of these compounds outweighed the demonstration of DOT1L binding. Therefore we ceased further characterization of the DFC compounds in order to identify more promising hits for potential lead development.

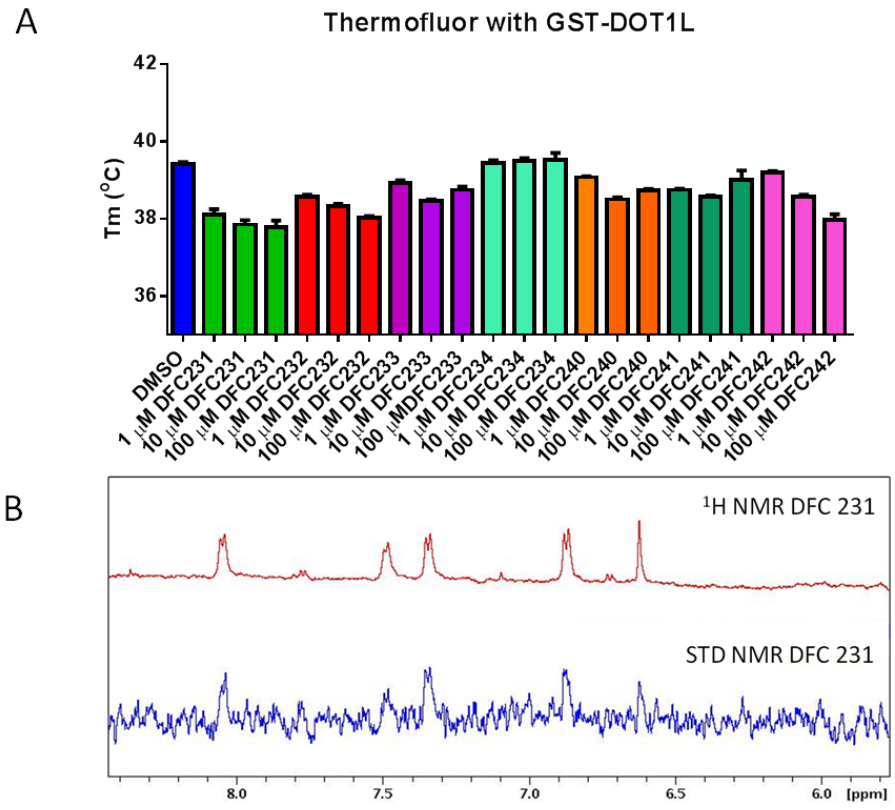

Figure 2.2.25 DFC compound binding to DOT1L. (a) ThermoFluor binding of DFC compounds to DOT1L. (b) 1H-NMR of 100 µM DFC 231 with 5 µM GST-DOT1L (red/top) and STD-NMR of 100 µM DFC 231 with 5 µM GST-DOT1L (blue/bottom).

2.3 Methods

2.3.1 Molecular modeling

The 1200 chemical structures of the focused library used in this study was downloaded in sdf format from the Substance database of the PubChem,(*29*) maintained by the NIH of the US government. These compounds were converted to 3D structures using the program of LigPrep 2.5. All parameters were set to the default values except that the "Ionization" was set to "Epik". The DOT1L:SAM complex (PDB ID: 1NW3) was downloaded from the website of PDB. Hydrogen atoms were added, and the complex was energy-minimized using the OPLS-AA 2005 force field within the Protein Preparation Wizard of Schrödinger.

To get a reasonable binding pose of EPZ004777 to the target of DOT1L, a molecule which is derived from EPZ00477 but does not have the tert-butylphenyl group was docked first into the active site of 1NW3. The tert-butylphenyl group was then manually built into the docked molecule. The artificial DOT1L:EPZ004777 complex was soaked in a box of TIP3P water molecules with a margin of 10 Å along each dimension. An appropriate number of counterions were added to neutralize the whole system. The gotten system was then minimized at three rounds, each of which consisted of 1000 steps, with harmonic constraints on all non-hydrogen atoms by employing the AMBER (version 11.0) program. The force constant was set to 100, 10 and 0 kcal/(mol*$Å^2$) respectively. The molecular dynamic simulation was started by heating the entire system from 0 to 300 *K* in 100 *ps* and equilibrating at 300 *K* for another 100 *ps*. A subsequent 2 *ns* production run was performed under a constant temperature of 300 *K* and a constant pressure of 1 *atm*. No other constraint was applied to either the protein or the ligand during the entire MD simulation. The final snapshot of DOT1L:EPZ004777 complex produced from the molecular dynamic was minimized again and then used in the virtual screening.

The compounds of the library were docked and scored using Glide 5.7 in standard precision (SP) and extra precision (XP) modes. The receptor grids were prepared with a 20 Å side length with the centroids in the centers of SAM (1NW3) and EPZ004777

(simulated DOT1L:EPZ004777 complex) respectively. All Glide options were kept at default settings except that for Glide SP, at most 1 pose per ligand was written out; for Glide XP, at most 5 poses per ligand was written out for analysis.

2.3.2 Expression and purification of recombinant DOT1L

The catalytic domain of DOT1L (1-416) was cloned into a pMCSG vector with an N-terminal His_6 –GST tag. Transformation of His-TEV-hDot1L 1-416 aa in pET28-MHL (Kanamycin resistance) vector into BL21*RIL (Chloramphenecol resistance) cells was carried out by thawing bacterial cells stocks from -80 C on ice. Pipette 50 uL of cell stock with a sterile tip to an autoclaved 1.5 mL microcentrifuge tube. Add 1 uL of plasmid DNA to cells and incubate on ice 30 min. Heat shock cells by incubating in 42° C water bath for 1 min followed by incubation on ice 2 min. Add the mixture to a warm LB-Kanamycin (50 ug/mL, antibiotic depends on resistance imparted by individual plasmid) plate and spread evenly with a sterilized tool. Allow it to sit 5 min at RT to absorb excess liquid. Alternatively, streak a small amount of transformed cells in glycerol stock on a warm LB-Kan plate with a sterile pipette tip. Incubate the plate upside down at 37°C for 12-16 hr. For growth and expression of protein in a 500 mL culture, use a sterile inoculation loop (or pipette tip), pick single colonies from the LB-Kan agar plate to inoculate five separate 4 ml cultures of LB + Kan (50 ug/mL) + Chloramphenocol (34 ug/mL) in 14 ml culture tubes and grow at 37^{o}C with shaking until cloudy (3.5 hr). Collect the 5 x 4 mL cultures by pipette and add to 500 mL autoclaved Terrific broth (TB) with Kan+Chlor added once cooled in a 2 L flask. Incubate with shaking at 37°C for about 3.5 hours until OD_{600nm} = 0.6-0.8 using TB as a reference to blank the spectrometer at 600 nm. Transfer to 20°C shaker and allow to cool for 15-20 min. Induce protein expression with 200 µM IPTG (100µL of 1M stock to 500 ml). Grow at 20°C with shaking overnight (~18hr). For purification of expressed protein, pour cells into large centrifuge jars and spin for 15 min x 6000rpm, pour off supernatant and keep the pellet on ice. Alternatively, store at -80°C and thaw on ice and skip the freeze thaw step. Freeze cells thoroughly in dry ice and ethanol and thaw in cold water. Mash the pellet around the sides of the centrifuge jar and resuspend in 40 ml Lysis Buffer **(**50 mM sodium phosphate dibasic pH 8.0, 500 mM NaCl, 1 mM PMSF, 5% Glycerol, 10 mM

Imidazole, 10 mM β-mercaptoethanol, 0.1% Triton X-100) with pipetting up and down until homogeneous. Transfer cell suspension to metal sonication cup and keep on ice. Sonicate 30 sec x 6 (on 30 sec/off 30 sec, constantly @ output 5) in cold room and keep on ice between cycles. Centrifuged at 10,000 xg for 20 min, 4^{o}C. Suspend 2 mL of Ni-NTA agarose beads per 500 mL culture (50% slurry in ethanol) in 30 mL PBS and shake on ice 5 min. Spin beads at 1500 rpm 7 min with centrifuge deceleration = 2 and aspirate off wash leaving beads. Add cleared cell lysate (supernatant from sonicated cell lysate after centrifugation) to Ni-NTA beads and rotate 1hr at 4^{o}C. Spin the beads 1500 rpm 7 min with centrifuge deceleration = 2 and pipette off supernatant keeping some for SDS-PAGE. Add 30mL wash buffer (50 mM sodium phosphate dibasic pH 8.0, 500 mM NaCl, 5% Glycerol, 25 mM Imidazole, 10 mM β-mercaptoethanol, 0.1% Triton X-100) to the beads, and rotate until beads are resuspended. Spin the beads 1500 rpm 7 min with centrifuge deceleration = 2 and pipette off supernatant keeping some for SDS-PAGE. Gently resuspend beads in 8 mL wash buffer with a Pasteur pipette and add to poly-prep column (BioRad) allowing the wash to flow through (collect some for SDS-PAGE). Wash the column by filling the column reservoir above the Ni-NTA packing with wash buffer and allow it to flow through. Once all the wash buffer has drained to the level of the Ni-NTA beads, add 7 mL of elution buffer **(**50 mM sodium phosphate dibasic pH 8.0, 500 mM NaCl, 5% Glycerol, 150 mM Imidazole, 10 mM β-mercaptoethanol, 0.1% Triton X-100) containing 150 mM imidazole to elute His-Dot1L (collect this 7 mL separate from wash). Dilute 20 uL of each sample with 20 uL of 2X SDS-sample buffer and boil for 10 min at 95^{o}C. Load 20 uL of sample on a 4-20% Tris-Glycine gel and run at 120V 2hr. Stain the gel with Coomassie blue and combine fractions containing product. Determine the concentration with Bradford protein assay with a BSA standard curve. Collect the elution fraction containing Dot1 and concentrate for FPLC, storage, or TEV cleavage.

At this stage in the purification, DOT1L likely has DNA bound and can be checked by measuring the absorbance spectra and if the absorbance at 260 nm is greater than 280 nm there is substantial DNA present. If no further purification is required then dialyze against 1L storage buffer **(**25 mM Tris pH 7.5, 100 mM NaCl, 3 mM DTT) in 10,000 MWCO tubing that has been wet and washed, change out buffer 2 times and leave for 3

hr for each change. Centrifuge the protein 5,000 RPM , 10 min to remove any precipitate. Determine the protein concentration by OD280 and extinction coefficient and/or Bradford method. Add glycerol to 20% and aliquot to microcentrifuge tubes and store at -80^{o}C.

If further purification and removal of DNA is required then concentrate protein to a volume of 4.5 mL using the centrifuge concentrator and load on S200 column with 20 mM Tris pH 8.0, 200 mM NaCl, 1 mM EDTA, 1 mM DTT (*7*). DOT1L elutes in the void volume due to aggregation with DNA (later peak around expected MW is DOT1L that did not bind to DNA and is inactive fraction, keep some and test it). Concentrate void fractions collected from S200 and load on to cation exchange column (SP sepharose) and run a salt gradient of 0 mM to 1,000 mM NaCl. Cleaved DOT1L elutes with at a conductivity of 60-70 mS. Run DOT1L fraction on S200 column in 20 mM Tris pH 8.0, 200 mM NaCl, 1 mM EDTA, 1 mM DTT. Or dialyze against 1L buffer with 3 exchanges overnight. Analyze fractions collected by SDS-PAGE and coomassie blue staining. Pool pure fractions and concentrate to around 1 mg/mL, centrifuge the protein 5,000 RPM 10 min to remove any precipitate and measure the concentration by OD280 and extinction coefficient and/or Bradford method. Add glycerol to 20% and aliquot to microcentrifuge tubes and store at -80^{o}C.

2.3.3 In vitro DOT1L histone methyltransferase assay

Enzymatic activity of DOT1L was assessed by incubating 125 nM of recombinantly expressed and purified GST-DOT1L in the presence of 125 nM (0.28 µCi) ^{3}H-S-adenosyl methionine (NET155250UC; Perkin Elmer), and 1 µg of core histones (Sigma-Aldrich) or 0.7 µg of recombinant nucleosomes in HMTase buffer (20 mM Tris pH 7.9, 4 mM EDTA, 1 mM DTT, 0.01% Triton X-100) at a final volume of 26.5 µL. For determination of inhibitor potency, compounds were added to the reaction mixture prior to initiation of the HMTase reaction with ^{3}H-SAM. The HMTase reaction was allowed to proceed for 1 hr at room temperature and was stopped by transferring 5 µL of reaction mixture to P81 filter paper. After drying, filter papers were washed three times with 50 mM $NaHCO_3$ pH 9.0. Filter papers were then dried and radioactivity measured in vials with 10 mL liquid scintillation fluid on a Tri-Carb 2800 TR liquid scintillation counter

(Perkin Elmer). IC_{50} values of compounds were determined by non-linear regression analysis of the plotted CPM values or percent inhibition values transformed according to DMSO control being 0% inhibition and no DOT1L protein control being 100 % inhibition using Graphpad Prism 6.0 software.

2.3.4 96-well plate in vitro DOT1L histone methyltransferase assay

To prepare the Millipore MultiScreen plates (Cat. No. MSHVN4B50) pre-wet the plate filters with addition of 50 uL of HMTase buffer (20 mM Tris pH 7.9, 4 mM EDTA, 1 mM DTT, 0.01% Triton X-100) to each well of the plate. Vacuum filter out buffer briefly to wet filters until buffer is removed (*do not* pull air through filter until filters are dry again).Blot excess droplets from bottom of filter on paper towel. To prepare the HMTase reaction in plate, add 20 uL of HMTase buffer to wells of pre-wet plate, add 5 uL of GST-DOT1L and core histone mixture to the plate (0.6625 uM GST-DOT1L for a final concentration of 125 nM and 0.2 ug/ul of core histones for a final amount of 1 ug/reaction), add 0.5 uL of compound or DMSO, add 1 uL of 0.28 uCi/uL 3H-S-adenosylmethionine (NET155250UC; Perkin Elmer; two-fold dilution from stock solution with HMTase buffer). Tap the plate gently to mix, cover with the plate cover and incubate at room temperature for 1 hr. To quench the reaction add 27 uL ice cold 50% TCA bringing the final concentration up to 25-30% TCA to precipitate the proteins. Equilibrate at 4^{o}C for 30 min-1 hr. Place the plate on the vacuum manifold. Remove the cover and apply vacuum (4-8 ” Hg maximum). Wash FC plate five times with 25 uL 25% cold TCA turning off the vacuum after each wash during addition of next wash. To perform in plate liquid scintillation counting, blot the plate on a lint-free absorbent surface to displace any droplets formed on the underside of the plate. Remove the plastic underdrain from the plate and snap on the Packard TopCount Adapter (Cat. No. MSTPCWH50). Add 50 uL of Ultima Gold liquid scintillation cocktail to each well with a multichannel pipette. Seal the top of the plate with clear sealing tape (Cat. No. MATAHCL00). After 1 hr measure ^{3}H-counts with a Packard TopCount instrument. Signal stable up to 18 hr.

2.3.5 Mechanism of action kinetic characterization

Kinetic characterization of DOT1L was carried out in the presence of DMSO or varying concentrations of compound. With respect to the substrate, the initial reaction velocity was determined at different substrate concentrations (0.021 –1.36 ug/uL) in the presence of saturating SAM concentration (600 nM). With respect to SAM the initial reaction velocity was determined with varying concentrations of SAM (12.5 – 800 nM) with a constant saturating concentration of substrat (0.76 ug/uL). The initial velocity was determined by removing 5 uL aliquots from the HMTase reaction at 5, 10, and 20 min. Michaelis-Menten kinetics were applied to the plot of reaction velocity vs concentration (SAM or substrate) to determine Km and Vmax. Kinetics analysis and double reciprocal Lineweaver-Burk plots were generated using Graphpad Prism 6.0.

2.3.6 UV-vis absorbance spectra measurements

Absorbance spectra of 100 µM UMD-7 and UMD-1 were measured in 100 uL of HMTase buffer (20 mM Tris pH 7.9, 4 mM EDTA, 1 mM DTT, 0.01% Triton X-100) at a final volume of 100 uL and measured in the presence of varying concentrations of substrates or histone proteins. Measurements were acquired in flat-bottom clear 96 well plates (Denville Scientific; P9734) on a BioTek Synergy H1 hybrid plate reader. Absorbance changes were quantified for the individual compounds respective maximum absorbance wavelength.

2.3.7 Saturation transfer difference NMR

All STD NMR experiments were performed on a 600 MHz Bruker Avance III equipped with a CryoProbe at 25°C as previously described (*30*). Samples were prepared in HMTase buffer with 7% D_2O, and 1% DMSO and contained 200 µM ligand and 5 µM GST-DOT1L with or without 1 mM SAH (Sigma-Aldrich). The on-resonance irradiation of the protein was performed using a 2s pulse train of 50ms gaussian pulses centered at 0 ppm and off-resonance irradiation was applied at 30 ppm as the reference. Experiments used 16 scans with 16 dummy scans and were processed using TOPSPIN 2.1 (Bruker).

2.3.8 Thermal stability shift assay

Thermal stability shift experiments were performed as previously described (*31*) using a Thermo Fluor 384-well plate reader (Johnson & Johnson). The melting temperature (T_m) of GST-DOT1L was determined by measuring the fluorescence of 1-Anilinonaphthalene-8-Sulfonic Acid (1,8-ANS) (Cayman Chemical) upon thermal denaturing of DOT1L heated in a continuous gradient with 1 min incubations at 1°C increments. Samples contained 4 µM DOT1L, 100 µM ligand, and 100 µM 1,8-ANS in 25 mM Tris pH 7.5, 100 mM NaCl, 3 mM DTT in a total volume of 11 µL overlaid with 2 µL of silicone oil in ABgene 384-well PCR microtiter plates (Thermo Scientific).

2.3.9 Western blot analysis of H3 lysine methylation

Murine bone marrow cells transformed with MLL-AF9 (*32*) were plated at 2 x 10^5 cells/mL in 12 well plates and treated with compounds for 3 days. Histones were isolated as previously described (*8*). The concentration of extracted histones was determined using the Bradford assay (BioRad). Equal quantities of histones were separated on a 4-20% Tris-glycine gel (Life Technologies) and transferred to PVDF membrane (Thermo Scientific). Membranes were probed with primary rabbit polyclonal antibodies against histone H3 (ab1791), H3K79Me1 (ab2886), H3K79Me2 (ab3594), H3K79Me3 (ab2621), H3K4Me3 (ab8580), H3K9Me3 (ab8898), H2K27Me3 (Millipore ABE44), H3K36Me3 (ab9050). Membranes were subsequently probed with HRP-conjugated goat anti rabbit secondary antibody (GenScript) and signal detected with Lumi-Light western blotting substrate (Roche) and exposure to autoradiography film (Denville).

2.3.10 qRT-PCR analysis of gene expression

Cells were treated as in the western blot assay and RNA was extracted using Trizol (Life technologies) and RNA purified using a RNeasy mini kit (Qiagen). RNA quantity was normalized and reverse transcription performed with SuperScript III first strand synthesis kit (Life technologies). Quantitivative PCR was carried out with Power SYBR

green PCR master mix (Life technologies) on a 7500 RT-PCR system instrument (Applied Biosystems).

2.3.11 Cell viability assay

Human leukemia cell lines in log phase growth were diluted with media and 5,000 cells were added to each well of a flat bottom 96-well plate (Corning). Compound or DMSO was added at the indicated concentrations and cells were incubated for 4 days at 37^{o}C. Viability was assessed by addition of 10 uL of the WST-assay reagent (CCK-8; Dojindo) and measurement of $OD_{450\ nm}$ after 2-4 hr.

2.3.12 Apoptosis analysis

Human leukemia cells were plated at 5 x 10^5 cells/mL in 12 well plates and treated with UMD-7 for 24 hr. 1.5 x 10^5 cells were collected and centrifuged at 200xg for 5 min. The media was aspirated off and cells were washed with PBS and centrifuged. Cells were resuspended in 100 uL of BD biding buffer (BD biosciences) and 4 uL of Annexin V (BD biosciences) and 5 uL of propidium iodide (PI) 1 ug/uL solution (Invitrogen) was added to the cells. Cells were allowed to stain 5 min and diluted with an additional 100 uL BD binding buffer and Annexin V and PI staining was analyzed on a Becton-Dickinson LSR-II flow cytometer.

2.3.13 Cell cycle analysis

Cells were treated the same as in apoptosis experiments. Collected all cells in the wells, centrifuged 250 xg 8 min, aspirate off media and wash with 2 mL cold PBS. Repeat centrifugation and aspirate wash off cells. Resusped cells in 500 uL cold PBS and add 1 mL of cold 100% ethanol to cell suspension while gently vortexing. Incubate cells on ice 30 min and centrifuge 400 xg 8 min, wash cells once with 2 mL PBS and resuspend in 500 uL PBS, add RNase A to a final concentration of 100 ug/mL, add PI to a final concentration of 10 ug/mL. Allowed staining for 30 min and analyzed on a Becton-Dickinson LSR-II flow cytometer.

2.3.14 Differentiation analysis

THP-1 cells were plated at 5 x 10^5 cells/mL in 12 well plates and treated with UMD-7 for 7 for 6 days. Cells are split and retreated with compound every 2 days. 1.5 x 10^5 cells were collected and centrifuged at 200xg for 5 min then washed with 1 mL PBS. Cells were resuspened in 100 uL of PBS + 0.1% FBS and 2 uL of Pacific Blue labeled CD11b antibody (company) was added and allowed to incubate 30 min. Cells were washed with 1 mL PBS + 0.1% FBS and resuspended in 100 uL of BD binding buffer then Annexin V and PI were added and analyzed the same as in the apopstosis experiment. CD11b expression was analyzed for the healthy living population of cells that was Annexin V and PI negative.

2.3.15 Colony forming units (CFU) assay

The soft agar colony forming units assay was carried out as previously described (*16*) with the addition of UMD-7 to the soft agar media at the indicated concentrations.

2.3.16 Cell growth assay

Murine bone marrow transformed with MLL-AF9 or E2A-HLF as described for the CFU assay (*16*) was grown in liquid culture media of IMDM, 15% fetal bovine serum, and 10 ng/mL IL-3. Cells were diluted to 250,000 cells/mL and treated with UMD-7 or DMSO at the indicated concentrations. Cells were split and fresh media with compound was added every 2-3 days.

2.3.17 OctetRED binding assay

Biolayer interferometry assays were carried out using a ForteBio OctetRED system as described (*33*) utilizing biotinylated His-DOT1L (1-416) and MBP as a control. Protein was biotinylated using EZ-Link NHS-PEG4 Biotinylation Kit (Thermo Scientific; 21329) following manufacturer instructions, Biotin in 1:1 molar ration with the protein incubated on ice for 1-2 hr. Biotinylated DOT1L activity was confirmed using the standard HMTase assay described above then immobilized on super-streptavidin biosensors (ForteBio; 18-5057) in binding buffer (20 mM Phosphate pH 7.4, 150 mM NaCl, 0.01% Tween20, 0.01% BSA) at 50 ug/mL and washed three times in binding buffer. Compounds were

serially diluted in binding buffer and binding association and dissociation monitored by OctetRED for 3 min. Non-specific signal was addressed by subtraction of the MBP control surface and data was analyzed with OctetRED software.

2.4 Conclusions

Based on the importance of DOT1L as a therapeutic target in MLL-rearrangement leukemias, we employed several approaches for the identification of small molecule inhibitors of DOT1L HMTase activity. Our experience shows that numerous secondary biophysical and cellular assays are required to thoroughly evaluate the quality of screening hits as potential lead compounds. In total over 5,500 compounds were screened in a preliminary assay for DOT1L inhibition. Stringent criteria were established for the identification of quality inhibitors of DOT1L including compound binding to the target DOT1L evaluated by STD NMR, ThermoFluor, and OctetRED assays. Compounds were also required to demonstrate selective cellular inhibition of H3K79 methylation.

Virtual screening of a focused nucleoside library resulted in identification of several SAM analogues that inhibit DOT1L *in vitro* by binding to the SAM binding site. This lead to the identification of the most potent SAM competitive compounds **2.2** which selectively inhibits DOT1L in a MLL-AF9 murine model cell line. Two classes of DOT1L inhibitors were identified through biochemical screening; class A naphthosulfonyl compounds, including UMD-7, and class B naphthoquinones**.** UMD-7 is a novel inhibitor of H3K79 methylation that works through a unique mechanism unlike other current DOT1L inhibitors by binding to histone proteins resulting in rapid cellular loss of H3K79 methylation. Furthermore, UMD-7 treatment phenocopies genetic loss of DOT1L resulting in apoptosis, cell cycle arrest, differentiation, and selective growth inhibition of MLL-rearrangement cell lines.

2.5 References

1. van Leeuwen, F., Gafken, P. R., and Gottschling, D. E. (2002) Dot1p modulates silencing in yeast by methylation of the nucleosome core, *Cell 109*, 745-756.
2. McGinty, R. K., Kohn, M., Chatterjee, C., Chiang, K. P., Pratt, M. R., and Muir, T. W. (2009) Structure-Activity Analysis of Semisynthetic Nucleosomes: Mechanistic Insights into the Stimulation of Dot1L by Ubipuitylated Histone H2B, *Acs Chem Biol 4*, 958-968.
3. Ng, H. H., Xu, R. M., Zhang, Y., and Struhl, K. (2002) Ubiquitination of histone H2B by Rad6 is required for efficient Dot1-mediated methylation of histone H3 lysine 79, *J Biol Chem 277*, 34655-34657.
4. Villoutreix, B. O., Eudes, R., and Miteva, M. A. (2009) Structure-based virtual ligand screening: recent success stories, *Comb Chem High Throughput Screen 12*, 1000-1016.
5. Cheng, T., Li, Q., Zhou, Z., Wang, Y., and Bryant, S. H. (2012) Structure-based virtual screening for drug discovery: a problem-centric review, *AAPS J 14*, 133-141.
6. Tuccinardi, T. (2009) Docking-based virtual screening: recent developments, *Comb Chem High Throughput Screen 12*, 303-314.
7. Min, J. R., Feng, Q., Li, Z. Z., Zhang, Y., and Xu, R. M. (2003) Structure of the catalytic domain of human DOT1L, a Non-SET domain nucleosomal histone methyltransferase, *Cell 112*, 711-723.
8. Daigle, S. R., Olhava, E. J., Therkelsen, C. A., Majer, C. R., Sneeringer, C. J., Song, J., Johnston, L. D., Scott, M. P., Smith, J. J., Xiao, Y., Jin, L., Kuntz, K. W., Chesworth, R., Moyer, M. P., Bernt, K. M., Tseng, J. C., Kung, A. L., Armstrong, S. A., Copeland, R. A., Richon, V. M., and Pollock, R. M. (2011) Selective killing of mixed lineage leukemia cells by a potent small-molecule DOT1L inhibitor, *Cancer Cell 20*, 53-65.
9. Seifert, M. H., and Lang, M. (2008) Essential factors for successful virtual screening, *Mini Rev Med Chem 8*, 63-72.
10. Harris, C. J., Hill, R. D., Sheppard, D. W., Slater, M. J., and Stouten, P. F. (2011) The design and application of target-focused compound libraries, *Comb Chem High Throughput Screen 14*, 521-531.
11. McGovern, S. L., Helfand, B. T., Feng, B., and Shoichet, B. K. (2003) A specific mechanism of nonspecific inhibition, *J Med Chem 46*, 4265-4272.
12. Fox, S., Farr-Jones, S., Sopchak, L., Boggs, A., Nicely, H. W., Khoury, R., and Biros, M. (2006) High-throughput screening: Update on practices and success, *J Biomol Screen 11*, 864-869.
13. Matulis, D., Kranz, J. K., Salemme, F. R., and Todd, M. J. (2005) Thermodynamic stability of carbonic anhydrase: Measurements of binding affinity and stoichiometry using ThermoFluor, *Biochemistry 44*, 5258-5266.
14. Benod, C., Villagomez, R., Filgueira, C. S., Hwang, P. K., Leonard, P. G., Poncet-Montange, G., Rajagopalan, S., Fletterick, R. J., Gustafsson, J. A., and Webb, P. (2014) The Human Orphan Nuclear Receptor Tailless (TLX, NR2E1) Is Druggable, *Plos One 9*.

15. Feng, Y., Li, M. Y., Wang, B. H., and Zheng, Y. G. (2010) Discovery and Mechanistic Study of a Class of Protein Arginine Methylation Inhibitors, *Journal of Medicinal Chemistry 53*, 6028-6039.
16. Jo, S. Y., Granowicz, E. M., Maillard, I., Thomas, D., and Hess, J. L. (2011) Requirement for Dot1l in murine postnatal hematopoiesis and leukemogenesis by MLL translocation, *Blood 117*, 4759-4768.
17. Wilson, S. J., Lovenberg, T. W., and Barbier, A. J. (2003) A high-throughput-compatible assay for determining the activity of fatty acid amide hydrolase, *Anal Biochem 318*, 270-275.
18. Yu, W. Y., Smil, D., Li, F. L., Tempel, W., Fedorov, O., Nguyen, K. T., Bolshan, Y., Al-Awar, R., Knapp, S., Arrowsmith, C. H., Vedadi, M., Brown, P. J., and Schapira, M. (2013) Bromo-deaza-SAH: A potent and selective DOT1L inhibitor, *Bioorgan Med Chem 21*, 1787-1794.
19. Min, J., Feng, Q., Li, Z., Zhang, Y., and Xu, R. M. (2003) Structure of the catalytic domain of human DOT1L, a non-SET domain nucleosomal histone methyltransferase, *Cell 112*, 711-723.
20. Basavapathruni, A., Jin, L., Daigle, S. R., Majer, C. R., Therkelsen, C. A., Wigle, T. J., Kuntz, K. W., Chesworth, R., Pollock, R. M., Scott, M. P., Moyer, M. P., Richon, V. M., Copeland, R. A., and Olhava, E. J. (2012) Conformational adaptation drives potent, selective and durable inhibition of the human protein methyltransferase DOT1L, *Chem Biol Drug Des 80*, 971-980.
21. Friesner, R. A., Murphy, R. B., Repasky, M. P., Frye, L. L., Greenwood, J. R., Halgren, T. A., Sanschagrin, P. C., and Mainz, D. T. (2006) Extra precision glide: Docking and scoring incorporating a model of hydrophobic enclosure for protein-ligand complexes, *Journal of Medicinal Chemistry 49*, 6177-6196.
22. Sitwala, K. V., Dandekar, M. N., and Hess, J. L. (2008) HOX Proteins and Leukemia, *Int J Clin Exp Patho 1*, 461-474.
23. Krivtsov, A. V., Feng, Z., Lemieux, M. E., Faber, J., Vempati, S., Sinha, A. U., Xia, X., Jesneck, J., Bracken, A. P., Silverman, L. B., Kutok, J. L., Kung, A. L., and Armstrong, S. A. (2008) H3K79 methylation profiles define murine and human MLL-AF4 leukemias, *Cancer Cell 14*, 355-368.
24. Bernt, K. M., Zhu, N., Sinha, A. U., Vempati, S., Faber, J., Krivtsov, A. V., Feng, Z. H., Punt, N., Daigle, A., Bullinger, L., Pollock, R. M., Richon, V. M., Kung, A. L., and Armstrong, S. A. (2011) MLL-Rearranged Leukemia Is Dependent on Aberrant H3K79 Methylation by DOT1L, *Cancer Cell 20*, 66-78.
25. Nguyen, A. T., Taranova, O., He, J., and Zhang, Y. (2011) DOT1L, the H3K79 methyltransferase, is required for MLL-AF9-mediated leukemogenesis, *Blood 117*, 6912-6922.
26. Chang, M. J., Wu, H. Y., Achille, N. J., Reisenauer, M. R., Chou, C. W., Zeleznik-Le, N. J., Hemenway, C. S., and Zhang, W. Z. (2010) Histone H3 Lysine 79 Methyltransferase Dot1 Is Required for Immortalization by MLL Oncogenes, *Cancer Res 70*, 10234-10242.
27. Lai, C. J., and Wu, J. C. (2003) A simple kinetic method for rapid mechanistic analysis of reversible enzyme inhibitors, *Assay Drug Dev Techn 1*, 527-535.
28. Daigle, S. R., Olhava, E. J., Therkelsen, C. A., Majer, C. R., Sneeringer, C. J., Song, J., Johnston, L. D., Scott, M. P., Smith, J. J., Xiao, Y. H., Jin, L., Kuntz, K.

W., Chesworth, R., Moyer, M. P., Bernt, K. M., Tseng, J. C., Kung, A. L., Armstrong, S. A., Copeland, R. A., Richon, V. M., and Pollock, R. M. (2011) Selective Killing of Mixed Lineage Leukemia Cells by a Potent Small-Molecule DOT1L Inhibitor, *Cancer Cell 20*, 53-65.

29. Li, Q. L., Chen, T. J., Wang, Y. L., and Bryant, S. H. (2010) PubChem as a public resource for drug discovery, *Drug Discov Today 15*, 1052-1057.
30. Mayer, M., and Meyer, B. (2001) Group epitope mapping by saturation transfer difference NMR to identify segments of a ligand in direct contact with a protein receptor, *Journal of the American Chemical Society 123*, 6108-6117.
31. Mezzasalma, T. M., Kranz, J. K., Chan, W., Struble, G. T., Schalk-Hihi, C., Deckman, I. C., Springer, B. A., and Todd, M. J. (2007) Enhancing recombinant protein quality and yield by protein stability profiling, *J Biomol Screen 12*, 418-428.
32. Muntean, A. G., Giannola, D., Udager, A. M., and Hess, J. L. (2008) The PHD fingers of MLL block MLL fusion protein-mediated transformation, *Blood 112*, 4690-4693.
33. Asangani, I. A., Dommeti, V. L., Wang, X. J., Malik, R., Cieslik, M., Yang, R. D., Escara-Wilke, J., Wilder-Romans, K., Dhanireddy, S., Engelke, C., Iyer, M. K., Jing, X. J., Wu, Y. M., Cao, X. H., Qin, Z. H. S., Wang, S. M., Feng, F. Y., and Chinnaiyan, A. M. (2014) Therapeutic targeting of BET bromodomain proteins in castration-resistant prostate cancer, *Nature 510*, 278.

CHAPTER 3

Design and novel synthetic pathway to S-adenosylmethionine analogues as DOT1L inhibitors

3.1 Introduction

There is significant interest in development of small molecule inhibitors of DOT1L histone methyltransferase activity for therapeutic intervention in MLL-translocation leukemias as discussed in chapter 1. In addition to biochemical screening approaches to identify inhibitors of DOT1L, discussed in chapter 2, here we present the *de novo* design and synthesis of small molecule DOT1L inhibitors. This approach has been successfully applied to numerous targets including protein kinases, RNA polymerase, and even protein/peptide interactions (*1-3*) . In the case of DOT1L, *de novo* design has the benefit of starting from a known small molecule ligand, SAM and a defined binding pocket, the SAM binding site.

The crystal structure between the co-factor SAM and the catalytic domain of DOT1L (PDB: 1NW3) (*4*) provide structural insights for the interactions between them, permitting a rational approach to the discovery, chemical synthesis and development of new DOT1L inhibitors. Analysis of the crystal structure showed that the active site consists of the SAM binding pocket and an orthogonal lysine binding channel directed at the methyl group of SAM. The SAM binding pocket is wider and more hydrophobic at the entrance formed by Phe 223, Leu 224, Val 249, Lys 187 and Pro 133, where the adenine moiety binds and interacts via hydrophobic interactions and π-π stacking interactions between the adenine ring and Phe 223. In addition, the adenosine moiety of SAM forms hydrogen bonds with Asp 222, Phe 223, Lys 187 and Glu 186. The methionyl moiety inserts deep into the pocket, which becomes narrower toward the center of the protein and negatively charged, forming a network of hydrogen bond

contacts with several amino acid side chains, namely, Asp 161, Gln 168, Glu 186, and Thr 139 (*4*). Utilizing this information, we designed, synthesized, and biochemically evaluated several SAM analogues for their ability to inhibit DOT1L *in vitro* and inhibit H3K79 methylation in cellular studies.

Our design strategy required modifications of the 5' position of adenosine. Current synthetic strategies for 5' modified adenosine analogues typically proceed via activation of the 5' hydroxyl with a chlorine leaving group and subsequent displacement with a thiol or amine (*5-7*). Alkyl groups can be introduced through a 5' thioacetic acid intermediate upon NaOMe hydrolysis and displacement of a bromo-alkyl group (*6*). Alternatively a 5' amine intermediate can be accessed through conversion of the adenosine 5' hydroxyl group via Mitsunobu reaction and hydrazine treatment (*5*).

3.2 Results

3.2.1 De novo design of SAM analogues as DOT1L inhibitors

The focus of the structure-based design of novel SAM analogues was on modifying the homocysteine moiety through exploring the flexibility and the length of the tail as well as the polar amino acid moiety of SAM, since at physiological pH it is charged and might negatively influence the compounds bioavailability. Based on these considerations, we proposed the design of two SAM analogues (Figure 3.2.1). A key feature of this design was replacement of the sulfur linkage between the ribose and homocysteine tail with an amino linker in order to increase the synthetic feasibility of the designed compounds, as well as to establish a general synthetic route for synthesis of novel adenosine analogues.

To explore the importance of the linker flexibility in the homocysteine moiety, the alkyl chain was substituted with a rigid phenyl ring (**2**, Figure 3.2.1). In addition, the methyl ester **3** was designed to assess the importance of hydrogen bonds formed by the terminal carboxylic acid of **2**. Next, the amino acid tail of SAM was replaced with a bioisostere, α-amino acetamide moiety, in an attempt to recapitulate the hydrogen bonding network of SAM with DOT1L (**4** and **5**, Figure 3.2.1). The crystal structure of DOT1L shows that SAM binds to the protein in a fully extended confirmation, suggesting

that the length of the linker is important in order for the α-amino acetamide moiety to reach its optimal binding site in the protein. Thus, we designed compounds with different alkyl linkers to explore the optimum length.

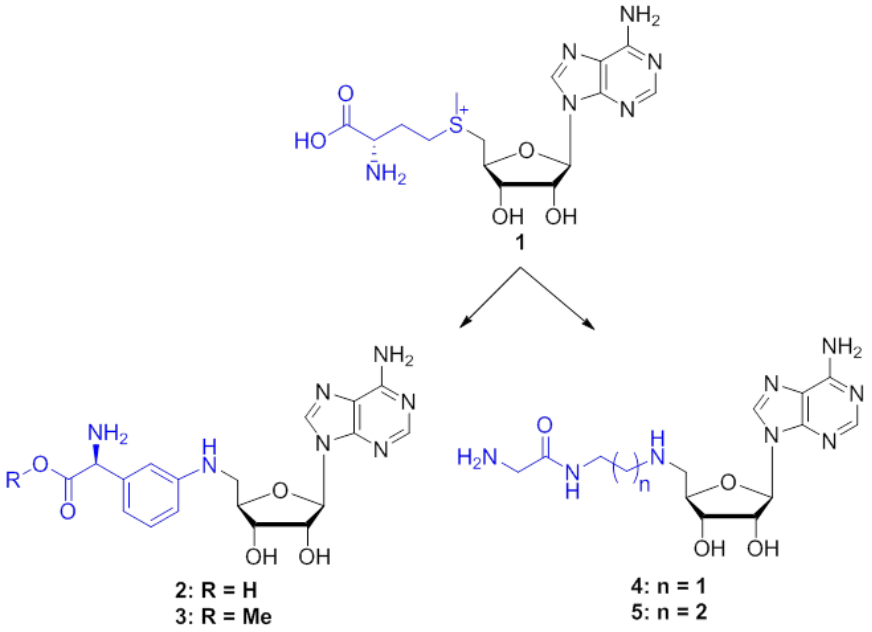

Figure 3.2.1 *De novo* design of novel DOT1L inhibitors.

To assess the proposed designed compounds *in silico*, docking studies were performed and their binding models were generated. The docking procedure was validated by docking SAM which provided a consistent binding pose with the crystal structure (Figure 3.2.2a). The predicted binding model of **2** showed that it binds in a very similar manner as SAM (Figure 3.2.2b). The adenine portion of **2** overlaps with SAM while maintaining the predicted π-π stacking interaction with Phe 223 and hydrogen bond contacts with Asp 222 and Lys 187. Some torsional strain shifts the ribose of **2** away from Glu 186 and may disrupt the formation of hydrogen bonds. However, the introduction of a rigid linker places the amino acid tail of **2** in the same position as in SAM and maintains the network of hydrogen bonds deep within the binding pocket. Based on the binding model it is also predicted that blocking the carboxylic acid tail as a methyl ester in analogue **3** should disrupt the hydrogen bonding network with Asn 241, Thr 139, and Gln 168, likely leading to lower potency. Designed compound **5** also showed similar binding pose as SAM (Figure 3.2.2c), but opposed to **2**, the ribose portion of **5** is predicted to maintain hydrogen bonds with Glu 186. However, the introduced α-amino acetamide

moiety is lacking the interaction with Gln 168 but maintain hydrogen bonds with Asp 161 and Gly 163. Based on the results from the predicted binding models, we synthesized the target compounds and tested their ability to inhibit DOT1L histone methyltransferase activity *in vitro*.

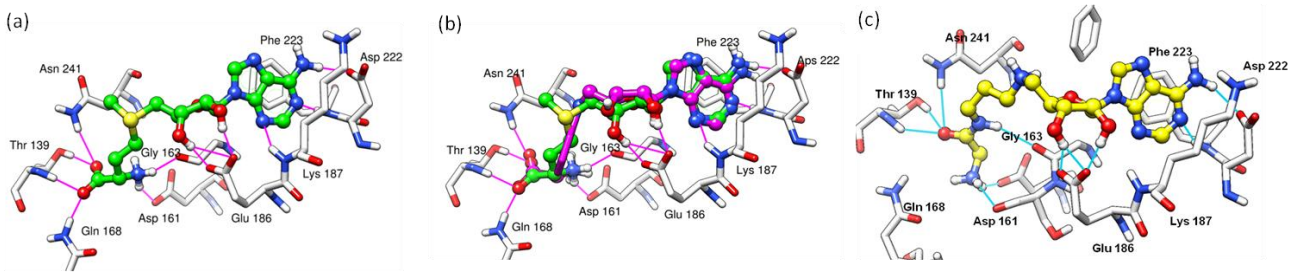

Figure 3.2.2 Validation of docking and predicted binding mode of designed DOT1L inhibitors. (a) Glide XP docking of SAM into 1NW3 structure. (b) Proposed binding mode of **2** (magenta) overlayed with SAM (green) demonstrating the predicted interactions with DOT1L. (c) Proposed binding mode of **5** (yellow) with DOT1L and predicted interactions.

3.2.2 Synthesis of designed compounds

Our synthetic strategy utilized a convergent approach in which a protected adenosine 5'-carboxaldehyde (**8**, Figure 3.2.3) was condensed with a requisite amine side chain via a reductive amination. The synthesis of the carboxyaldehyde **8** provides a novel and efficient method to access 5' amine linked adenosine derivatives.

The synthesis of **8** is shown in Scheme 3.2.1. Accordingly, hexamethyldisilazane (HMDS) persilylation of 2**',**3'-(isopropylidene)adenosine , **6**, followed by treatment with di-*t*-butyl dicarbonate was carried out by modification of a generalized procedure used to introduce N^6-Boc functionality onto nucleosides (*8*). This gave an intermediate N^6,N^6-bis(*tert*-butoxycarbonyl)-5'-*O*-(trimethylsilyl)adenosine, which was not isolated but was reacted directly with methanol : triethylamine (5:1) to simultaneously cleave the TMS ether and one of the N^6-Boc groups. This provided **7** in quantitative yield with the overall sequence representing a much superior method to make this reported compound(*9*). Subsequent conversion of **7** to the novel 5'-carboxaldehyde **8** was then carried out by oxidation with Dess-Martin periodinane. This novel intermediate, **8**, was used for synthesis of targeted designed compounds. The side chain of **2** was derived from (*S*)-

(+)-phenylglycine **12** in a series of standard reactions. Nitration followed by α-amine Boc protection was carried out by a literature procedure to provide compound **13**(*10*). Methyl ester formation gave **14**, which was then hydrogenated to amine **15**. Reductive amination of aldehyde **8** with **15** then provided compound **9** in modest overall yield.

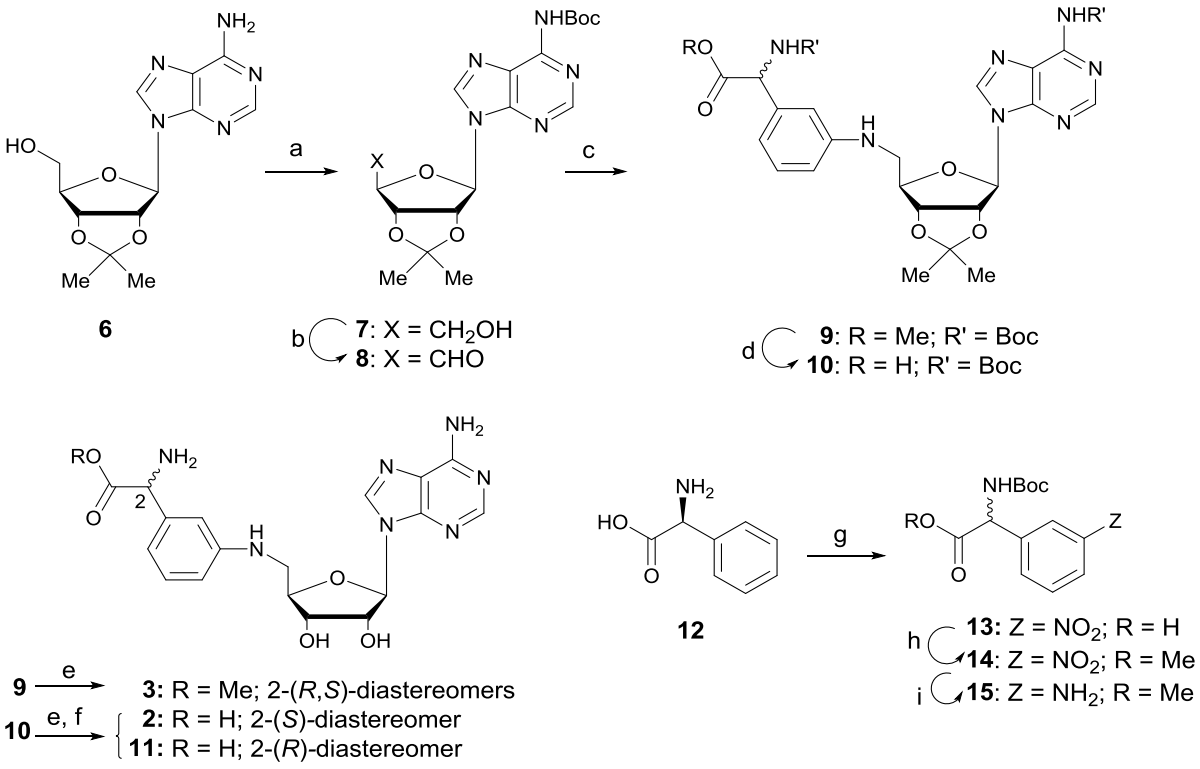

Figure 3.2.3 Synthesis of *de novo* designed rigid DOT1L inhibitors. Reagents and conditions: (a) 1. HMDS, DMAP, TMSOTf; 2. Boc_2O, THF; 3. 5:1 MeOH:TEA (100%, 3 steps); (b) Dess-Martin periodinane, DCM, 0°C - rt (99%) ; (c) **15**, 1,2-DCE, $NaBH(OAc)_3$ (26%); (d) LiOH, MeOH (39%); (e) aq. TFA (35% for **9**); (f) hplc purification; (g) ref (*10*); (h) MeI, K_2CO_3, THF (65%); (i) H_2, 10% Pd/C, MeOH (87%). See Supplemental Information for experimental details.

HPLC analysis of this product showed a ~1:1 mixture of diastereomers, indicating that racemization had taken place in the earlier nitration step of building up the side chain as previously documented (*11*). Hydrolysis of the methoxy ester with LiOH gave **10**, which was subjected to aqueous T FA hydrolyis to simultaneously remove the Boc and isopropylidene protecting groups. Upon HPLC purification, the target compound **2** could

be separated from its 2-(*R*)-diastereomer **11**. Alternatively, **9** was also subjected to TFA deprotection to provide the methyl ester **3** for testing.

For target compound **5**, the same general synthetic approach was utilized (Figure 3.2.4). Amidation of 1,3-propanediamine (**17**) with *N*-Boc-glycine methylester by the method of Morandeau et al.(*12*) gave **19** which was then coupled to aldehyde **8** under the same reductive amination conditions shown above. Subsequent global hydrolysis of the Boc and isopropylidene protecting groups provided **5** in good overall yield. The same sequence of steps was repeated on ethylenediame (**16**) to make target compound **4** with the truncated linker.

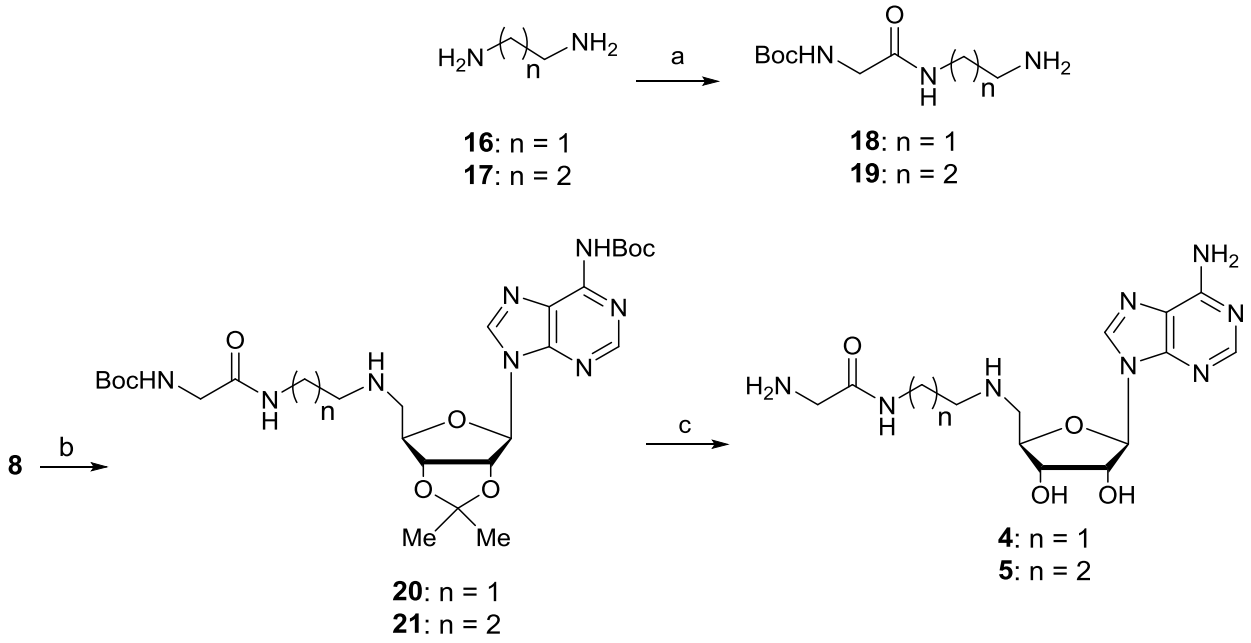

Figure 3.2.4 Synthesis of *de novo* designed flexible DOT1L inhibitors. Reagents and conditions**:** (a) *N*-(Boc)-glycine methyl ester, MeOH, 0^{o}C – rt (50-52% yield); (b) **18** or **19**, NaBH(OAc)$_3$, 1,2-DCE (43-48% yield); (c) aq. TFA (54-56% yield).

3.2.3 Evaluation of in vitro DOT1L inhibition

An *in vitro* DOT1L histone methyltransferase (HMTase) assay was used to evaluate the ability of our designed compounds to inhibit DOT1L. Using ^{3}H-methyl-S-adenosylmethionine (^{3}H-SAM) as the source of radioisotopically labeled methyl donor, in the presence of DOT1L the ^{3}H-methyl group is transferred from ^{3}H-SAM to the

substrate H3K79 in a milieu of extracted core histones. The dose dependent curves together with the IC_{50} values are presented in Figure 3.2.5. SAH was used as a positive control and showed inhibition of the methyltransferase activity of DOT1L with IC_{50} of 1.6 $\pm$ 0.4 µM, consistent with the reported results. Interestingly, both targeted compounds, **2** and **5**, showed significantly less potency in inhibiting the methyltransferase activity of DOT1L with IC_{50} values 270 µM and > 1,500 µM, although the predicted binding model showed very similar conformation as SAM with only several lost hydrogen bonds. Of the two diastereomers **2** and **11**, we assign **2** with the natural 2-(*S*)-stereochemistry in the side chain since it showed higher potency (270 µM vs. 1,055 µM, respectively). As expected, methyl ester **3** was less potent based on the prediction that substitution of the carboxylic acid function of **2**/**11** with an ester eliminates a key hydrogen bond with DOT1L.

Replacing the amino acid tail of SAM with a bioisostere, α-amino acetamide moiety, resulted in a detrimental effect on the activity of compounds **5** and **4** with IC_{50} values > 1,500 µM. In addition, the different length of the linker in these two compounds seemed that has no influence on their potency.

We believe that much of the loss of potency for our inhibitors can be attributed to disruption of the hydrogen bond network formed with DOT1L. In addition a SAR study of SAM analogues published while our work was in progress confirmed that slight alterations of the structure of SAM can dramatically affect the ability of small molecules to inhibit DOT1L (*6*). Several classes of potent and selective inhibitors of DOT1L (*13-15*) were reported which exploit an unexpected structural flexibility to induce a conformational change that opens a large hydrophobic pocket next to the SAM binding site (*16, 17*).

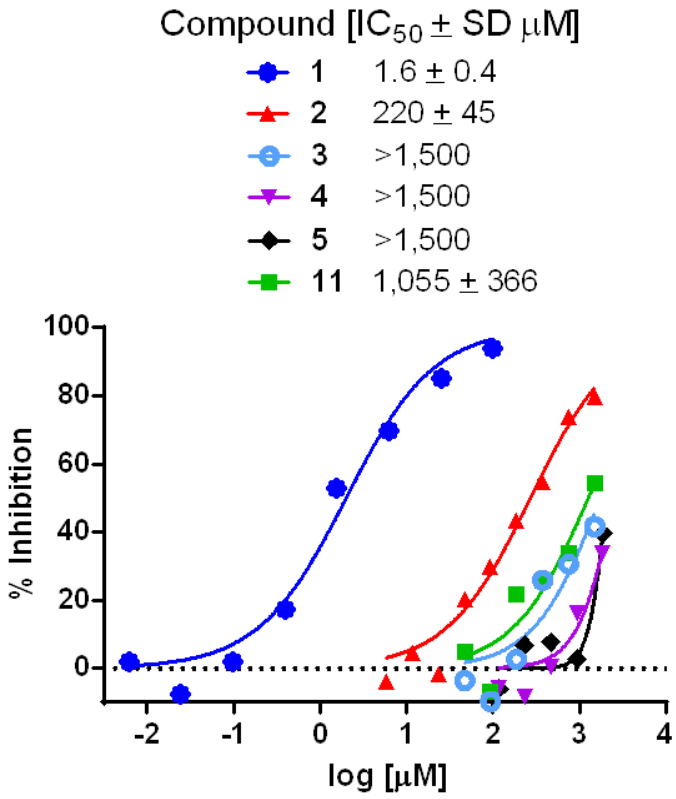

Figure 3.2.5 DOT1L inhibition by designed compounds. Potency of synthesized inhibitors assessed by *in vitro* DOT1L HMTase assay.

3.3 Methods

3.3.1 Chemistry General Procedures

All starting materials were obtained from commercial suppliers and were used without further purification. ^{1}H NMR spectra were recorded on a Varian 400 instrument and are provided in Appendix 1. Chemical shift values are recorded in δ units (ppm). Mass spectra were recorded on a Micromass TofSpec-2E Matrix-Assisted, Laser-Desorption, Time-of-Flight Mass Spectrometer in positive ESI mode unless otherwise noted. Analytical HPLC was run on a reverse-phase column (Restek Ultra C18, 5 µm, 150 x 4.6mm column; flow rate of 1 mL/min using a gradient of 40 – 80% acetonitrile in water over 20 min). Thin-layer chromatography (TLC) was performed on silica gel GHLF plates (250 microns) purchased from Analtech. Column chromatography was carried

out in the flash mode utilizing silica gel. Extraction solutions were dried over $MgSO_4$ prior to concentration.

3.3.2 Synthetic procedures

***tert*-Butyl (9-((3a*R*,4*R*,6*R*,6a*R*)-6-(hydroxymethyl)-2,2-dimethyltetrahydrofuro[3,4-*d*][1,3]dioxol-4-yl)-9*H*-purin-6-yl)carbamate (7)**(*9*). A suspension of **6** (1.54 g, 5 mmol), hexamethyldisilazane (HMDS; 2 mL), and 4-dimethylaminopyridine (DMAP; 120 mg) was stirred together at 25 °C in an oven-dried flask. To this was added drop-wise trimethylsilyl trifluoromethanesulfonate (TMSOTf ; 20 uL), and the resultant suspension was heated at 75 °C for 2 h. The mixture was concentrated to an oil that was dissolved in 3 mL of dry THF with gentle warming. The solution was ice-cooled and treated with 3.27 g (15 mmol) of di-*t*-butyl dicarbonate and an additional 7 ml of THF, and allowed to stir at 25 °C for 4 h. The solution was concentrated and then treated with 18 mL of 5:1(v/v) methanol : triethylamine. Following vigorous evolution of CO_2, the solution was stirred at 55 °C for 16 h and then concentrated to an oil that was distributed between dichloromethane and water. The dichloromethane phase was dried and concentrated to an oil that was purified by flash chromatography, eluting with hexanes : ethyl acetate (1:1). Combined product fractions were concentrated to an oil that was pumped *in vacuo* at 60 °C to leave **7** (2.53 g; 100% yield) as a white foam: NMR and mass spec data were identical to those previously reported (*9*).

***tert*-Butyl (9-((3a*R*,4*R*,6*S*,6a*S*)-6-formyl-2,2-dimethyltetrahydrofuro[3,4-*d*][1,3]dioxol-4-yl)-9*H*-purin-6-yl)carbamate (8).** To an ice-cooled stirred suspension of Dess-Martin periodinane (674 mg, 1.6 mmol) in dichloromethane (7.5 mL) was added **7** (589 mg, 1.45 mmol) and the resultant mixture was allowed to warm to room temperature over 3 h. The mixture was concentrated to a white powder that was suspended in ethyl acetate, and the insoluble Dess-Martin reagent was removed by filtration. The filtrate was concentrated and additional residual amounts of Dess-Martin reagent were removed by the same process. The filtrate was concentrated to leave fairly pure **8** (583 mg, 99% crude yield) as a solid, which was suitable for use in the next reaction: ^{1}H NMR (400 MHz, $CDCl_3$): δ 9.25 (s, 1H), 8.54 (s, 1H), 7.96 (s,1H), 6.17 (s,

1H), 5.49 (d, *J* = 6.1 Hz, 1H), 5.28 (d, *J* = 6.1 Hz, 1H), 4.62 (s, 1H), 1.54 (s, 3H), 1.50 (s, 9H), 1.34 (s, 3H); MS (ESI): *m/z* 438.1 $(M+Na)^+$.

Methyl (*S*)-2-((*tert*-butoxycarbonyl)amino)-2-(3-((((3a*R*,4*R*,6*R*,6a*R*)-6-(6-((*tert*-butoxycarbonyl)amino)-9*H*-purin-9-yl)-2,2-dimethyltetrahydrofuro[3,4-*d*][1,3]dioxol-4-yl)methyl)amino)phenyl)acetate and *R*-diastereomer (9). To an ice-cold solution of **8** (370 mg, 0.91 mmol) in 1,2-dichloroethane (DCE; 2.5 mL) was added a solution of **15** (280 mg, 1 mmol) in 1,2-dichloroethane (2.5 mL) followed by sodium triacetoxyborohydride (STAB; 270 mg, 1.3 mmol). The reaction mixture was stirred overnight at room temperature and quenched with saturated aq. $NaHCO_3$. The mixture was diluted with water and extracted with ethyl acetate (3x). The combined extracts were dried and concentrated to an oil that was purified by flash chromatography, eluting with hexanes : ethyl acetate (2:1) to give **9** (157 mg, 26% yield) as a ~1:1 ratio of diastereomers by HPLC: ^{1}H NMR (400 MHz, $CDCl_3$): δ 8.84, 8.67 (s each, 0.57H & 0.43H, H-8 of each diastereomer), 8.03 (br s, 1H), 7.97, 7.94 (s each, 0.49 & 0.51H, H-2 of each diastereomer), 7.10 (q, *J* = 8.1 Hz, 1H), 6.65 (t, *J* = 9.0 Hz, 1H), 6.61-6.51 (m, 2H), 6.03, 5.96 (s each, 0.44H & 0.56H, anomeric H of each diastereomer), 5.54 - 5.09 (m, 4H), 4.60 – 4.50 (m,1H), 3.67 (s, 3H), 3.53 - 3.45 (m, 2H), 1.61 (s, 3H), 1.55 (s, 9H), 1.42 (s, 9H), 1.36 (s, 3H); MS (ESI): *m/z* 670.2 $(M+1)^+$, 692.2 $(M+Na)^+$.

(*S*)-2-((*tert*-Butoxycarbonyl)amino)-2-(3-((((3a*R*,4*R*,6*R*,6a*R*)-6-(6-((*tert*-butoxycarbonyl)amino)-9*H*-purin-9-yl)-2,2-dimethyltetrahydrofuro[3,4-*d*][1,3]dioxol-4-yl)methyl)amino)phenyl)acetic acid and (*R*)-diastereomer (10). To a stirred solution of **9** (160 mg, 0.24 mmol) in methanol (1 mL) at 0 ^oC was added LiOH (11 mg, 0.26 mmol). Cooling was removed and reaction mixture was stirred at room temperature overnight. TLC showed incomplete conversion with a new spot of R_f ~0.4 (2:1 ethyl acetate : methanol). Additional LiOH (11 mg) was added and stirring was continued for 4 h. The mixture was concentrated and the residue was distributed between 5% aq. acetic acid added and ethyl acetate. The combined ethyl acetate extracts were dried and concentrated to an oil that was purified by flash chromatography, eluting with ethyl acetate : methanol (9:1). Product fractions were

combined and concentrated to give **10** (61 mg, 39% yield): ^{1}H NMR (400 MHz, $CDCl_3$): δ 8.66 (s, 1H), 7.98 (s, 1H), 7.11 – 6.97 (m, 1H), 6.71 - 6.45 (m, 3H), 6.03 (d, *J* = 4.4 Hz, 1H), 5.91 - 5.84 (m, 1H), 5.50 - 4.99 (m, 3H), 4.57 (m, 1H), 3.40 - 3.20 (m, 2H), 1.56 (s, 3H), 1.52 (s, 9H), 1.39 (s, 3H), 1.37 (s, 9H); MS (ESI): *m/z* 656.2 $(M+1)^+$.

Methyl (*S*)-2-amino-2-(3-((((2*R*,3*S*,4*R*,5*R*)-5-(6-amino-9*H*-purin-9-yl)-3,4-dihydroxytetrahydrofuran-2-yl)methyl)amino)phenyl)acetate and *R*-diastereomer (3). To a solution of **9** (173.5 mg, 0.26 mmol) in ice-cold water (3 mL) was added trifluoroacetic acid (TFA; 3 mL) at 0 ^{o}C. The mixture was stirred at room temperature overnight, concentrated and then diluted with aq. $NaHCO_3$. The mixture was extracted with ethyl acetate (3x), and the combined extracts were dried and concentrated to a residue that precipitated solids upon addition of ethyl acetate. The solids were collected and washed well with hexanes. The filtrate was concentrated and processed in a similar fashion to provide a second crop that was combined with the first to give **3** (39 mg, 35% yield): ^{1}H NMR (400 MHz, $CDCl_3$): δ 8.23 (s, 1H), 7.86 (s, 1H), 7.12 (t, *J* = 7.7 Hz, 1H), 6.64 (d, *J* = 7.5 Hz, 1H), 6.56 (d, *J* = 10.7 Hz, 1H), 6.40 (d, *J* = 7.0 Hz, 1H), 6.30 (s, 1H), 6.00 (s, 1H), 5.51 (d, *J* = 5.9 Hz, 1H), 5.40 (d, *J* = 7.0 Hz, 1H), 5.23 (d, *J* = 5.4 Hz, 1H), 4.60 (m, 1H), 3.68 (s, 3H), 3.60 - 3.35 (m, 2H); MS (ESI): *m/z* 430.9 $(M+1)^+$, 452.1 $(M+Na)^+$.

(*S*)-2-Amino-2-(3-((((2*R*,3*S*,4*R*,5*R*)-5-(6-amino-9*H*-purin-9-yl)-3,4-dihydroxytetrahydrofuran-2-yl)methyl)amino)phenyl)acetic acid (2) and (*R*)-diastereomer (11). To a solution of **10** (61 mg, 0.09 mmol) in dichloromethane (0.4 mL) at 0 ^{o}C was added water (0.1 mL) and TFA (0.5 mL). The mixture was stirred at room temperature overnight and concentrated to a residue that was dissolved in H_2O : methanol (95:5). The solution was then purified by reverse-phase HPLC (Restek Ultra C18, 5 µm, 150 x 21.2 mm column; flow rate of 10 mL/min using a gradient of 10 – 30% acetonitrile in water over 25 min) followed by concentration and lyophilization of fractions corresponding to each isomer provided purified diastereomers. Diastereomer **11:** ^{1}H NMR (400 MHz, DMSO-d_6 + D_2O): δ 8.34 (s, 1H), 8.12 (s, 1H), 7.10 (t, *J* = 7.8 Hz, 1H), 6.70 - 6.59 (m, 3H), 5.88 (d, *J* = 7.4 Hz, 1H), 4.99 (d, *J* = 11.0 Hz, 1H), 4.73 (s, 1H), 4.65 - 4.57 (m, 1H), 4.23 – 4.17 (m, 1H), 3.26 - 3.20 (m, 2H); MS (ESI): *m/z* 416.2

$(M+1)^+$; Diastereomer **2:** ^{1}H NMR (400 MHz, DMSO-d_6): δ 8.58 (br s, 2H; exchanges with D_2O), 8.38 (s, 1H), 8.24 (s,1H), 7.69 (br s, 2H; exchanges with D_2O), 7.12 (t, *J* = 7.8 Hz, 1H), 6.68 - 6.61 (m, 3H), 5.87 (d, *J* = 6.0 Hz,1H), 5.47 (br s, 1H; exchanges with D_2O), 5.27(br s, 1H; exchanges with D_2O), 4.88 (d, *J* = 18.0 Hz,1H; collapses to s with D_2O wash), 4.77 – 4.68 (m, 1H), 4.14 (t, *J* = 4.3 Hz, 1H), 4.07 (d, *J* = 3.5 Hz, 1H), 3.32 (d, *J* = 7.2 Hz, 2H; peak revealed with D_2O wash); MS (ESI): *m/z* 416.2 $(M+1)^+$.

Methyl (*S*)-2-((*tert*-butoxycarbonyl)amino)-2-(3-nitrophenyl)acetate (14) (*18*)**.** A stirred solution of partially racemized (*S*)-2-((*tert*-butoxycarbonyl)amino)-2-(3-nitrophenyl)acetic acid (*10*) (**13**; 600 mg, 2.03 mmol), iodomethane (140 uL, 2.2 mmol), anhydrous potassium carbonate (415 mg, 3 mmol) and THF (10 mL) was heated at 60 ^oC for 18 h. The mixture was filtered and the filtrate was diluted with water and extracted with dichloromethane (3x). The combined organic extracts were dried and concentrated to an oil that was purified by flash chromatography, eluting with hexanes : ethyl acetate (6:1). Product fractions were combined and concentrated to leave **14** (409 mg, 65% yield): (400 MHz, $CDCl_3$): δ 8.23 (t, *J* = 2.0 Hz, 1H), 8.19 – 8.15 (m, 1H), 7.72 (d, *J* = 7.7 Hz, 1H), 7.57 – 7.49 (m, 1H), 5.78 (s, 1H), 5.42 (d, *J* = 6.7 Hz, 1H), 3.73 (s, 3H), 1.51 (s, 9H).

Methyl (*S*)-2-(3-aminophenyl)-2-((*tert*-butoxycarbonyl)amino)acetate (15)(*18*). A mixture of **14** (720 mg, 2.3 mmol), 10% Pd/C (catalytic) and methanol (35 mL) was hydrogenated at 50 psi at room temperature overnight. The mixture was filtered over Celite® and the filtrate concentrated to leave **15** (566 mg, 87% yield) as a viscous yellow oil: ^{1}H NMR (400 MHz, $CDCl_3$): δ 7.10 (t, *J* = 7.8 Hz, 1H), 6.70 (dt, *J* = 7.7, 1.2 Hz, 1H), 6.64 (t, *J* = 2.0 Hz, 1H), 6.62 – 6.59 (m, 1H), 5.46 (d, *J* = 7.5 Hz, 1H), 5.18 (d, *J* = 7.5 Hz, 1H), 3.69 (s, 3H), 1.41 (s, 9H).

***tert*-Butyl (2-((2-aminoethyl)amino)-2-oxoethyl)carbamate (18)**(*12*)**.** To ethylenediamine (**16**; 13.5 mL, 200 mmol) at 0 ^oC was added drop-wise a solution of *N*-Boc-glycine methyl ester (948 mg, 5 mmol) in methanol (20 mL). The reaction mixture was stirred at room temperature for 6 h and concentrated to an oil that was partitioned

between water and dichloromethane. The combined organic extracts were dried and concentrated to an oil that was purified by flash chromatography eluting with ethyl acetate : methanol : triethylamine (50:50:1). Product fractions were concentrated to give **18** (544 mg, 50% yield) as an oil: ^{1}H NMR (400 MHz, $CDCl_3$): δ 6.58 (br s, 1H), 5.23 (br s, 1H), 3.77 (d, *J* = 5.8 Hz, 2H), 3.31 (m, 2H), 2.83 (br s, 2H), 1.44 (s, 9H), 1.26 (s, 2H); MS (ESI): *m/z* 218.2 $(M+1)^+$.

***Tert*-Butyl (2-((3-aminopropyl)amino)-2-oxoethyl)carbamate (19).** Reaction of 1,3-propanediamine (**17**; 16.8 ml, 200 mmol), as described for the synthesis of **18**, gave **19** (600 mg, 52% yield): ^{1}H NMR (400 MHz, $CDCl_3$): δ 7.10 (br s, 1H), 5.29 (br s, 1H), 3.74 (d, *J* = 5.8 Hz, 2H), 3.35 (q, *J* = 6.2 Hz, 2H), 2.77 (t, *J* = 6.3 Hz, 2H), 1.75 – 1.60 (m, 4H), 1.42 (s, 9H); MS (ESI): *m/z* 232.1 $(M+1)^+$, 254.1 $(M+Na)^+$.

***Tert*-Butyl (9-((3a*R*,4*R*,6*R*,6a*R*)-6-(11,11-dimethyl-6,9-dioxo-10-oxa-2,5,8-triazadodecyl)-2,2-dimethyltetrahydrofuro[3,4-*d*][1,3]dioxol-4-yl)-9*H*-purin-6-yl)carbamate (20).** To a solution of **8** (203 mg, 0.5 mmol) in 1,2-DCE (2 mL) at 0 ^oC was added **18** (120 mg, 0.55 mmol) dissolved in 1,2-DCE (1 mL), followed by sodium triacetoxyborohydride (148 mg, 0.7 mmol). The reaction mixture was stirred overnight at room temperature, quenched with saturated aq. $NaHCO_3$, and distributed between dichloromethane and water. The combined organic extracts were dried and concentrated to an oil that was purified by flash chromatography eluting with dichloromethane : methanol (19:1). Product fractions were combined and concentrated to give **20** (130 mg, 43% yield): ^{1}H NMR (400 MHz, $CDCl_3$ + D_2O): δ 8.72 (s, 1H), 8.13 (s, 1H), 6.07 (s, 1H), 5.48 – 5.41 (m, 1H), 4.99 (s, 1H), 4.35 (s, 1H), 3.77 (d, *J* = 5.3 Hz, 2H), 3.34 – 3.21 (m, 2H), 2.92 – 2.60 (m, 4H), 1.61 (s, 3H), 1.56 (s, 9H), 1.42 (s, 9H), 1.39 (s, 3H).

***tert*-Butyl (9-((3aR,4R,6R,6aR)-6-(12,12-dimethyl-7,10-dioxo-11-oxa-2,6,9-triazatridecyl)-2,2-dimethyltetrahydrofuro[3,4-d][1,3]dioxol-4-yl)-9*H*-purin-6-yl)carbamate (21).** Reaction of **19** (127 mg, 0.55 mmol) with **8** followed by purification, as described for the synthesis of **20**, gave **21** (153 mg, 48% yield): ^{1}H NMR (400 MHz, $CDCl_3$): δ 8.70 (s, 1H), 8.10 (s, 1H), 7.15 (d, *J* = 6.5 Hz, 1H), 6.09 (d, *J* = 2.5 Hz, 1H),

5.47 – 5.36 (m, 2H), 5.07 (dd, *J* = 6.4, 3.4 Hz, 1H), 4.50 – 4.47 (m, 1H), 3.68 (d, *J* = 5.8 Hz, 2H), 3.30 (d, *J* = 6.2 Hz, 2H), 3.20 – 3.08 (m, 2H), 2.81 – 2.71 (m, 2H), 1.80 – 1.70 (m, 2H), 1.60 (s, 3H), 1.55 (s, 9H), 1.42 (s, 9H), 1.37 (s, 3H).

2-Amino-*N*-(2-((((2*R*,3*S*,4*R*,5*R*)-5-(6-amino-9*H*-purin-9-yl)-3,4-dihydroxytetrahydrofuran-2-yl)methyl)amino)ethyl)acetamide (4). To a solution of **20** (130 mg, 0.21 mmol) in dichloromethane (0.8 mL) at 0 ^{o}C was added water (0.2 mL) and TFA (1.1 mL). The mixture was stirred at room temperature overnight and concentrated to a residue that was dissolved in methanol : water (5:95) and purified by preparative reverse-phase HPLC (Restek Ultra C18, 5 µm, 150 x 21.2 mm column; flow rate of 10 mL/min using an isocratic elution of 2% acetonitrile in water for 10 min) followed by concentration and lyophilization of fractions yielding **4** (44 mg, 56% yield): ^{1}H NMR (400 MHz, DMSO-d_6 + D_2O): δ 8.47 (s, 1H), 8.31 (s, 1H), 5.97 (d, *J* = 5.4 Hz, 1H), 4.65 (t, *J* = 5.0 Hz, 1H), 4.23 – 4.19 (m, 2H), 3.51 (s, 2H), 3.46 – 3.30 (m, 4H), 3.08 – 2.99 (m, 2H); MS (ESI): *m/z* 367.1 $(M+1)^{+}$.

2-Amino-*N*-(3-((((2*R*,3*S*,4*R*,5*R*)-5-(6-amino-9*H*-purin-9-yl)-3,4-dihydroxytetrahydrofuran-2-yl)methyl)amino)propyl)acetamide (5). To a solution of **21** (185 mg, 0.3 mmol) in dichloromethane (1.2 mL) at 0 ^{o}C was added water (0.3 mL) and TFA (1.5 mL). The mixture was stirred at room temperature overnight and concentrated to a residue that was dissolved in methanol : water (5:95) and purified by preparative reverse-phase HPLC (Restek Ultra C18, 5 µm, 150 x 21.2 mm column; flow rate of 10 mL/min using an isocratic elution of 2% acetonitrile in water for 10 min) followed by concentration and lyophilization of fractions yielding **5** (62 mg, 54% yield): ^{1}H NMR (400 MHz, DMSO-d_6 + D_2O): δ 8.42 (s, 1H), 8.31 (s, 1H), 5.95 (d, *J* = 5.3 Hz, 1H), 4.63 (t, *J* = 5.0 Hz, 1H), 4.25 – 4.15 (m, 2H), 3.50 (s, 2H), 3.36 (dd, *J* = 13.2, 9.6 Hz, 1H), 3.24 (dd, *J* = 13.4, 2.8 Hz, 1H), 3.12 (t, *J* = 6.8 Hz, 2H), 2.90 (t, *J* = 7.7 Hz, 2H), 1.79 – 1.64 (m, 2H); MS (ESI): *m/z* 381.1 $(M+1)^{+}$.

3.3.3 Molecular Modeling

The designed compounds were converted to 3D structures using the program of LigPrep 2.5. All parameters were set to the default values except that the “Ionization” was set to “Epik”. The DOT1L:SAM complex (PDB ID: 1NW3) was energy-minimized, upon addition of hydrogen atoms, using the OPLS-AA 2005 force field within the Protein Preparation Wizard of Schrödinger. The compounds were docked and scored using Glide 5.7 extra precision (XP) with options kept at default settings. The receptor grids were prepared with a 20 Å side length with the centroids in the centers of SAM.

3.3.4 In vitro DOT1L histone methyltransferase assay

The evaluation of DOT1L inhibitors by *in vitro* histone methyltransferase assay was carried out as described in chapter 2.

3.4 Conclusions

In this chapter, we have applied de novo ligand design using the crystal structure of the DOT1L catalytic domain (1NW3) towards developing SAM derivatives as novel DOT1L inhibitors followed by biochemical evaluation of synthesized compounds. A convergent synthetic approach was utilized to install different moieties as bioisosteres of the methionine tail of SAM. Introduction of a rigid linker between adenosine and the amino acid tail, **2**, compromised hydrogen bonding interactions between the ribose portion of adenosine and Glu 186, but positioned the amino acid portion of **2** in the same orientation as SAM. Two analogues, **5** and **4**, with a flexible amide linker off the 5’-position of adenosine and α-amino acetamide tail, allowed interactions between ribose and Glu 186 to be maintained, but did not fully recapitulate the network of hydrogen bonding between amino acid tail of SAM and DOT1L. Overall, disruption of the hydrogen bond network between our designed small molecules and DOT1L resulted in a marked loss of potency for inhibition of DOT1L HMTase activity *in vitro*.

Importantly, the synthetic strategy described here for the convergent synthesis of SAM analogues represents a novel synthetic methodology for a range of 5’-position adenosine modifications. This synthetic route will be useful for making related

compounds in which moieties off the 5'-position of adenosine (or related nucleoside congeners) can be easily constructed via reductive amination of a precursor 5'-carboxaldehyde. Thus, the utility clearly extends beyond SAM analogues, as adenosine is a useful scaffold for the development of numerous potential classes of inhibitors.

3.5 References

1. Cavalluzzo, C., Voet, A., Christ, F., Singh, B. K., Sharma, A., Debyser, Z., De Maeyer, M., and Van der Eycken, E. (2012) De novo design of small molecule inhibitors targeting the LEDGF/p75-HIV integrase interaction, *Rsc Adv 2*, 974-984.
2. Agarwal, A. K., Johnson, A. P., and Fishwick, C. W. G. (2008) Synthesis of de novo designed small-molecule inhibitors of bacterial RNA polymerase, *Tetrahedron 64*, 10049-10054.
3. Urich, R., Wishart, G., Kiczun, M., Richters, A., Tidten-Luksch, N., Rauh, D., Sherborne, B., Wyatt, P. G., and Brenk, R. (2013) De Novo Design of Protein Kinase Inhibitors by in Silico Identification of Hinge Region-Binding Fragments, *Acs Chem Biol 8*, 1044-1052.
4. Min, J., Feng, Q., Li, Z., Zhang, Y., and Xu, R. M. (2003) Structure of the catalytic domain of human DOT1L, a non-SET domain nucleosomal histone methyltransferase, *Cell 112*, 711-723.
5. Yao, Y., Chen, P., Diao, J., Cheng, G., Deng, L., Anglin, J. L., Prasad, B. V., and Song, Y. (2011) Selective inhibitors of histone methyltransferase DOT1L: design, synthesis, and crystallographic studies, *J Am Chem Soc 133*, 16746-16749.
6. Anglin, J. L., Deng, L., Yao, Y., Cai, G., Liu, Z., Jiang, H., Cheng, G., Chen, P., Dong, S., and Song, Y. (2012) Synthesis and structure-activity relationship investigation of adenosine-containing inhibitors of histone methyltransferase DOT1L, *J Med Chem 55*, 8066-8074.
7. Llewellyn, D. B., and Wahhab, A. (2009) An efficient synthesis of base-substituted analogues of S-adenosyl-DL-homocysteine, *Tetrahedron Lett 50*, 3939-3941.
8. Sikchi, S. A., and Hultin, P. G. (2006) Solventless protocol for efficient bis-N-boc protection of adenosine, cytidine, and guanosine derivatives, *J Org Chem 71*, 5888-5891.
9. Lu, X., Zhang, H., Tonge, P. J., and Tan, D. S. (2008) Mechanism-based inhibitors of MenE, an acyl-CoA synthetase involved in bacterial menaquinone biosynthesis, *Bioorg. Med. Chem. Lett. 18*, 5963-5966.
10. Sassatelli, M., Debiton, E., Aboab, B., Prudhomme, M., and Moreau, P. (2006) Synthesis and antiproliferative activities of indolin-2-one derivatives bearing amino acid moieties, *Eur. J. Med. Chem. 41*, 709-716.
11. Friis, P., and Kjaer, A. (1963) Absolute configuration of m-carboxyphenylglycine, an amino acid from a higher plant, Iris tingitana, *Acta Chem. Scand. 17*, 2391-2396.
12. Morandeau, L., Remaud-Le Saec, P., Ouadi, A., Bultel-Riviere, K., Mougin-Degraef, M., de France-Robert, A., Faivre-Chauvet, A., and Gestin, J.-F. (2006)

Synthesis and evaluation of a novel samarium-153 bifunctional chelating agent for radioimmunotargeting applications, *J. Labelled Compd. Radiopharm. 49*, 109-123.

13. Daigle, S. R., Olhava, E. J., Therkelsen, C. A., Basavapathruni, A., Jin, L., Boriack-Sjodin, P. A., Allain, C. J., Klaus, C. R., Raimondi, A., Scott, M. P., Waters, N. J., Chesworth, R., Moyer, M. P., Copeland, R. A., Richon, V. M., and Pollock, R. M. (2013) Potent inhibition of DOT1L as treatment of MLL-fusion leukemia, *Blood 122*, 1017-1025.
14. Daigle, S. R., Olhava, E. J., Therkelsen, C. A., Majer, C. R., Sneeringer, C. J., Song, J., Johnston, L. D., Scott, M. P., Smith, J. J., Xiao, Y. H., Jin, L., Kuntz, K. W., Chesworth, R., Moyer, M. P., Bernt, K. M., Tseng, J. C., Kung, A. L., Armstrong, S. A., Copeland, R. A., Richon, V. M., and Pollock, R. M. (2011) Selective Killing of Mixed Lineage Leukemia Cells by a Potent Small-Molecule DOT1L Inhibitor, *Cancer Cell 20*, 53-65.
15. Yu, W. Y., Smil, D., Li, F. L., Tempel, W., Fedorov, O., Nguyen, K. T., Bolshan, Y., Al-Awar, R., Knapp, S., Arrowsmith, C. H., Vedadi, M., Brown, P. J., and Schapira, M. (2013) Bromo-deaza-SAH: A potent and selective DOT1L inhibitor, *Bioorgan Med Chem 21*, 1787-1794.
16. Yu, W. Y., Chory, E. J., Wernimont, A. K., Tempel, W., Scopton, A., Federation, A., Marineau, J. J., Qi, J., Barsyte-Lovejoy, D., Yi, J. N., Marcellus, R., Iacob, R. E., Engen, J. R., Griffin, C., Aman, A., Wienholds, E., Li, F. L., Pineda, J., Estiu, G., Shatseva, T., Hajian, T., Al-awar, R., Dick, J. E., Vedadi, M., Brown, P. J., Arrowsmith, C. H., Bradner, J. E., and Schapira, M. (2012) Catalytic site remodelling of the DOT1L methyltransferase by selective inhibitors, *Nat Commun 3*.
17. Basavapathruni, A., Jin, L., Daigle, S. R., Majer, C. R. A., Therkelsen, C. A., Wigle, T. J., Kuntz, K. W., Chesworth, R., Pollock, R. M., Scott, M. P., Moyer, M. P., Richon, V. M., Copeland, R. A., and Olhava, E. J. (2012) Conformational Adaptation Drives Potent, Selective and Durable Inhibition of the Human Protein Methyltransferase DOT1L, *Chem Biol Drug Des 80*, 971-980.
18. Greig, I. R., Sheridan, R. M., Fisher, R., Tozer, M. J., Clase, J. A., Smith, A., Tuffnell, A. R., and Van 'T Hof, R. J. (2010) Preparation of aryl-phenyl-sulfonamide-phenylene compounds useful in treatment of diseases mediated by inappropriate activation of immune system, p 171pp., Pimco 2664 Limited, UK .

CHAPTER 4

Regulation of the Wnt Signaling Target Gene Expression by the Histone Methyltransferase DOT1L

4.1 Introduction

The “classical,” also called canonical, Wingless-type (Wnt) signaling pathway is one of the most relevant pathways involved in normal cell growth and differentiation (*1*). Some of the Wnt pathway antagonists are epigenetically deregulated in cancer models and many studies attempted to characterize the role of epigenetic alterations of the Wnt pathway in human cancers (*2-6*). Upon activation of Wnt signaling the central effector molecule, β-catenin, translocates to the nucleus and interacts with TCF/LEF transcription factors to activate the expression of Wnt-pathway target genes (*7*). Additional transcriptional coactivators are recruited by β-catenin including several chromatin modifying enzymes such as the histone acetyltransferases CBP/P300 and TRRAP/TIP60 as well as the histone methyltransferase complexes MLL1/MLL2 (*8*).

In order to investigate the composition of DOT1L containing multi-protein complexes in MLL-translocation leukemias and to identify novel interacting partners, DOT1L was immunoprecipitated and interacting proteins were identified by mass spectrometry. These studies led to the identification of a multi-protein complex known as Dot1-containing complex (DotCom), comprising MLL fusion partners together with known components of the Wnt signaling pathway, Skp1, TRRAP, and β-catenin, linked H3K79 methylation to the Wnt signaling pathway (*9*). Subsequently, knockdown of Dot1 and Dot1-associated proteins in Drosophila decreased expression of a subset of Wingless target genes (*9*). In mouse intestinal crypts and human colon cancer cells DOT1L and a

known interacting partner, AF10, were identified in complex with the Tcf4 transcription factor, a key effector molecule for β-catenin (*10*). Functional studies demonstrated that β-catenin recruits AF10/DOT1L proteins to the regulatory regions of several Wnt target genes, resulting in deposition of H3K79 methylation over their coding regions. Depletion of AF10 in cell lines impaired DOT1L recruitment to TCF4/β-catenin target genes and identifies AF10 and DOT1L as essential co-activators of Wnt-dependent transcription (*10*). In a model of chondrogenesis, the inhibition of DOT1L expression by RNAi led to reduced expression of three Wnt-regulated genes (Tcf1, AXIN2, c-MYC) (*11*). While these studies suggest a key role for DOT1L in Wnt signaling, others have demonstrated that DOT1L is not required for homeostasis of the intestinal epithelium which is regulated through Wnt signaling. A conditional DOT1L knockout murine model demonstrated no gross defects of the intestinal epithelium despite the absence of H3K79 methylation (*12*). Additionally, a tissue specific genetic approach was used to investigate a large number of Wnt target genes in mammalian $LGR5^{+}$ intestinal epithelial cells and demonstrated that DOT1L is not essential for activation of Wnt target genes or maintenance of intestinal homeostasis and function (*13*).

Based on these complex findings, there is a need for further studies to elucidate the role of DOT1L in Wnt signaling. Of note, in all these reports, DOT1L's biological role was studied by utilizing genetic approaches to knockdown DOT1L protein levels and H3K79 methylation. However, it is not clear at this time whether previous findings of the functional consequences of genetic loss of DOT1L are due to disruption of DOT1L containing multi-protein complexes or loss of H3K79 methylation. Therefore, our approach to assess the role of DOT1L in Wnt signaling was to specifically inhibit methyltransferase activity of DOT1L using the small molecule inhibitor EPZ004777 as a chemical tool.

4.2 Results

4.2.1 DOT1L H3K79 methylation affect on canonical Wnt-pathway reporter gene expression

To examine whether DOT1L mediated methylation of H3K79 is required for activation of canonical Wnt signaling, the TOPflash luciferase reporter assay which contains

TCF/LEF binding sites in a reporter plasmid and is specifically activated in response to Wnt pathway agonists was utilized (*14*) in conjunction with the control plasmid with mutated TCF binding sites, FOPflash. Due to the inactive basal activity of Wnt signaling in HEK293 cells, activation of the Wnt signaling pathway was achieved by inhibition of GSK3 with the small molecule SB-216763 in HEK293 cells (*15*). Inhibition of GSK3 prevents phosphorylation and degradation of β-catenin, resulting in transcriptional activation of β-catenin/TCF targets in HEK293 cells. As was expected, the TOPflash expression in HEK293 cells was significantly induced upon treatment with SB-216763 (Figure 4.2.1). To determine whether H3K79 methylation is required for the activation of TOPflash expression, HEK293 cells were pretreated with the DOT1L inhibitor EPZ004777 for four days, prior to transfection with the TOPflash reporter and activation with SB-216763. Cells were maintained in the presence of 3 µM EPZ004777 for the duration of the experiment and the inhibition of DOT1L resulted in decrease of H3K79 methylation (Figure 4.2.1a). However, the TOPflash reporter activation was not affected by the loss of H3K79 methylation (Figure 4.2.1a).

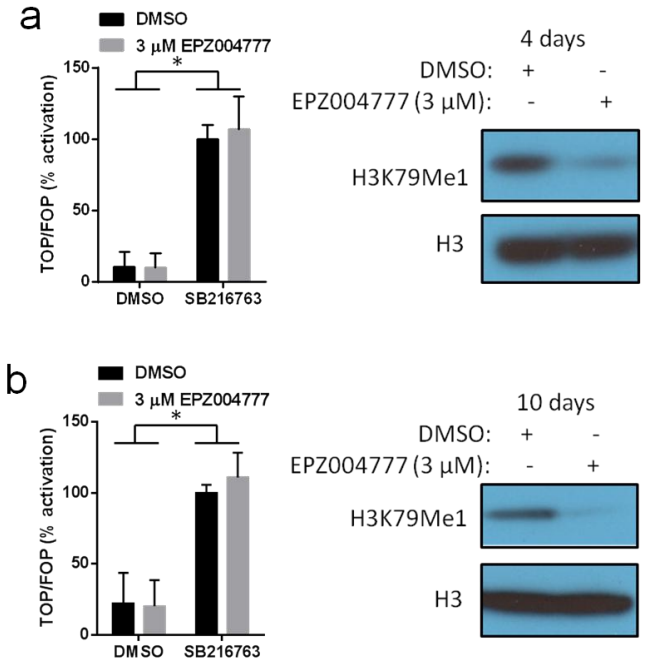

Figure 4.2.1 Activation of a β-catenin-TCF/LEF regulated reporter gene by SB-216763 in HEK293 cells after inhibition of DOT1L histone methyltransferase activity. Relative luciferase expression ratio of TOPflash/FOPflash reporter activity and western blot of histone extracts from HEK293 cells after (a) four days and (b) ten days

treatment with 3 µM EPZ004777, followed by 24 hour Wnt-signaling pathway activation with 5 µM SB-216763. (*p = <0.05, n= 6, two-way ANOVA)

It is known that EPZ004777 requires longer time of treatment in order to show effect and influence the expression of MLL target genes such as Hoxa9 and Meis1 (*16*). Thus, HEK293 cells were pretreated with EPZ004777 for ten days and as expected H3K79 methylation was significantly reduced (Figure 4.2.1b). Nevertheless, the TOPflash expression was not affected (Figure 4.2.1b) consistent with the four day time point. These results demonstrate that expression of the TOPflash luciferase reporter does not require DOT1L HMTase activity or H3K79 methylation.

4.2.2 Effects of DOT1L inhibition on activation of the endogenous Wnt target gene AXIN2

To further confirm this result, the expression of the representative, well characterized, endogenous Wnt target gene *AXIN2* was measured in HEK293 cells upon activation of the Wnt signaling pathway and treatment with EPZ004777. It has been reported that DOT1L is recruited to the *AXIN2* gene upon induction of Wnt signaling in an AF10-dependent manner resulting in increased H3K79 methylation at the gene promoter and transcribed gene body (*10*). Reports also demonstrate that *AXIN2* gene expression is induced upon GSK3 inhibition with SB-216763 (*17*). Consistent with these reports, after treatment of HEK293 cells with GSK3 inhibitor, *AXIN2* gene expression was significantly induced. However, loss of H3K79 methylation after treatment with EPZ004777 for two and seven days (Figure 4.2.2) did not affect the expression of *AXIN2* (Figure 4.2.2). Importantly, the housekeeping control gene *β-actin* was the same under EPZ004777 treatment conditions demonstrating that the activation of *AXIN2* was specific to Wnt signaling and not a broad transcriptional change. These results are consistent with the observations from the TOPflash reporter assay and demonstrate that H3K79 methylation is not required for Wnt-regulated transcription and activation of the representative canonical Wnt signaling target gene, *AXIN2*.

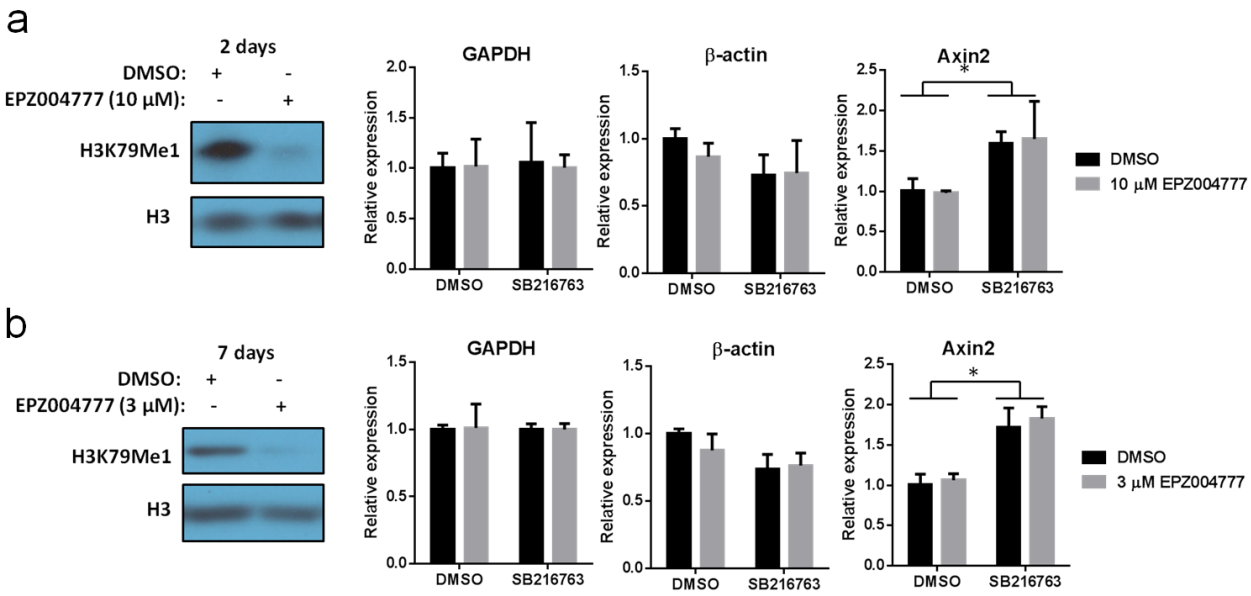

Figure 4.2.2 Expression of the endogenous Wnt target gene *AXIN2* in HEK293 cells after inhibition of DOT1L histone methyltransferase activity. Western blot of histone extracts and qRT-PCR analysis of gene expression normalized to GAPDH from HEK293 cells after (a) two days and (b) seven days treatment with EPZ004777 (10 µM and 3 µM, respectively) followed by 24 hours Wnt-signaling pathway activation with 10 µM SB-216763 treatment. (* p = <0.05, n= 6, two-way ANOVA)

4.2.3 Effects of DOT1L inhibition on human colon carcinoma cell lines

Because these studies were performed in HEK293 cells which do not have constitutively activated Wnt signaling, we next examined two human colon adenocarcinoma-derived cell lines containing mutations in β-catenin, LS174T (*18*), and APC, SW480 (*14*), leading to constitutive activation of the Wnt signaling pathway and expression of target genes. Activation of the Wnt signaling pathway is a critical event in the development of colon cancer, thus understanding the regulatory pathways that influence Wnt signaling might led to novel therapies beyond that of APC and β-catenin.

To investigate the requirement of DOT1L HMTase activity for maintaining expression of endogenous Wnt target genes in these two cell lines, cells were treated with EPZ004777 using three different concentrations. Four days treatment of SW480 cells with EPZ004777 resulted in decreased H3K79 methylation (Figure 4.2.3a). TOPflash expression was analyzed in SW480 cells upon inhibition of DOT1L HMTase activity. SW480 cells have a high TOP/FOP expression ratio, as expected due to the “Wnt on”

state of the cells and were able to maintain similar expression of the TOPflash luciferase reporter even after treatment with 3 μM EPZ004777 for four days and loss of H3K79 methylation (Figure 4.2.3a). Quantitative RT-PCR analysis of treated cells revealed that selected known Wnt-dependent target genes, *AXIN2, EPHB3, LGR5, ASCL2,* and *c-MYC*, were present in H3K79me2-decreased cells at levels similar to or slightly higher than the levels in control untreated cells (Figure 4.2.3a). Inhibition of DOT1L HMTase activity over a longer time period of seven and ten days produced the same result (Figure 4.2.4). These results are consistent with the effects on TOPflash reporter gene expression. Importantly, the cell growth of SW480 cells was not affected after treatment with the DOT1L inhibitor up to ten days (Figure 4.2.5). Overall, the results demonstrate that DOT1L-mediated H3K79 methylation is not essential to maintain the expression of Wnt pathway target genes in SW480 cells.

In LS174T cells decreased H3K79 methylation (Figure 4.2.3b), resulted in mixed dose-dependent effects on Wnt target gene expression (Figure 4.2.3b). The well characterized and validated Wnt target genes, *LGR5*, *EPHB3* and *c-MYC (19-21)* were significantly decreased by loss of H3K79 methylation. These results are consistent with the previous report which showed that H3K79Me2 marks on *LGR5* and *EPHB3* genes correlate with their expression (*13*). *ASCL2* gene expression was not affected by EPZ004777 treatment (Figure 4.2.3b). Surprisingly, LS174T cells with reduced H3K79 methylation had 3-fold greater TOPflash reporter expression, consistent with the higher expression of the Wnt target gene *AXIN2* in the presence of the DOT1L inhibitor (Figure 4.2.3b). These results suggest that in this cell line there is not a direct correlation between H3K79 methylation and Wnt pathway gene activation, consistent with a prior study using crypt basal columnar cells (CBC) expressing the cell surface protein LGR5 (*13*). This study showed that *LGR5*, *EPBH3*, and *AXIN2* are highly expressed in LGR5+ cells compared with villi cells, but H3K79 methylation levels only correlate with expression of *LGR5* and *EPBH3*, while *AXIN2* expression is low in villi cells regardless of high H3K79 methylation levels The treatment of LS174T cells with DOT1L inhibitor for four days did not affect the cell growth indicating that identified changes in the Wnt target genes are not essential for the cell growth and proliferation (Figure 4.2.5).

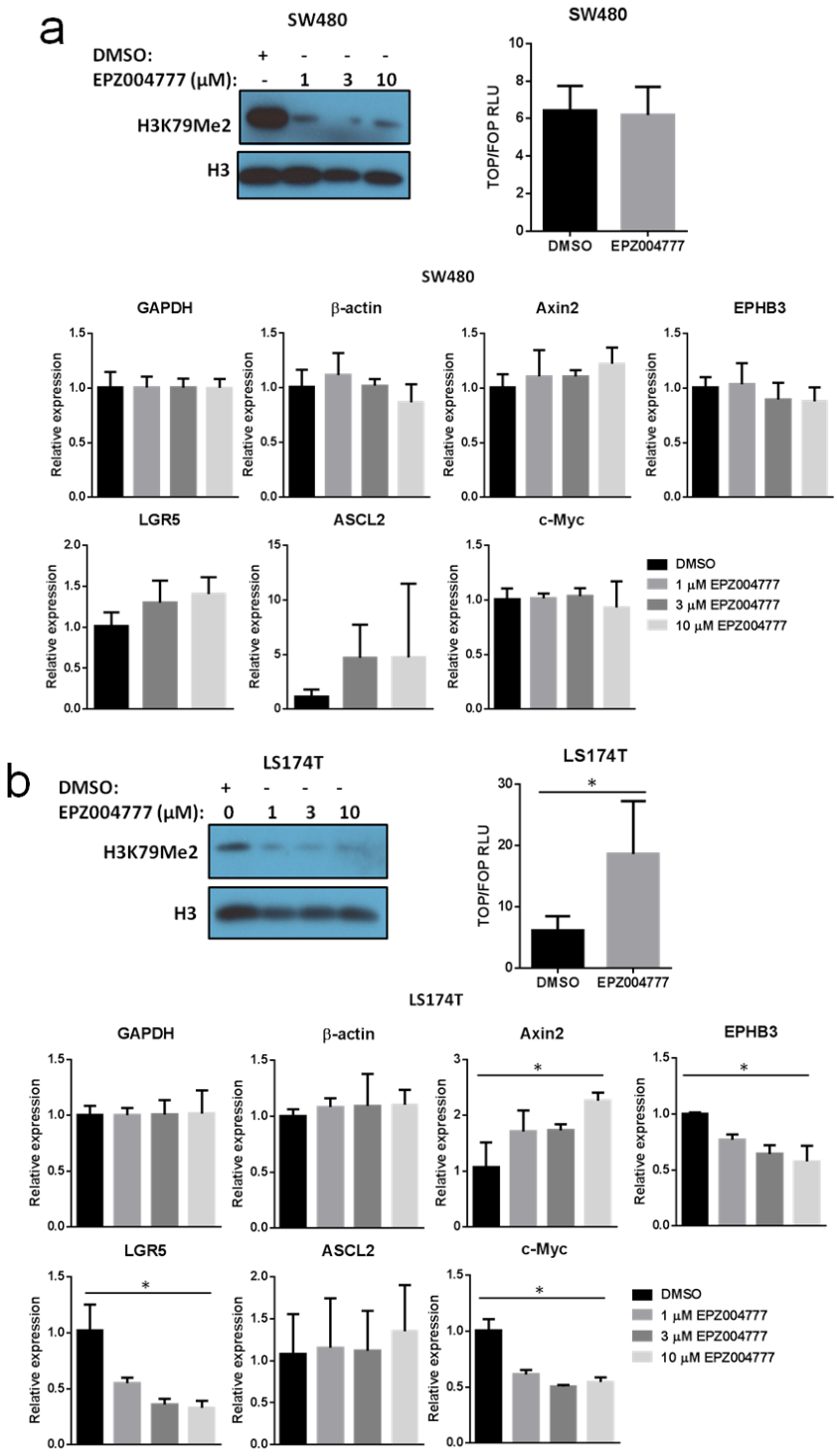

Figure 4.2.3 Wnt target gene expression and TCF/LEF reporter activity in human colon adenocarcinoma-derived cell lines in the absence of DOT1L enzyme activity. Western blot of histone extracts, TOPflash TCF/LEF luciferase reporter assay and qRT-PCR analysis of well characterized Wnt target genes in (a) SW480 and (b) LS174T cell lines after four days treatment with 3 μM EPZ004777. (* $p < 0.05$, n=4, unpaired t-test)

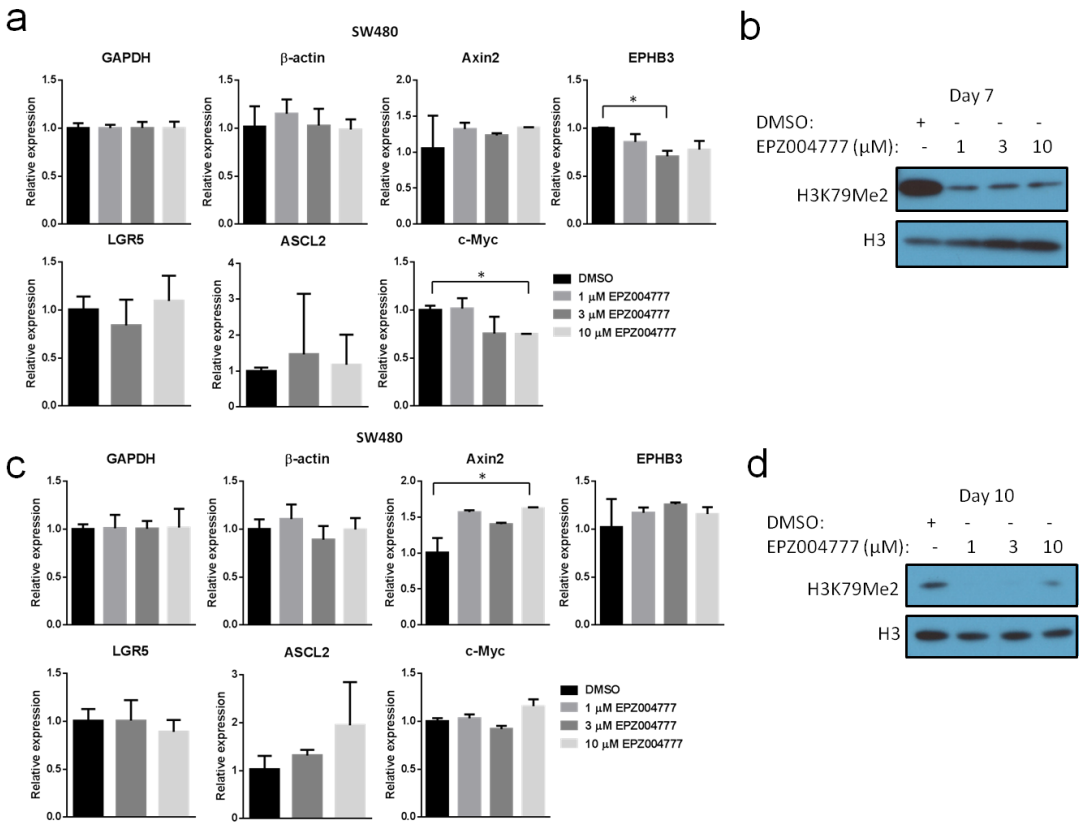

Figure 4.2.4 Wnt target gene expression is not affected by loss of H3K79 methylation in SW480 cells over a time course. (a) qRT-PCR analysis of well characterized Wnt target genes (b) western blot of H3K79 dimethylation in SW480 cells upon 7 days DOT1L inhibition with EPZ004777 at indicated concentrations. (c) qRT-PCR analysis of well characterized Wnt target genes (d) western blot of H3K79 dimethylation in SW480 cells upon 10 days DOT1L inhibition with EPZ004777 at indicated concentrations.

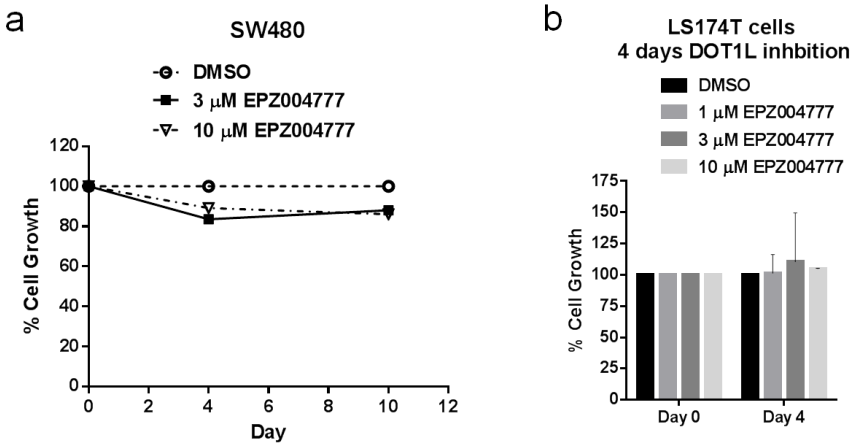

Figure 4.2.5 Proliferation of human colon cancer cell lines is not inhibited by EPZ004777. Cell counts of (a) SW480 cells over at 10 day time course and (b) LS174T cells after 4 days of EPZ04777 treatment at the indicated concentrations.

The results obtained using two human colorectal adenocarcinoma derived cell lines suggest that inhibition of DOT1L activity has cell context-dependent effects, demonstrating either no effect on Wnt signaling pathway as in SW480 or a differential effects on target genes as in LS174T cells. Furthermore, these results indicate that H3K79 methylation is not required for maintaining the cell growth of constitutively “Wnt on” human colon cancer-derived cell lines.

4.2.4 H3K79 methylation distribution in normal and colon cancer human tissue

In order to further assess the importance of DOT1L in colon cancer, we investigated whether H3K79 methylation was altered in patient samples. Using immunohistochemical staining to probe for H3K79 dimethylation, we observed that in three of four tissue samples examined, H3K79 dimethylation was similar in colon adenocarcinoma and adjacent normal colon tissue (Figure 4.2.6a). In one of four cases examined, H3K79 methylation was reduced in the adenocarcinoma tissue compared with normal adjacent colon. Importantly, H3K79 methylation has similar distribution in Wnt-active basal crypts as well as Wnt-inactive superficial crypts of normal and cancerous colon (Figure 4.2.6).

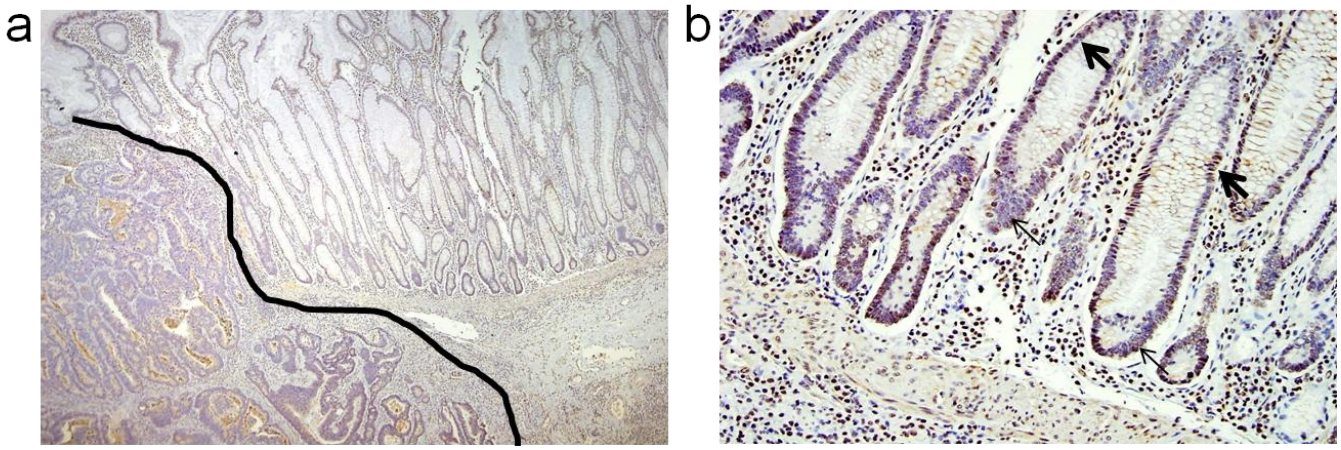

Figure 4.2.6. Immunohistochemical staining of H3K79 dimethylation in (a) colon adenocarcinoma (left) and adjacent normal colon tissue (right); (b) Normal colonic mucosa at high magnification showing positive H3K79 dimethylation staining in basal crypts (narrow arrows) and more superficial crypts (bold arrows).

These results demonstrate that colon carcinomas and Wnt-active tissue do not contain increased H3K79 methylation compared with normal and Wnt-inactive colon tissue. This evidence supports our findings in human colon cancer cell lines that DOT1L is not required for maintenance or activation of Wnt gene expression.

4.3 Methods

4.3.1 Cell culture and compound treatment

293, SW480, or LS174T cells were cultured in DMEM (Life Technologies), 10% fetal bovine serum (FBS; FisherBrand), and 1% Penicillin/Streptomycin (Life Techlonogies) in the presence of EPZ004777 or DMSO control and were split and replated with fresh media and compound every 3-4 days. 293 cells were treated with 5 or 10 μM SB-261763 (Selleck Chemicals) for 24 hr prior to harvesting.

4.3.2 β-catenin-TCF/LEF luciferase reporter (TOPflash) assay

Upon pretreatment of cells with indicated concentrations of EPZ004777 or DMSO, cells were transfected with TOPflash or FOPflash reporter plasmids in conjunction with a renilla-luciferase reporter as a transfection control using Fugene6 (Roche) following manufacturer recommendations. After 24 hr 293 cells were treated with 5 μM SB-216763 after an additional 24 hr cell lysate was collected and luciferase measured using the dual luciferase reporter assay (Promega).

4.3.3 qRT-PCR analysis of gene expression

RNA was isolated by Trizol (Invitrogen) and purified by RNeasy mini kit (Qiagen). cDNA was synthesized using SuperScript III first-strand synthesis (Invitrogen). qPCR analysis was carried out using Power SYBR green PCR master mix (Applied Biosystems) on an 7500 RT-PCR system instrument (Applied Biosystems).

4.3.4 Western blot analysis of H3K79 methylation

Histones were extracted as described (*16*) and protein concentration was determined using Bradford assay (Bio-Rad) and normalized. Samples were denatured by in SDS-

loading buffer and heating and separated on 4-20% Tris-Glycine gel (Invitrogen). Protein was transferred to PVDF membrane (Millipore) and probed with antibodies from Abcam, histone H3 (ab1791), H3K79 Me1 (ab2886), or H3K79Me2 (ab3594). Followed by goat anti rabbit HRP conjugated secondary antibody (GenScript) and signal developed with Lumi-light western blot substrate (Roche) before exposure to autoradiography film (Denville).

4.3.5 Immunohistochemical staining

Immunohistochemical analysis of H3K79Me2 was carried out as previously described (*12*) using anti-H3K79Me2 (ab3594) rabbit polyclonal antibody 1:1,500, 30 minutes.

4.4 Conclusion

Utilizing a chemical biology approach enabled a novel perspective on the role of DOT1L in Wnt signaling by specifically inhibiting H3K79 methylation activity as opposed to genetic elimination of all DOT1L protein expression and function. The studies of DOT1L activity in human colorectal adenocarcinoma cell lines indicate that there is not a conserved dependence on DOT1L H3K79 methylation for expression of Wnt target genes or maintenance of cell growth. Taken together, these results demonstrate that DOT1L H3K79 methylation activity is not essential for a general mechanism of activation or maintenance of Wnt target gene expression. For some Wnt target genes such as EPHB3, LGR5 and c-MYC, DOT1L H3K79 methylation may play a role in sustaining gene expression. As is the case for most cellular genes with complex regulation by a constellation of different transcription factors and chromatin remodeling complexes, variation in the expression of Wnt pathway-regulated genes by DOT1L H3K79 methylation may reflect effects on other proteins and pathways in cultured human cancer cell lines, indicating cell context-dependent mechanism. For example it is known that C-MYC gene is also regulated by p53 (*22*), the transciption factor NFAT1 (*23*), and AKT kinase (*24*). Thus, the effects seen on some Wnt target genes upon DOT1L H3K79 methylation inhibition in the LS174T cell line may reflect the broader role of DOT1L in transcriptional regulation as opposed to a specific role for DOT1L function as a cofactor in Wnt pathway-dependent transcriptional regulation. Furthermore, the

TOPflash reporter system does not require H3K79 methylation for activation or maintnance of a TCF/LEF reporter activity.

In conclusion, DOT1L is an important general regulator of transcriptional activation through H3K79 methylation but is not essential for Wnt pathway target genes. Thus, the use of a potent and selective DOT1L inhibitor as a targeted therapy for treatment of patients with MLL rearrangement leukemia would seem to pose little risk for disruption of Wnt signaling in intestinal homeostasis or potential side effects in intestinal tissues. Furthermore, the results demonstrate that TCF/β-catenin target genes do not require H3K79 methylation for continued expression and H3K79 methylation is not dysregulated in human colorectal cancer samples. As such, DOT1L would not seem to represent a good candidate for therapeutic intervention in colon cancer.

4.5 References

1. Logan, C. Y., and Nusse, R. (2004) The Wnt signaling pathway in development and disease, *Annu Rev Cell Dev Bi 20*, 781-810.
2. Aguilera, O., Munoz, A., Esteller, M., and Fraga, M. F. (2007) Epigenetic alterations of the Wnt/beta-catenin pathway in human disease, *Endocr Metab Immune Disord Drug Targets 7*, 13-21.
3. Roth, W., Wild-Bode, C., Platten, M., Grimmel, C., Melkonyan, H. S., Dichgans, J., and Weller, M. (2000) Secreted Frizzled-related proteins inhibit motility and promote growth of human malignant glioma cells, *Oncogene 19*, 4210-4220.
4. Takada, T., Yagi, Y., Maekita, T., Imura, M., Nakagawa, S., Tsao, S. W., Miyamoto, K., Yoshino, O., Yasugi, T., Taketani, Y., and Ushijima, T. (2004) Methylation-associated silencing of the Wnt antagonist SFRP1 gene in human ovarian cancers, *Cancer Sci 95*, 741-744.
5. Suzuki, H., Watkins, D. N., Jair, K. W., Schuebel, K. E., Markowitz, S. D., Chen, W. D., Pretlow, T. P., Yang, B., Akiyama, Y., Van Engeland, M., Toyota, M., Tokino, T., Hinoda, Y., Imai, K., Herman, J. G., and Baylin, S. B. (2004) Epigenetic inactivation of SFRP genes allows constitutive WNT signaling in colorectal cancer, *Nat Genet 36*, 417-422.
6. Mazieres, J., He, B., You, L., Xu, Z., Lee, A. Y., Mikami, I., Reguart, N., Rosell, R., McCormick, F., and Jablons, D. M. (2004) Wnt inhibitory factor-1 is silenced by promoter hypermethylation in human lung cancer, *Cancer Res 64*, 4717-4720.
7. Anastas, J. N., and Moon, R. T. (2013) WNT signalling pathways as therapeutic targets in cancer, *Nat Rev Cancer 13*, 11-26.
8. Sierra, J., Yoshida, T., Joazeiro, C. A., and Jones, K. A. (2006) The APC tumor suppressor counteracts beta-catenin activation and H3K4 methylation at Wnt target genes, *Gene Dev 20*, 586-600.

9. Mohan, M., Herz, H. M., Takahashi, Y. H., Lin, C. Q., Lai, K. C., Zhang, Y., Washburn, M. P., Florens, L., and Shilatifard, A. (2010) Linking H3K79 trimethylation to Wnt signaling through a novel Dot1-containing complex (DotCom), *Gene Dev 24*, 574-589.
10. Mahmoudi, T., Boj, S. F., Hatzis, P., Li, V. S. W., Taouatas, N., Vries, R. G. J., Teunissen, H., Begthel, H., Korving, J., Mohammed, S., Heck, A. J. R., and Clevers, H. (2010) The Leukemia-Associated Mllt10/Af10-Dot1lAreTcf4/beta-Catenin Coactivators Essential for Intestinal Homeostasis, *Plos Biol 8*.
11. Betancourt, M. C. C., Cailotto, F., Kerkhof, H. J., Cornelis, F. M. F., Doherty, S. A., Hart, D. J., Hofman, A., Luyten, F. P., Maciewicz, R. A., Mangino, M., Metrustry, S., Muir, K., Peters, M. J., Rivadeneira, F., Wheeler, M., Zhang, W. Y., Arden, N., Spector, T. D., Uitterlinden, A. G., Doherty, M., Lories, R. J. U., Valdes, A. M., and van Meurs, J. B. J. (2012) Genome-wide association and functional studies identify the DOT1L gene to be involved in cartilage thickness and hip osteoarthritis, *P Natl Acad Sci USA 109*, 8218-8223.
12. Jo, S. Y., Granowicz, E. M., Maillard, I., Thomas, D., and Hess, J. L. (2011) Requirement for Dot1l in murine postnatal hematopoiesis and leukemogenesis by MLL translocation, *Blood 117*, 4759-4768.
13. Ho, L. L., Sinha, A., Verzi, M., Bernt, K. M., Armstrong, S., and Shivdasani, R. A. (2013) DOT1L-mediated H3K79 methylation in chromatin is dispensable for Wnt pathway-specific and other intestinal epithelial functions, *Mol Cell Biol*.
14. Korinek, V., Barker, N., Morin, P. J., vanWichen, D., deWeger, R., Kinzler, K. W., Vogelstein, B., and Clevers, H. (1997) Constitutive transcriptional activation by a beta-catenin-Tcf complex in APC(-/-) colon carcinoma, *Science 275*, 1784-1787.
15. Coghlan, M. P., Culbert, A. A., Cross, D. A., Corcoran, S. L., Yates, J. W., Pearce, N. J., Rausch, O. L., Murphy, G. J., Carter, P. S., Roxbee Cox, L., Mills, D., Brown, M. J., Haigh, D., Ward, R. W., Smith, D. G., Murray, K. J., Reith, A. D., and Holder, J. C. (2000) Selective small molecule inhibitors of glycogen synthase kinase-3 modulate glycogen metabolism and gene transcription, *Chem Biol 7*, 793-803.
16. Daigle, S. R., Olhava, E. J., Therkelsen, C. A., Majer, C. R., Sneeringer, C. J., Song, J., Johnston, L. D., Scott, M. P., Smith, J. J., Xiao, Y. H., Jin, L., Kuntz, K. W., Chesworth, R., Moyer, M. P., Bernt, K. M., Tseng, J. C., Kung, A. L., Armstrong, S. A., Copeland, R. A., Richon, V. M., and Pollock, R. M. (2011) Selective Killing of Mixed Lineage Leukemia Cells by a Potent Small-Molecule DOT1L Inhibitor, *Cancer Cell 20*, 53-65.
17. Hirsch, C., Campano, L. M., Wohrle, S., and Hecht, A. (2007) Canonical Wnt signaling transiently stimulates proliferation and enhances neurogenesis in neonatal neural progenitor cultures, *Exp Cell Res 313*, 572-587.
18. Li, V. S. W., Ng, S. S., Boersema, P. J., Low, T. Y., Karthaus, W. R., Gerlach, J. P., Mohammed, S., Heck, A. J. R., Maurice, M. M., Mahmoudi, T., and Clevers, H. (2012) Wnt Signaling through Inhibition of beta-Catenin Degradation in an Intact Axin1 Complex, *Cell 149*, 1245-1256.
19. Barker, N., van Es, J. H., Kuipers, J., Kujala, P., van den Born, M., Cozijnsen, M., Haegebarth, A., Korving, J., Begthel, H., Peters, P. J., and Clevers, H. (2007)

Identification of stem cells in small intestine and colon by marker gene Lgr5, *Nature 449*, 1003-U1001.

20. van de Wetering, M., Sancho, E., Verweij, C., de Lau, W., Oving, I., Hurlstone, A., van der Horn, K., Batlle, E., Coudreuse, D., Haramis, A. P., Tion-Pon-Fong, M., Moerer, P., van den Born, M., Soete, G., Pals, S., Eilers, M., Medema, R., and Clevers, H. (2002) The beta-catenin/TCF-4 complex imposes a crypt progenitor phenotype on colorectal cancer cells, *Cell 111*, 241-250.
21. He, T. C., Sparks, A. B., Rago, C., Hermeking, H., Zawel, L., da Costa, L. T., Morin, P. J., Vogelstein, B., and Kinzler, K. W. (1998) Identification of c-MYC as a target of the APC pathway, *Science 281*, 1509-1512.
22. Ho, J. S. L., Ma, W. L., Mao, D. Y. L., and Benchimol, S. (2005) p53-dependent transcriptional repression of c-myc is required for G(1) cell cycle arrest, *Molecular and Cellular Biology 25*, 7423-7431.
23. Mognol, G. P., de Araujo-Souza, P. S., Robbs, B. K., Teixeira, L. K., and Viola, J. P. B. (2012) Transcriptional regulation of the c-Myc promoter by NFAT1 involves negative and positive NFAT-responsive elements, *Cell Cycle 11*, 1014-1028.
24. Vartanian, R., Masri, J., Martin, J., Cloninger, C., Holmes, B., Artinian, N., Funk, A., Ruegg, T., and Gera, J. (2011) AP-1 Regulates Cyclin D1 and c-MYC Transcription in an AKT-Dependent Manner in Response to mTOR Inhibition: Role of AIP4/Itch-Mediated JUNB Degradation, *Mol Cancer Res 9*, 115-130.

CHAPTER 5

5.1 Conclusions and future directions

The histone methyltransferase DOT1L plays a critical role in leukemias bearing translocations of the *MLL* gene. Inhibiting the histone H3 lysine 79 (H3K79) methyltransferase activity of DOT1L represents an attractive therapeutic strategy for the treatment of ALL and AML leukemias resulting from MLL-rearrangements. Furthermore, DOT1L has been implicated as a possible transcriptional coactivator of TCF/β-catenin in Wnt signaling. However, the role of DOT1L HMTase activity has not been fully addressed by present studies utilizing genetic approaches. Herein we have presented several approaches for the identification and biological characterization of novel DOT1L inhibitors and utilized a potent and selective small molecule as a chemical tool to probe the function of DOT1L HMTase activity in Wnt signaling.

5.1.1 Inhibitors of H3K79 methylation identified through biochemical screening

In chapter one, we disclosed several inhibitors of H3K79 methylation. The most potent of which, UMD-7, was identified through biochemical screening. Through secondary validation studies we demonstrated that UMD-7 and related sulfo-naphthyl compounds inhibit H3K79 methylation by binding to the substrate core histones and not the target, DOT1L. These compounds demonstrate rapid inhibition of H3K79 methylation within 24-48 hr as compared to SAM analog DOT1L inhibitors (*1*). Furthermore, UMD-7 inhibition of H3K79 methylation recapitulates the cellular phenotype observed by genetic loss of DOT1L including induction of apoptosis, cell cycle arrest in G0/G1 phase, and induction of differentiation.

Due to the novel mechanism of H3K79 methylation inhibition, UMD-7 may offer a unique chemical tool to study the effect of rapid loss of H3K79 methylation. Several

questions remain to be clarified for this class of compounds. A rigorous demonstration of UMD-7 binding to the biologically relevant nucleosome substrate is important to support binding to histones as the proposed cellular mechanism of H3K79 methylation inhibition. Isothermal titration calorimetry (ITC) is one biophysical method that could be used to verify binding of UMD-7 to nucleosomes and has been used to demonstrate binding of other compounds to histone H3 (*2*). Determining exact binding site of UMD-7 to core histones would facilitate the chemical optimization of these compounds and lead to a mechanistic understanding of its specificity for H3K79 methylation inhibition. It is possible that UMD-7 binds to a region of histone H3 around lysine 79 or perhaps and allosteric site. It is know that H2B ubitquitination (*3-5*) and an acidic patch of histone H4 effect H3K79 methylation (*6, 7*).

Additionally, it will be interesting to investigate how UMD-7 results in rapid H3K79 methylation mark removal in contrast to DOT1L-binding inhibitors which require longer treatment. One possibility is that small molecule binding to the histones induces a histone turnover as a quality control mechanism. Until now, inhibitors of H3K79 methylation acting through direct targeting of DOT1L demonstrate slow kinetics of H3K79 methylation inhibition. The slow loss of H3K79 methylation is attributed to replication dependent histone turnover (*8*) . However, histone turnover at specific gene loci is a dynamic process regulated by numerous histone chaperone proteins and incorporation of histone variants such as H3.3 is associated with active gene transcription and corresponding epigenetic marks (*9*). To further probe the rapid H3K79 methylation loss, the rate of histone turnover should be measured in the presence of UMD-7 in mammalian cells as demonstrated by others to investigate the incorporating of histone variants into chromatin (*9*). It is possible that binding to nucleosomes directly induces a replication-independent mechanism of histone turnover responsible for the rapid loss of H3K79 methylation. Should UMD-7 demonstrate H3K79 methylation inhibition regardless of replication it may provide a useful tool for investigating the role of H3K79 methylation in cell culture systems with little to no replication such as in primary cultured neurons. In summary, UMD-7 provides a chemical tool for inhibition of H3K79 methylation in cells with a novel mechanism that warrants further investigation.

5.1.2 DOT1L inhibitors identified by virtual screening and de novo design

DOT1L binding small molecule inhibitors of H3K79 methylation were identified through structure based virtual screening followed by biochemical validation discussed in Chapter 2. Using the reported structure of DOT1L with SAM (PB ID 1NW3) (*10*) and a modeled complex between DOT1L and EPZ004777, virtual screening was employed and a nucleoside analog focused library of SAM analogues was screened. Based on the obtained results, 210 compounds were selected for biochemical validation as DOT1L inhibitors. This resulted in identification of 7 inhibitors with IC_{50} from 32 – 168 μM. Biophysical evaluation of these compounds demonstrated that they bind to DOT1L in the SAM binding site as predicted by computational modeling. Furthermore, the most potent of these compounds demonstrated selective cellular inhibition of H3K79 methylation in a murine model cell line containing the MLL fusion protein MLL-AF9.

To establish a robust chemical synthetic route which will allow synthesis of novel, more potent nucleoside analogs based on the confirmed hits, a novel synthetic pathway was established. For this purpose, we designed and synthesized several SAM analogues modified at the 5' position of adenosine, discussed in Chapter 3. Our designed SAM analogues took advantage of the crystal structure of DOT1L with SAM (PB ID 1NW3) and led to introduction of a rigid linker between the ribose and the amino acid tail of SAM and bioisosteric replacement of the amino acid with an α-amino acetamide moiety. Ultimately, we established a novel and convenient synthetic pathway for installing modifications at the 5' adenosine or related nucleoside congeners that has utility beyond SAM analogues to build off of nucleoside scaffolds for numerous potential classes of inhibitors. However, the *in vitro* DOT1L inhibition potency of synthesized compounds was low compared to SAM which demonstrates the exquisite sensitivity of the SAM binding pocket to alterations in small molecule ligand structure confirmed by others (*11*).

Future studies of the confirmed nucleoside based DOT1L inhibitors should entail optimization of the chemical structures for improved potency and pharmacokinetic properties. A great deal of progress has been made on DOT1L inhibitors during the course of our studies and others have reported thorough SAR of the 5' tail modifications

of adenosine (*11-14*). However, even the most potent DOT1L inhibitor, EPZ-5676, suffers from poor biological stability due to the inherent metabolically labile adenosine based scaffold (*8*). Some efforts have been made to replace the ribose portion of DOT1L inhibitors with cyclopentane or cyclopentene derivatives with modest improvement in metabolic *in vitro* stability assays (*12*). Future efforts to improve DOT1L inhibitor stability could possibly take advantage of the optimized tail portion of SAM in EPZ-5676 with designed bioisosteres of the ribose and adenine moieties.

5.1.3 Expanding therapeutic implications for DOT1L inhibitors

In addition to chemical modifications of current inhibitors, expanding the implications for these compounds as therapeutics is important. Due to the early phase I success of DOT1L inhibitors demonstrating low toxicity, it may prove useful to test the suitability of DOT1L inhibitors in other forms of leukemia with MLL-translocations that do not directly interact with DOT1L or do not contain MLL-translocation. For instance, EPZ004777 has been demonstrated to be effective in inhibiting the growth of MLL-AF6 transformed murine cells and the AML cell line ML2, containing the MLL-AF6 fusion protein (*15*). The effectiveness of DOT1L inhibition in MLL-AF6 transformed cell lines is intriguing because MLL-AF6 is a cytoplasmic fusion protein and contrary to other MLL-fusion partners such as AF9, AF10, and ENL, AF6 has not been shown to directly interact with DOT1L. Other MLL-translocations resulting in internal partial tandem duplications (PTDs) of MLL which lead to leukemia have also been shown to be sensitive to inhibition of DOT1L. In human leukemia cell lines bearing MLL-PTDs, MUTZ-11 and EOL-1, treatment with EPZ004777 reduced cellular proliferation and lead to apoptosis and differentiation (*16*). Interestingly the downstream effects of *Hoxa* gene cluster downregulation as a result of DOT1L inhibition are similar in MLL-AF6 and MLL-PTD leukemias compared with MLL-translocations that directly interact with DOT1L. The mechanism of DOT1L recruitment and H3K79 dysregulation at *Hoxa* genes in these cell lines may be different from the C-terminal fusion protein mediated recruitment model proposed for other MLL-fusion proteins.

Further studies elucidating the role for DOT1L and H3K79 methylation dysregulation in leukemias with MLL-translocations that do not directly interact with DOT1L would be

useful to predict which genetic aberrations leading to leukemia would be sensitive to DOT1L inhibition as a therapeutic strategy. As MLL and DOT1L both exist in multi-protein complexes it is possible that other MLL-interacting factors such as the polymerase associated factor complex (PAFc) may play a role in indirectly regulating H3K79 methylation. Recruitment of PAFc to MLL-target genes through the N-terminal portion of MLL, maintained in MLL-fusion proteins and MLL-PTDs has been shown to promote Hox gene expression and leukemogenesis (*17*). The hypothesis that PAFc mediated dysregulation of H3K79 methylation could be tested by investigating the localization of DOT1L to MLL target genes such as *Hoxa* genes in the presence of wild type or MLL-PTDs with partial deletions of PAFc or expression of dominant negative fragments that block PAFc recruitment to MLL-target genes. Furthermore, PAFc is important for regulating H2B-ubiquitination which promotes H3K79 methylation through histone cross talk (*17*). Probing the levels of H2B ubiquitination and H3K79 methylation at MLL-target genes upon disruption of PAFc recruitment could help to elucidate whether PAFc is important for mediating the sensitivity of MLL-PTD cell lines to DOT1L inhibition.

Furthermore, some evidence shows that EPZ004777 has efficacy in reducing the proliferation of primary AML cells without any MLL translocations, but instead harboring mutations of the isocitrate dehydrogenase (IDH) genes *IDH1* and *IDH2* (*18*). These mutations lead to important epigenetic changes unrelated to histone methylation but rather DNA hypermethylation as a result of inhibition of TET-2 mediated 5-hydroxymethylation (*19*). This process occurs as a result of mutations in IDH that produce the oncometabolite 2-hydroxygluterate (2-HG) which inhibits numerous enzymes involved in epigenetic regulation (*20*). Interestingly, mutations in IDH1 and IDH2 show dysregulation of numerous histone methylation marks, including increased global H3K79 methylation. The mechanism by which these mutations lead to alterations in H3K79 methylation and how they may regulate DOT1L is not understood and presents an attractive avenue for future investigation.

Although our studies demonstrate that DOT1L is not likely a viable therapeutic target colon cancer, it may prove useful to investigate the targeting of DOT1L in other solid

tumors. Due to the diverse role of DOT1L in normal development and the availability of low toxicity potent and selective inhibitors, EPZ004777 and EPZ-5676 the efficacy of DOT1L inhibition should be investigated in numerous human malignancies. One possibility is to screen a diverse panel of human cancer cell lines for growth inhibition in the presence of DOT1L inhibitors. The National Cancer Institute (NCI) provides a panel of 60 human cancer cell lines for the screening of potential anticancer drugs that would provide and important starting point for this experiment. An additional important consideration for this type of study is that DOT1L inhibition shows slow growth inhibition kinetics in sensitive leukemia cell lines often taking seven days or more for noticeable effects.

5.1.4 DOT1L in Wnt signaling

We investigated the role of DOT1L in Wnt signaling using a chemical biology approach in human cell lines including two colon carcinoma cell lines with mutations in the Wnt signaling pathway. Our findings indicate that there is a cell context dependent effect of H3K79 methylation on the expression of endogenous Wnt target genes. Importantly, DOT1L HMTase activity is not required for activation or maintenance of expression of a TCF/β-catenin dependent reporter gene. These findings are in agreement with previous studies utilizing genetic approaches (*21-23*) and suggests that DOT1L is likely not a viable therapeutic target in colon cancer.

Due to the importance of Wnt signaling in maintenance of leukemia stem cells (*24-28*), investigating the role of DOT1L as a transcriptional coactivator of Wnt target genes in the context of leukemia could provide valuable insight into the contribution of Wnt signaling in leukemia and broaden the scope and implications of DOT1L in leukemia. In order to address whether or not DOT1L is important for Wnt signaling in the context of leukemia, chemical and genetic approaches can be used in parallel.

Utilizing the conditional knockout model of DOT1L (*22*), murine bone marrow can be transformed with various leukemogenic oncogenes such as MLL-AF9, Hoxa9/Meis1, and E2A-HLF. Upon transformation with each of these oncogenes, exogenous wild type DOT1L, an enzymatically inactive RCR DOT1L mutant, a ten amino acid deletion

(Δ10aa) DOT1L mutant, or a control vector can be introduced to replace the subsequent removal of endogenous DOT1L. Next, endogenous DOT1L can be knocked out upon treatment with 4-hydroxy tamoxifen (4-OHT) which induces the expression of Cre recombinase that excises the floxed DOT1L gene. Based on previous studies, the MLL-AF9 transformed cells proliferation will be inhibited after several days of DOT1L knockout with vector control unless rescued by exogenous wild type DOT1L. Thus, the wild type DOT1L will rescue the colony forming ability and growth potential of MLL-AF9 cells upon the excision of endogenous DOT1L. However, introducing an enzymatically inactive RCR mutant or a mutant with a 10 amino acid deletion (Δ10aa), mediating the interaction with MLL-AF9, will not rescue the colony forming abilities of MLL-AF9 transformed bone marrow (*22, 29*). Hoxa9/Meis1 and E2A-HLF transformed cells will proliferate without the presence of endogenous DOT1L since they do not depend on DOT1L and the removal of endogenous DOT1L by Cre excision provides an excellent genetic tool to examine the effects of reintroduced DOT1L mutants.

This system can be utilized to study the role of DOT1L in Wnt signaling in leukemic cells by using the MLL-AF9, Hoxa9/Meis1, and E2A-HLF transformed cells, transfecting them with wild type DOT1L, enzymatically inactive RCR DOT1L mutant, or Δ10aa DOT1L followed by inducing knockout of endogenous DOT1L, then measuring the effects on Wnt target gene expression. Depending on the basal level of Wnt signaling in these cells, if Wnt signaling is low, exogenous Wnt ligand or chemical activators of Wnt signaling such as SB216763 can be added to induce activation of Wnt target genes.

Additionally, these tools could be used to address the differences between DOT1L enzymatic activity and recruitment by MLL-AF9. If DOT1L enzymatic activity and recruitment are important for Wnt signaling, we would expect that wild type DOT1L would be able to facilitate active Wnt target gene expression but the RCR or Δ10aa DOT1L mutants would have decreased Wnt target gene expression. However, as our data show that enzymatic activity of DOT1L is not required for Wnt target gene expression it is possible that previous affects observed using genetic knockdown of DOT1L were mediated by recruitment or scaffolding functions mediated DOT1L. In this

case, if recruitment but not enzymatic activity of DOT1L is essential for Wnt target gene expression,

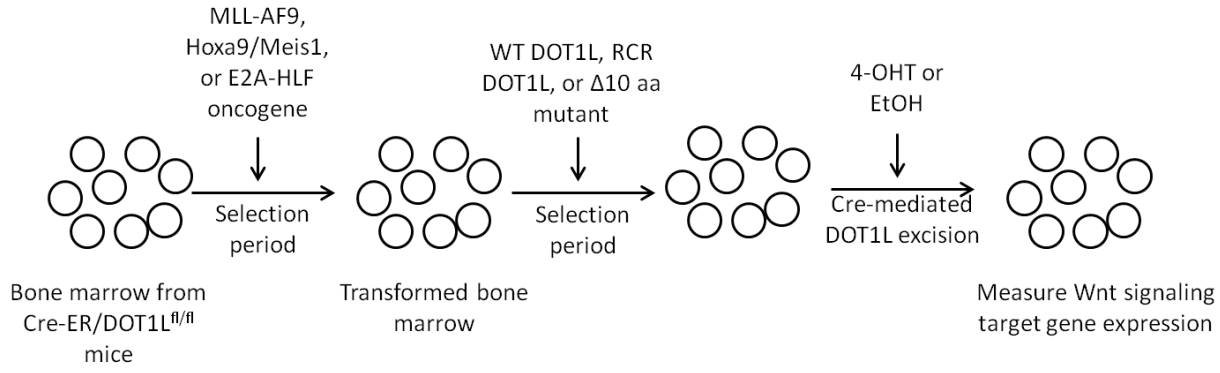

Figure 5.1.1 Schematic experimental design testing the role of DOT1L in Wnt signaling in leukemia.

Alternatively, a chemical biology approach can be used to inhibit DOT1L H3K79 methylation activity in MLL-AF9, Hoxa9/Meis1, and E2A-HLF transformed murine bone marrow. Upon inhibition of DOT1L, analysis of Wnt target gene expression can be used to determine whether H3K79 methylation is required for activation or maintenance of Wnt target genes in hematopoietic progenitor cells. These results may either confirm the observations made in human colorectal cancer cell lines, or provide different results that could implicate a tissue specific role for DOT1L in Wnt signaling.

5.1.5 The role of DOT1L in normal hematopoiesis

Initially, it was demonstrated that DOT1L is required for embryonic development and DOT1L null mice die between 9.5-13.5 days post coitum (*23, 30*). DOT1L deficient mice suffered from anemia and defective erythroid differentiation (*23*). Considering the potential for targeting DOT1L in leukemia, there is significant interest to investigate the role of DOT1L in normal hematopoiesis in developed mice. Therefore, conditional knockout models of DOT1L were developed and demonstrated that DOT1L is essential for maintenance of normal adult hematopoiesis and inducible knockout lead to depletion of hematopoietic stem cells and various lineage progenitors (granulocyte, monocyte, megakaryocyte, erythrocyte, and common myeloid) resulting in severe anemia and hypocellularity in the bone marrow (*22, 31*). These two studies indicate that DOT1L

inhibitors may potentially have serious side effects. In contrast, a third study using DOT1L knockout in the hematopoietic compartment starting during embryonic development reported that mice display anemia with hypocellularity in the bone marrow, but DOT1L depletion did not cause a total loss of myeloid or lymphoid development (*32*). Additional studies which target the enzymatic activity of DOT1L by treating with with the small molecule inhibitor EPZ004777 for 14 days demonstrate a decrease in committed progenitor cells that was most apparent in common myeloid progenitors and megakaryocyte/erythroid common progenitors; however the hematopoietic stem cell population was not affected (*1*). All of these studies provided different conclusions which may be caused by the differences in experimental models or the levels of DOT1L deletion.

Thus, these results prompt the need for further studies to investigate the role of DOT1L in normal hematopoiesis as well as different strategies to target DOT1L. One particularly attractive approach is the targeting of protein-protein interactions between DOT1L and MLL-fusion proteins such as MLL-AF9 and MLL-ENL. This approach offers the potential benefit of inhibiting DOT1L recruitment to MLL-target genes while allowing for normal H3K79 methylation regulation in hematopoietic stem cells and other cellular lineages. Therefore, we predicted that cells containing the MLL-fusion proteins will be selectively sensitive to inhibitors blocking the AF9 or ENL interaction with DOT1L. Although it has been shown that preventing the interaction between MLL-AF9 and DOT1L results in a failure in transformation capabilities of MLL-AF9 (*29*), it needs to be investigated whether disruption of the AF9 or ENL interaction affects normal hematopoietic stem cells and lineage progenitors.

In order to test whether inhibiting DOT1L interaction with AF9 and ENL has less affect on normal hematopoiesis than inhibition of H3K79 methylation activity, exogenous DOT1L constructs can be introduced into bone marrow from mice with conditionally excisable endogenous DOT1L as previously described. The ability of reintroduced DOT1L constructs to recapitulate the function of endogenous DOT1L shall provide insight into the requirement for DOT1L interaction with AF9 and ENL in normal hematopoiesis. To test this, the control would be introduction of wild-type DOT1L

construct into bone marrow of mice with floxed DOT1L allele and induction of Cre expression with 4-OHT to induce excision of endogenous DOT1L. The introduced wild-type DOT1L is predicted to function in place of lost endogenous DOT1L and upon transplantation of that bone marrow into lethally irradiated recipient mice, should be able to properly restore the hematopoietic compartment, allowing the restoration of hematopoietic lineages and allowing the mice to survive. This system will then allow us to compare the differences between reintroducing DOT1L lacking enzymatic activity (RCR mutant) or lacking the ten amino acid sequence of DOT1L required for interaction with AF9 and ENL (Δ10 aa). Based on previous studies for the requirement of DOT1L in maintenance of adult hematopoiesis (*22, 31*) we predict that the DOT1L enzymatically inactive construct will not be able to replace lost endogenous DOT1L and that the bone marrow will fail to rescue the lethally irradiated recipient mice. The critical unknown that this experiment seeks to address is whether or not the DOT1L mutant lacking the ability to interact with AF9 and ENL will be able to recapitulate the function of endogenous DOT1L. If this is the case and bone marrow containing DOT1L with a disrupted protein –protein interaction motif is able to rescue lethally irradiated recipient mice, then this will strongly support the idea that targeting the protein-protein interaction between DOT1L and AF9 or ENL is more therapeutically attractive and there is less concern for toxicity of normal bone marrow and disruption of hematopoietic stem cells using this targeting approach.

5.1.6 Summary

The histone H3K79 methyltransferase DOT1L is an important therapeutic target in MLL-translocations leukemias. When this work began, there were no reported inhibitors of DOT1L methyltransferase activity. Here we present the identification of several classes of novel small molecule inhibitors of H3K79 methylation with both SAM competitive binding to DOT1L, **2.2**, and with a unique histone binding mechanism of action UMD-7. While this work was in progress, several other SAM competitive inhibitors have been reported, of which, the most developed, EPZ-5676, has entered clinical trials. The DOT1L inhibitors we identified and characterized in this work contribute to the growing knowledge of SAM analog activity as DOT1L inhibitors. Furthermore, we present a

novel synthetic pathway for 5' adenosine modifications that has utility beyond DOT1L inhibitors for the synthesis and modification of various nucleosides. Our discovery of the histone binding UMD-7 presents a novel mechanism of H3K79 methylation inhibition and phenocopies genetic loss of DOT1L, therefore offering a valuable chemical tool for probing the biological effects of H3K79 methylation inhibition.

Lastly, we applied a chemical biology approach to investigate the role of DOT1L in Wnt signaling. The specific inhibition of H3K79 methylation with a chemical tool, EPZ004777, represents a novel approach for elucidating the function of DOT1L in Wnt signaling. Previous genetic approaches resulted in apparently contradictory implications for the necessity of DOT1L as a transcriptional coactivator of Wnt signaling. Here we contributed to the field of epigenetic regulation of Wnt signaling by demonstrating that H3K79 methylation activity is not essential for activation of canonical Wnt-pathway target genes.

5.2 References

1. Daigle, S. R., Olhava, E. J., Therkelsen, C. A., Majer, C. R., Sneeringer, C. J., Song, J., Johnston, L. D., Scott, M. P., Smith, J. J., Xiao, Y. H., Jin, L., Kuntz, K. W., Chesworth, R., Moyer, M. P., Bernt, K. M., Tseng, J. C., Kung, A. L., Armstrong, S. A., Copeland, R. A., Richon, V. M., and Pollock, R. M. (2011) Selective Killing of Mixed Lineage Leukemia Cells by a Potent Small-Molecule DOT1L Inhibitor, *Cancer Cell 20*, 53-65.
2. Selvi, B. R., Batta, K., Kishore, A. H., Mantelingu, K., Varier, R. A., Balasubramanyam, K., Pradhan, S. K., Dasgupta, D., Sriram, S., Agrawal, S., and Kundu, T. K. (2010) Identification of a Novel Inhibitor of Coactivator-associated Arginine Methyltransferase 1 (CARM1)-mediated Methylation of Histone H3 Arg-17, *J Biol Chem 285*, 7143-7152.
3. Nakanishi, S., Lee, J. S., Gardner, K. E., Gardner, J. M., Takahashi, Y., Chandrasekharan, M. B., Sun, Z. W., Osley, M. A., Strahl, B. D., Jaspersen, S. L., and Shilatifard, A. (2009) Histone H2BK123 monoubiquitination is the critical determinant for H3K4 and H3K79 trimethylation by COMPASS and Dot1, *J Cell Biol 186*, 371-377.
4. Ng, H. H., Xu, R. M., Zhang, Y., and Struhl, K. (2002) Ubiquitination of histone H2B by Rad6 is required for efficient Dot1-mediated methylation of histone H3 lysine 79, *J Biol Chem 277*, 34655-34657.
5. McGinty, R. K., Kim, J., Chatterjee, C., Roeder, R. G., and Muir, T. W. (2008) Chemically ubiquitylated histone H2B stimulates hDot1L-mediated intranucleosomal methylation, *Nature 453*, 812-U812.

6. Altaf, M., Utley, R. T., Lacoste, N., Tan, S., Briggs, S. D., and Cote, J. (2007) Interplay of chromatin modifiers on a short basic patch of histone H4 tail defines the boundary of telomeric heterochromatin, *Mol Cell 28*, 1002-1014.
7. Fingerman, I. M., Li, H. C., and Briggs, S. D. (2007) A charge-based interaction between histone H4 and Dot1 is required for H3K79 methylation and telomere silencing: identification of a new trans-histone pathway, *Gene Dev 21*, 2018-2029.
8. Daigle, S. R., Olhava, E. J., Therkelsen, C. A., Basavapathruni, A., Jin, L., Boriack-Sjodin, P. A., Allain, C. J., Klaus, C. R., Raimondi, A., Scott, M. P., Waters, N. J., Chesworth, R., Moyer, M. P., Copeland, R. A., Richon, V. M., and Pollock, R. M. (2013) Potent inhibition of DOT1L as treatment of MLL-fusion leukemia, *Blood 122*, 1017-1025.
9. Kraushaar, D. C., Jin, W. F., Maunakea, A., Abraham, B., Ha, M., and Zhao, K. J. (2013) Genome-wide incorporation dynamics reveal distinct categories of turnover for the histone variant H3.3, *Genome Biol 14*.
10. Min, J. R., Feng, Q., Li, Z. Z., Zhang, Y., and Xu, R. M. (2003) Structure of the catalytic domain of human DOT1L, a Non-SET domain nucleosomal histone methyltransferase, *Cell 112*, 711-723.
11. Anglin, J. L., Deng, L. S., Yao, Y., Cai, G. B., Liu, Z., Jiang, H., Cheng, G., Chen, P. H., Dong, S., and Song, Y. C. (2012) Synthesis and Structure-Activity Relationship Investigation of Adenosine-Containing Inhibitors of Histone Methyltransferase DOT1L, *J Med Chem 55*, 8066-8074.
12. Deng, L. S., Zhang, L., Yao, Y., Wang, C., Redell, M. S., Dong, S., and Song, Y. C. (2013) Synthesis, activity and metabolic stability of non-ribose containing inhibitors of histone methyltransferase DOT1L, *Medchemcomm 4*, 822-826.
13. Yao, Y., Chen, P. H., Diao, J. S., Cheng, G., Deng, L. S., Anglin, J. L., Prasad, B. V. V., and Song, Y. C. (2012) Selective Inhibitors of Histone Methyltransferase DOT1L: Design, Synthesis, and Crystallographic Studies, *J Am Chem Soc 134*, 17834-17834.
14. Yu, W. Y., Smil, D., Li, F. L., Tempel, W., Fedorov, O., Nguyen, K. T., Bolshan, Y., Al-Awar, R., Knapp, S., Arrowsmith, C. H., Vedadi, M., Brown, P. J., and Schapira, M. (2013) Bromo-deaza-SAH: A potent and selective DOT1L inhibitor, *Bioorgan Med Chem 21*, 1787-1794.
15. Deshpande, A. J., Chen, L., Fazio, M., Sinha, A. U., Bernt, K. M., Banka, D., Dias, S., Chang, J., Olhava, E. J., Daigle, S. R., Richon, V. M., Pollock, R. M., and Armstrong, S. A. (2013) Leukemic transformation by the MLL-AF6 fusion oncogene requires the H3K79 methyltransferase Dot1l, *Blood 121*, 2533-2541.
16. Kuhn, M. W. M., Hadler, M., Daigle, S. R., Chen, C. W., Sinha, A. U., Krivtsov, A. V., Olhava, E. J., Caligiuri, M. A., Bradner, J. E., Pollock, R. M., and Armstrong, S. A. (2013) Myeloid Leukemia Cells With MLL partial Tandem Duplication Are Sensitive To Pharmacological Inhibition Of The H3K79 Methyltransferase DOT1L, *Blood 122*.
17. Muntean, A. G., Tan, J. Y., Sitwala, K., Huang, Y. S., Bronstein, J., Connelly, J. A., Basrur, V., Elenitoba-Johnson, K. S. J., and Hess, J. L. (2010) The PAF Complex Synergizes with MLL Fusion Proteins at HOX Loci to Promote Leukemogenesis, *Cancer Cell 17*, 609-621.

18. Sarkaria, S. M., Christopher, M. J., Klco, J. M., and Ley, T. J. (2014) Primary acute myeloid leukemia cells with IDH1 or IDH2 mutations respond to a DOT1L inhibitor in vitro, *Leukemia*.
19. Rakheja, D., Konoplev, S., Medeiros, L. J., and Chen, W. N. (2012) IDH mutations in acute myeloid leukemia, *Hum Pathol 43*, 1541-1551.
20. Lu, C., Ward, P. S., Kapoor, G. S., Rohle, D., Turcan, S., Abdel-Wahab, O., Edwards, C. R., Khanin, R., Figueroa, M. E., Melnick, A., Wellen, K. E., O'Rourke, D. M., Berger, S. L., Chan, T. A., Levine, R. L., Mellinghoff, I. K., and Thompson, C. B. (2012) IDH mutation impairs histone demethylation and results in a block to cell differentiation, *Nature 483*, 474-U130.
21. Ho, L. L., Sinha, A., Verzi, M., Bernt, K. M., Armstrong, S. A., and Shivdasani, R. A. (2013) DOT1L-mediated H3K79 methylation in chromatin is dispensable for Wnt pathway-specific and other intestinal epithelial functions, *Mol Cell Biol 33*, 1735-1745.
22. Jo, S. Y., Granowicz, E. M., Maillard, I., Thomas, D., and Hess, J. L. (2011) Requirement for Dot1l in murine postnatal hematopoiesis and leukemogenesis by MLL translocation, *Blood 117*, 4759-4768.
23. Feng, Y., Yang, Y. P., Ortega, M. M., Copeland, J. N., Zhang, M. C., Jacob, J. B., Fields, T. A., Vivian, J. L., and Fields, P. E. (2010) Early mammalian erythropoiesis requires the Dot1L methyltransferase, *Blood 116*, 4483-4491.
24. Lu, D. S., Zhao, Y. D., Tawatao, R., Cottam, H. B., Sen, M., Leoni, L. M., Kipps, T. J., Corr, M., and Carson, D. A. (2004) Activation of the Wnt signaling pathway in chronic lymphocytic leukemia, *P Natl Acad Sci USA 101*, 3118-3123.
25. Anastas, J. N., and Moon, R. T. (2013) WNT signalling pathways as therapeutic targets in cancer, *Nat Rev Cancer 13*, 11-26.
26. Wang, Y. Z., Krivtsov, A. V., Sinha, A. U., North, T. E., Goessling, W., Feng, Z. H., Zon, L. I., and Armstrong, S. A. (2010) The Wnt/beta-Catenin Pathway Is Required for the Development of Leukemia Stem Cells in AML, *Science 327*, 1650-1653.
27. Ysebaert, L., Chicanne, G., Demur, C., De Toni, F., Prade-Houdellier, N., Ruidavets, J. B., Mansat-De Mas, V., Rigal-Huguet, F., Laurent, G., Payrastre, B., Manenti, S., and Racaud-Sultan, C. (2006) Expression of beta-catenin by acute myeloid leukemia cells predicts enhanced clonogenic capacities and poor prognosis, *Leukemia 20*, 1211-1216.
28. Zhao, C., Blum, J., Chen, A., Kwon, H. Y., Jung, S. H., Cook, J. M., Lagoo, A., and Reyal, T. (2007) Loss of beta-catenin impairs the renewal of normal and CML stem cells in vivo, *Cancer Cell 12*, 528-541.
29. Shen, C. X., Jo, S. Y., Liao, C. Z., Hess, J. L., and Nikolovska-Coleska, Z. (2013) Targeting Recruitment of Disruptor of Telomeric Silencing 1-like (DOT1L) CHARACTERIZING THE INTERACTIONS BETWEEN DOT1L AND MIXED LINEAGE LEUKEMIA (MLL) FUSION PROTEINS, *J Biol Chem 288*, 30585-30596.
30. Jones, B., Su, H., Bhat, A., Lei, H., Bajko, J., Hevi, S., Baltus, G. A., Kadam, S., Zhai, H. L., Valdez, R., Gonzalo, S., Zhang, Y., Li, E., and Chen, T. P. (2008) The Histone H3K79 Methyltransferase Dot1L Is Essential for Mammalian Development and Heterochromatin Structure, *Plos Genet 4*.

31. Nguyen, A. T., He, J., Taranova, O., and Zhang, Y. (2011) Essential role of DOT1L in maintaining normal adult hematopoiesis, *Cell Res 21*, 1370-1373.
32. Bernt, K. M., Zhu, N., Sinha, A. U., Vempati, S., Faber, J., Krivtsov, A. V., Feng, Z. H., Punt, N., Daigle, A., Bullinger, L., Pollock, R. M., Richon, V. M., Kung, A. L., and Armstrong, S. A. (2011) MLL-Rearranged Leukemia Is Dependent on Aberrant H3K79 Methylation by DOT1L, *Cancer Cell 20*, 66-78.

Appendix I

^{1}H NMR spectra of synthesized compounds described in chapter 3.

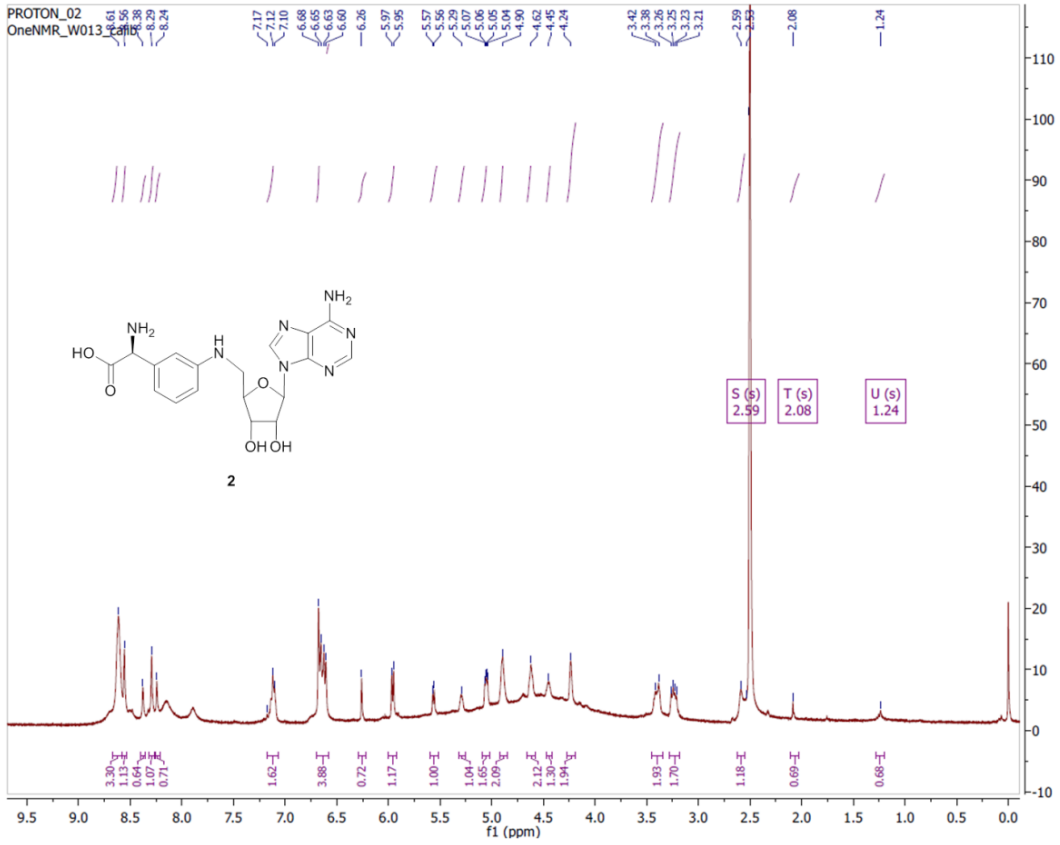

2

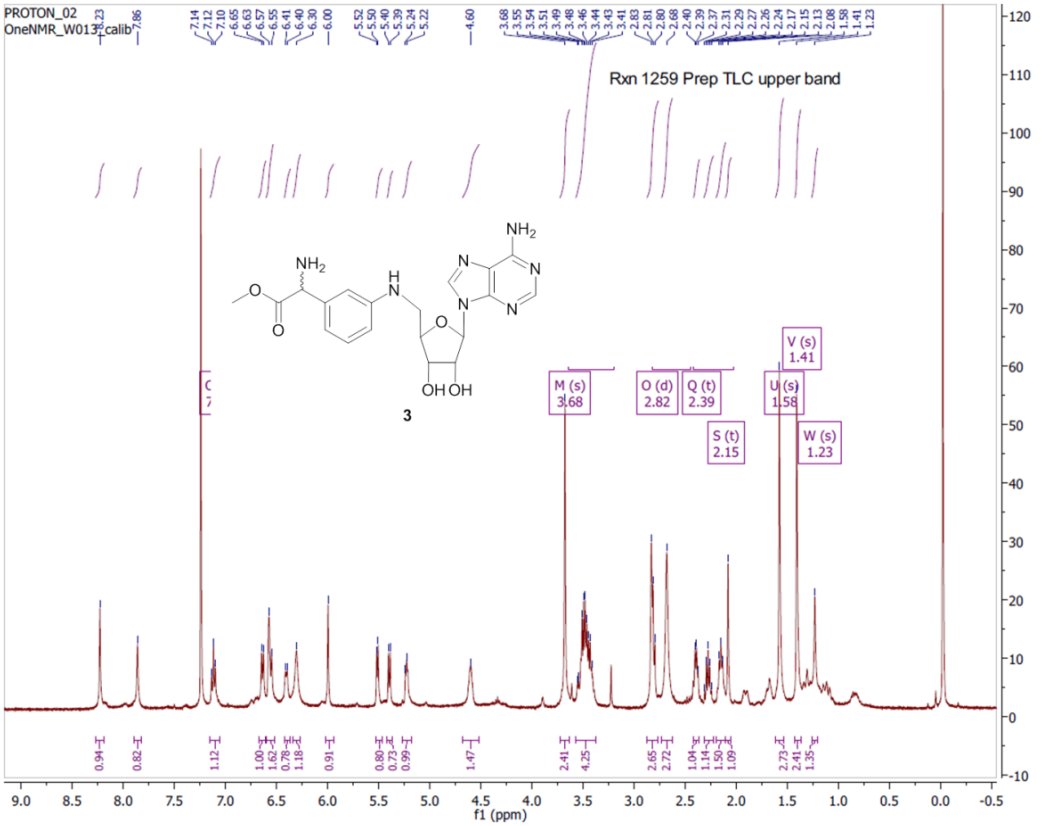
PROTON_02
OneNMR_W013_calib
Rxn 1259 Prep TLC upper band
M (s)
3.68
O (d)
2.82
Q (t)
2.39
S (t)
2.15
V (s)
1.41
W (s)
1.23
3
f1 (ppm)

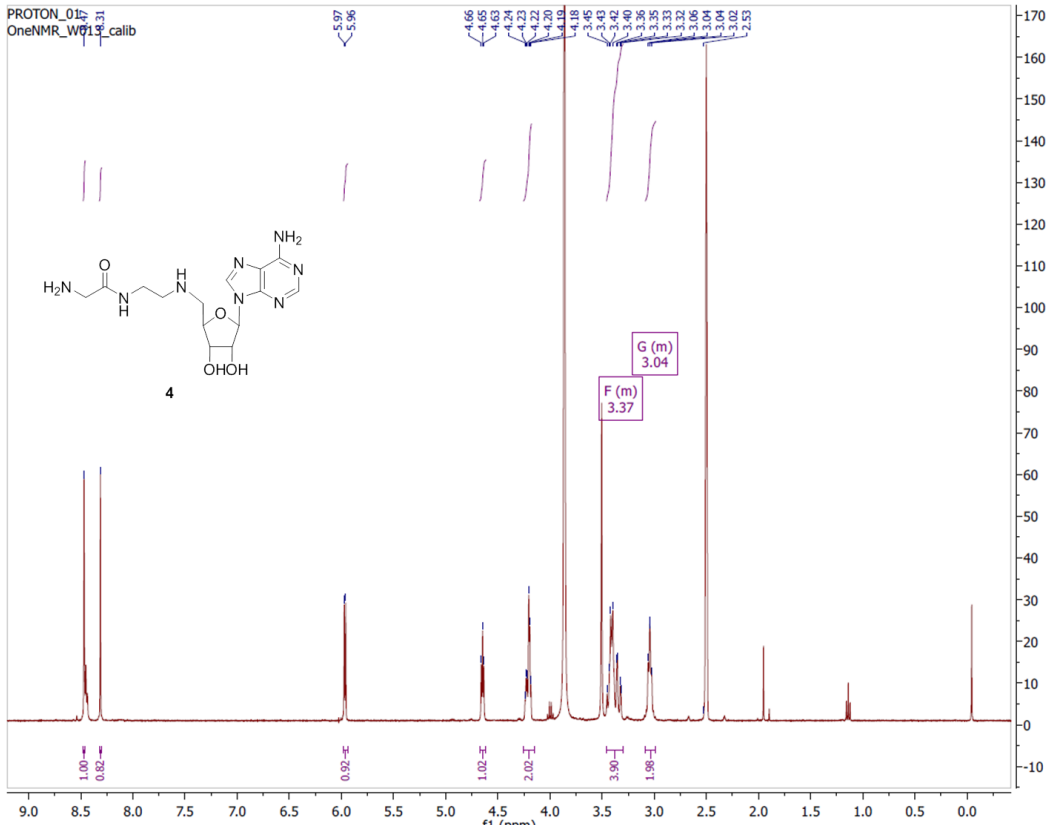
PROTON_01
OneNMR_W013_calib
G (m)
3.04
F (m)
3.37
4
f1 (ppm)

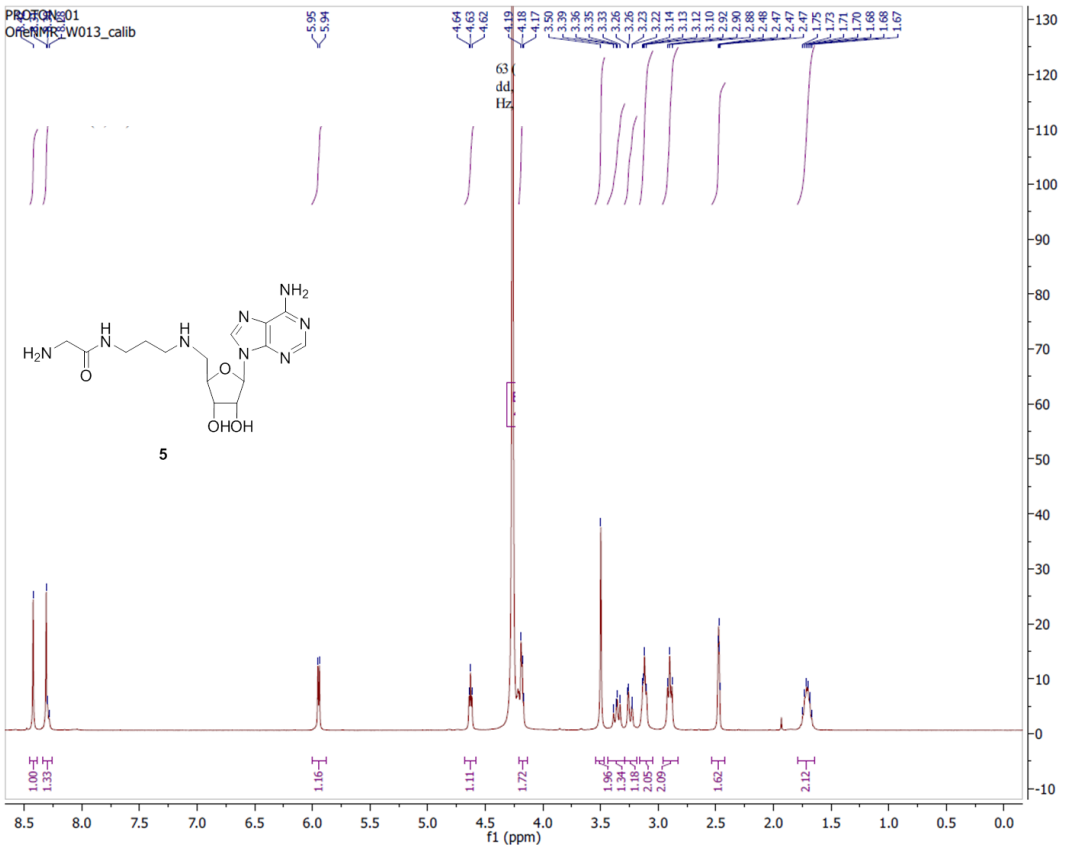
PROTON_01
One_NMR_W013_calib
5.95
5.94
4.64
4.63
4.62
4.19
4.18
4.17
3.50
3.39
3.36
3.35
3.33
3.26
3.26
3.23
3.22
3.14
3.13
3.12
3.10
2.92
2.90
2.88
2.48
2.47
2.47
2.47
1.75
1.73
1.71
1.70
1.68
1.68
1.67
NH2
H2N
OHOH
5
1.00
1.33
1.16
1.11
1.72
1.96
1.34
1.18
2.05
2.09
1.62
2.12
f1 (ppm)

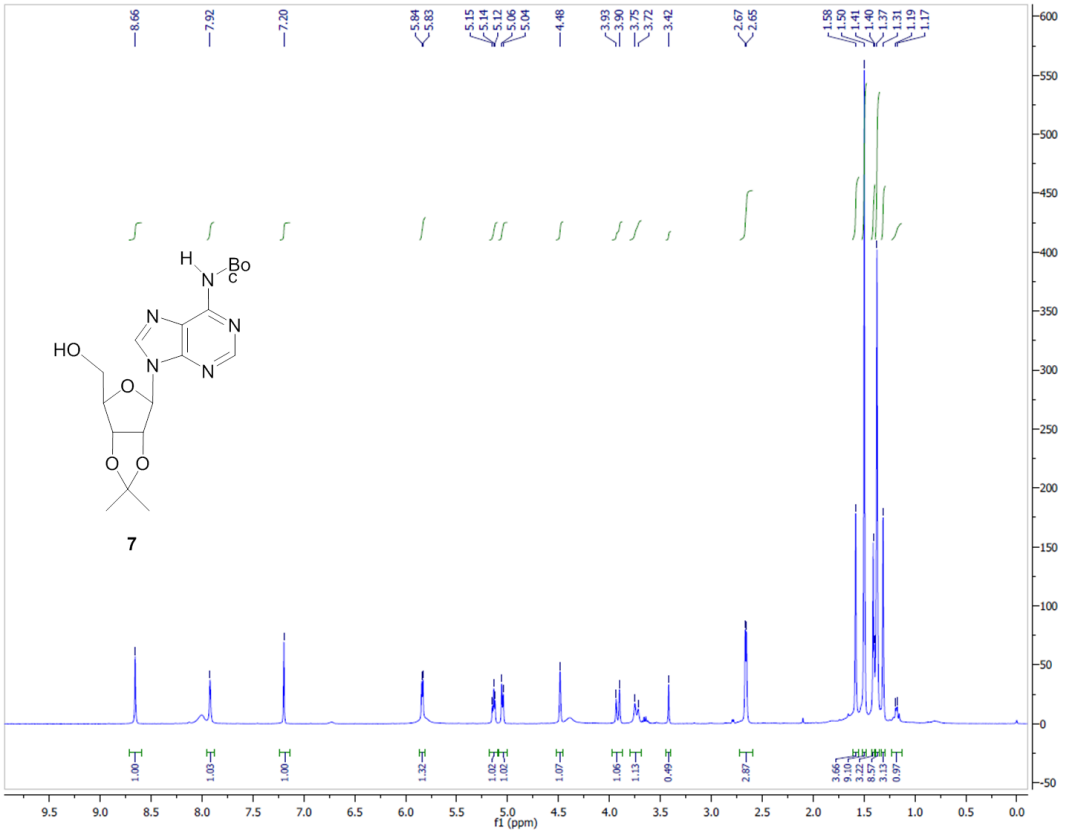
8.66
7.92
7.20
5.84
5.83
5.15
5.14
5.12
5.06
5.04
4.48
3.93
3.90
3.75
3.72
3.42
2.67
2.65
1.58
1.50
1.41
1.40
1.37
1.31
1.19
1.17
Boc
HO
7
1.00
1.03
1.00
1.32
1.02
1.02
1.07
1.06
1.13
0.49
2.87
3.66
9.10
3.22
8.57
3.13
0.97
f1 (ppm)

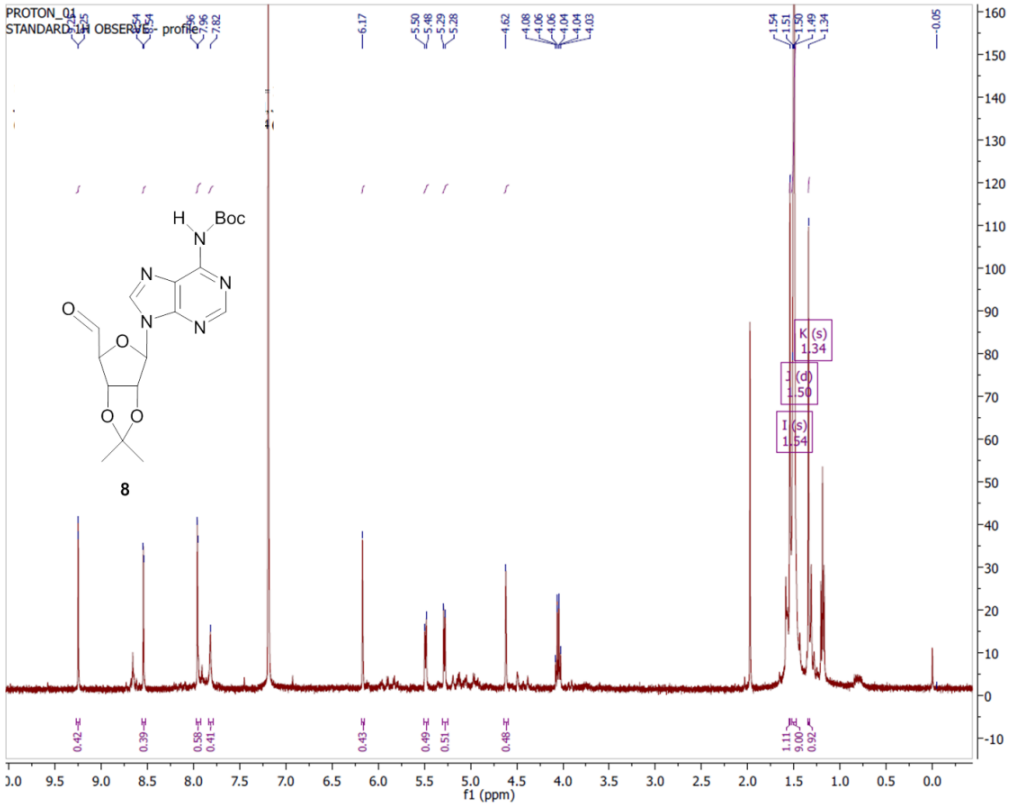
PROTON_01
STANDARD_1H OBSERVE_ profile
H
Boc
N
O
O
O
O
8
K (s)
1.34
I (s)
1.54
f1 (ppm)

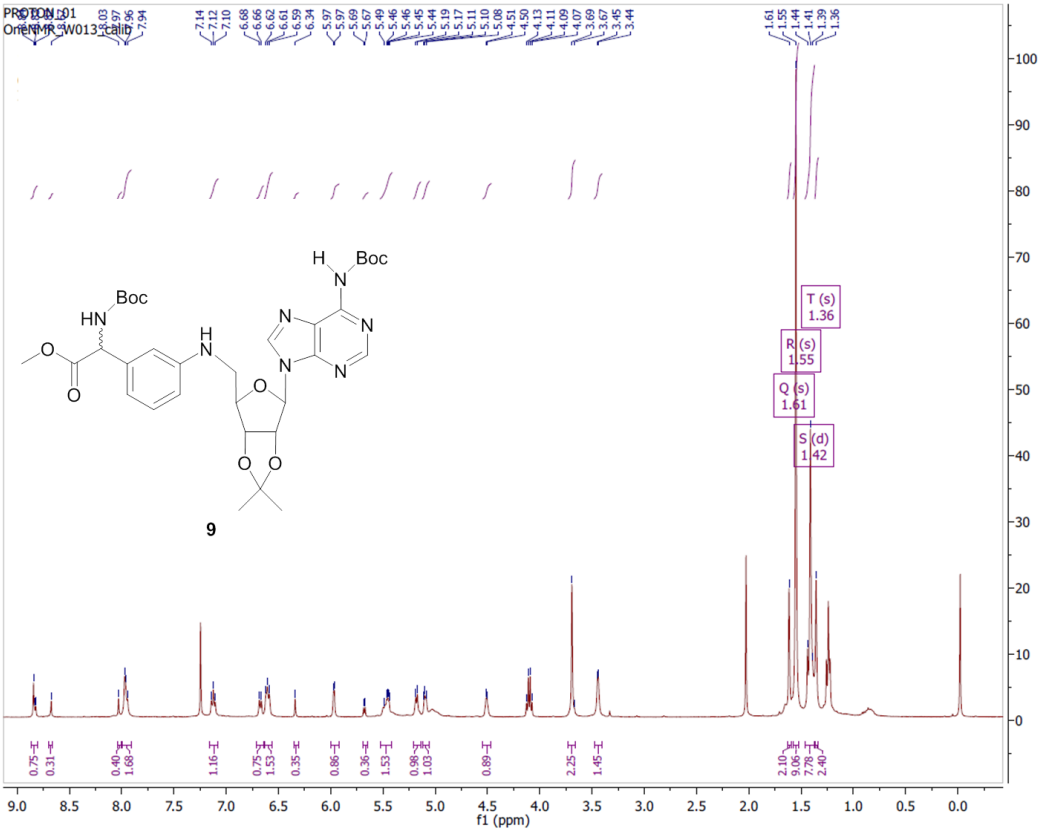
PROTON_01
OneNMR-W013-calib
H
Boc
HN
Boc
H
N
O
O
O
O
9
T (s)
1.36
R (s)
1.55
Q (s)
1.61
S (d)
1.42
f1 (ppm)

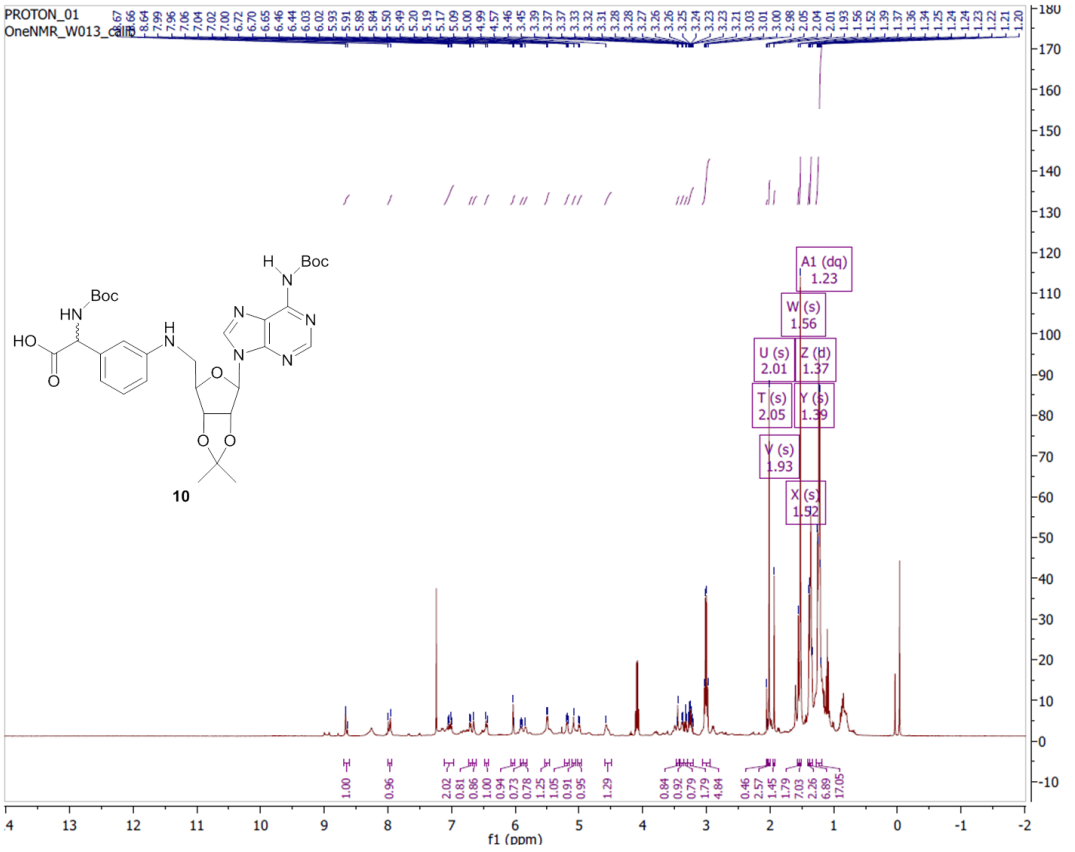
PROTON_01
OneNMR_W013_cal8
A1 (dq)
1.23
W (s)
1.56
U (s)
2.01
Z (d)
1.37
T (s)
2.05
Y (s)
1.39
V (s)
1.93
X (s)
1.92
f1 (ppm)

10

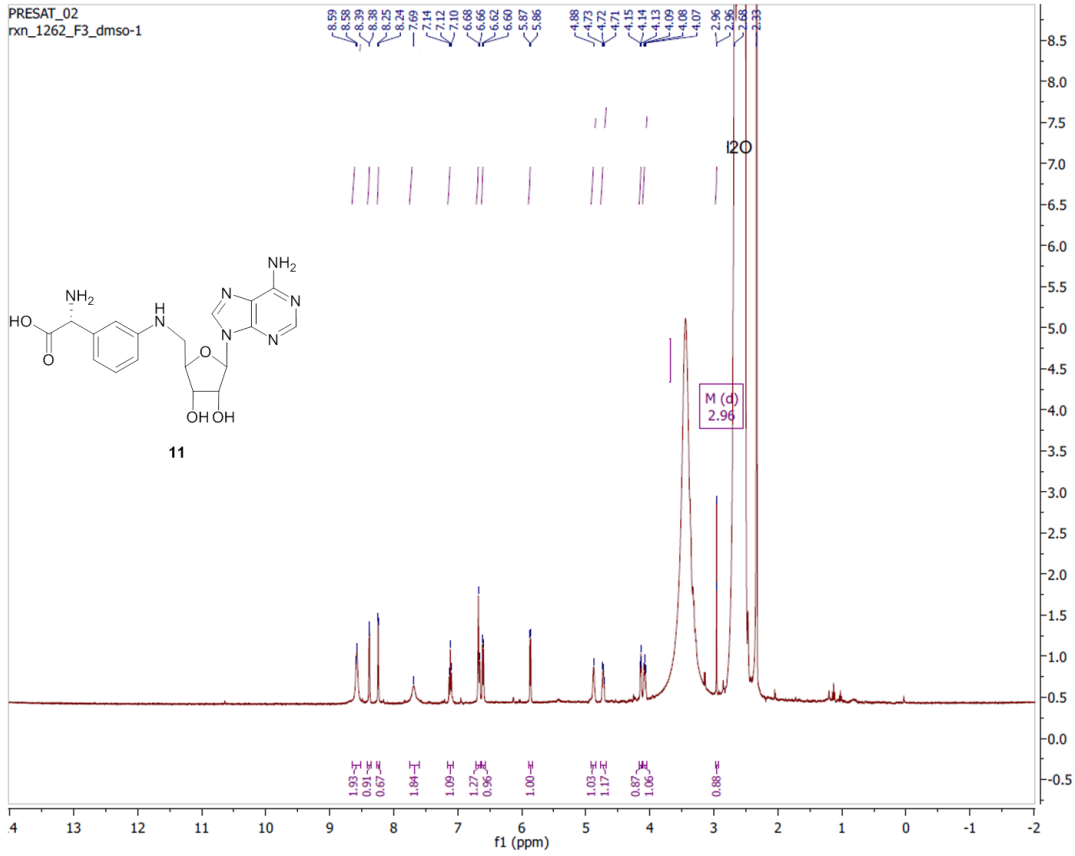
PRESAT_02
rxn_1262_F3_dmso-1
120
M (d)
2.96
f1 (ppm)

11

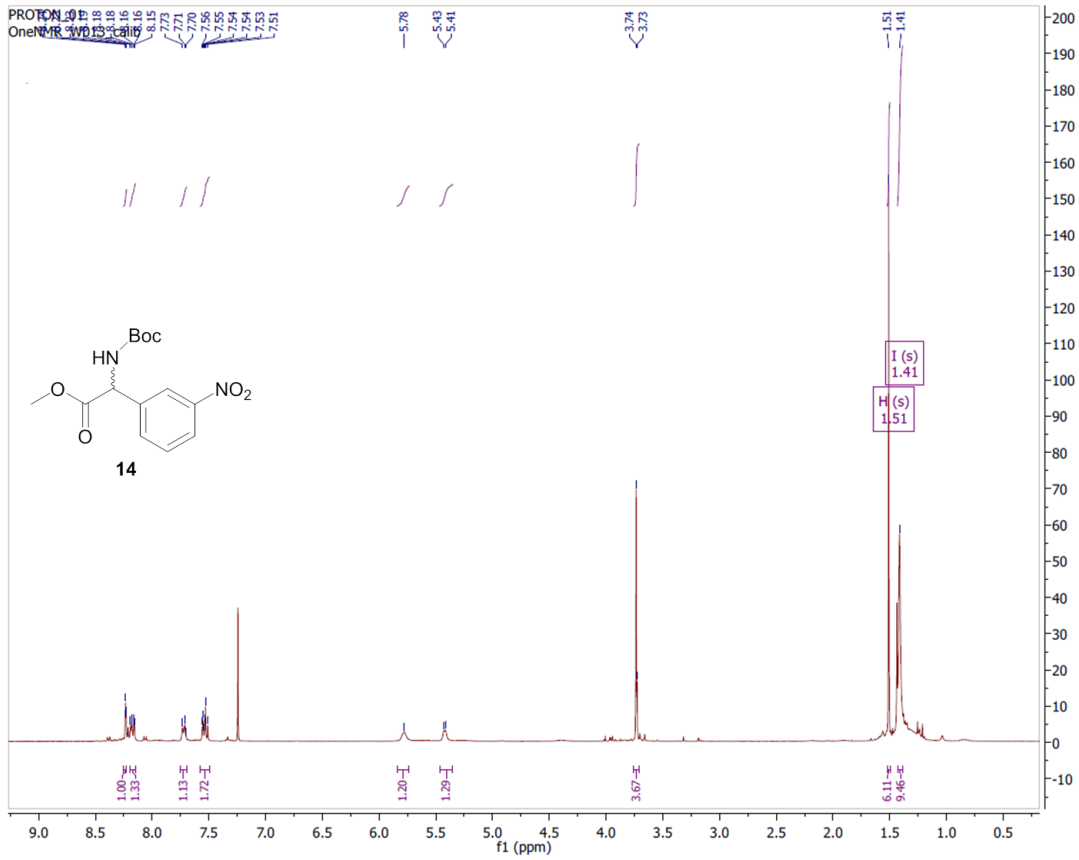
PROTON_01
OneNMR_W013_calib
Boc
HN
O
O
NO2
14
I (s)
1.41
H (s)
1.51
f1 (ppm)

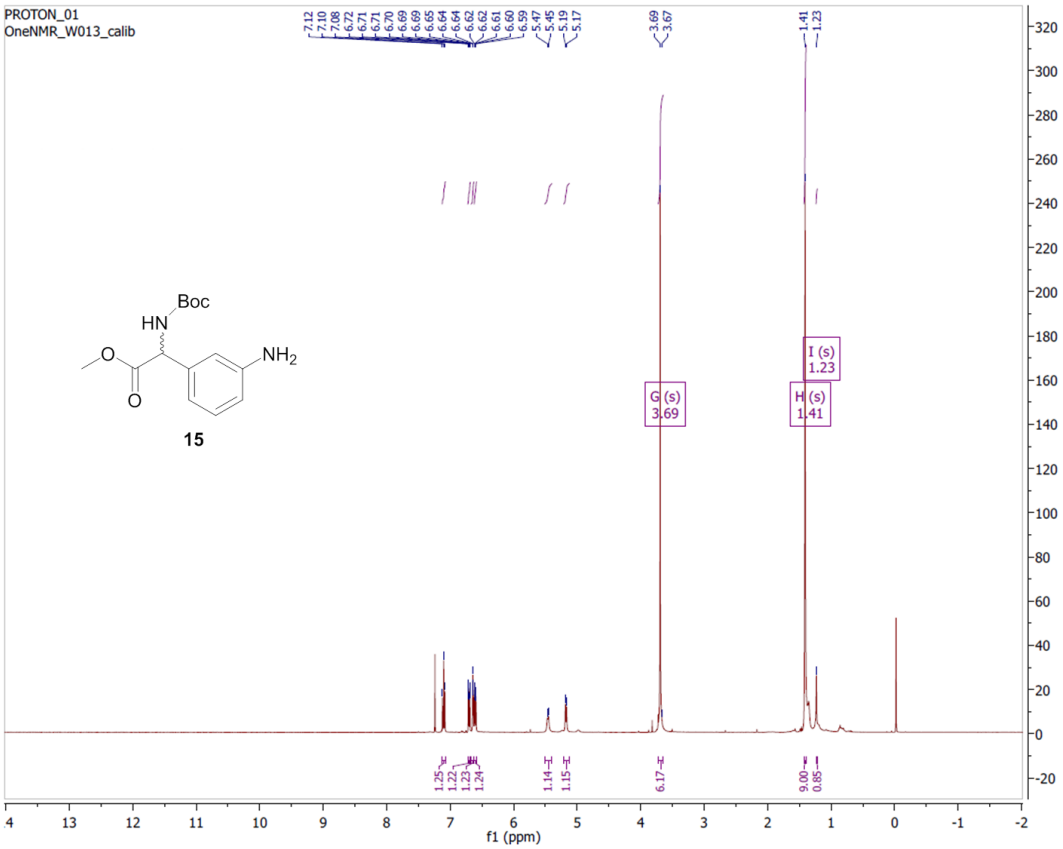
PROTON_01
OneNMR_W013_calib
Boc
HN
O
O
NH2
15
I (s)
1.23
H (s)
1.41
G (s)
3.69
f1 (ppm)

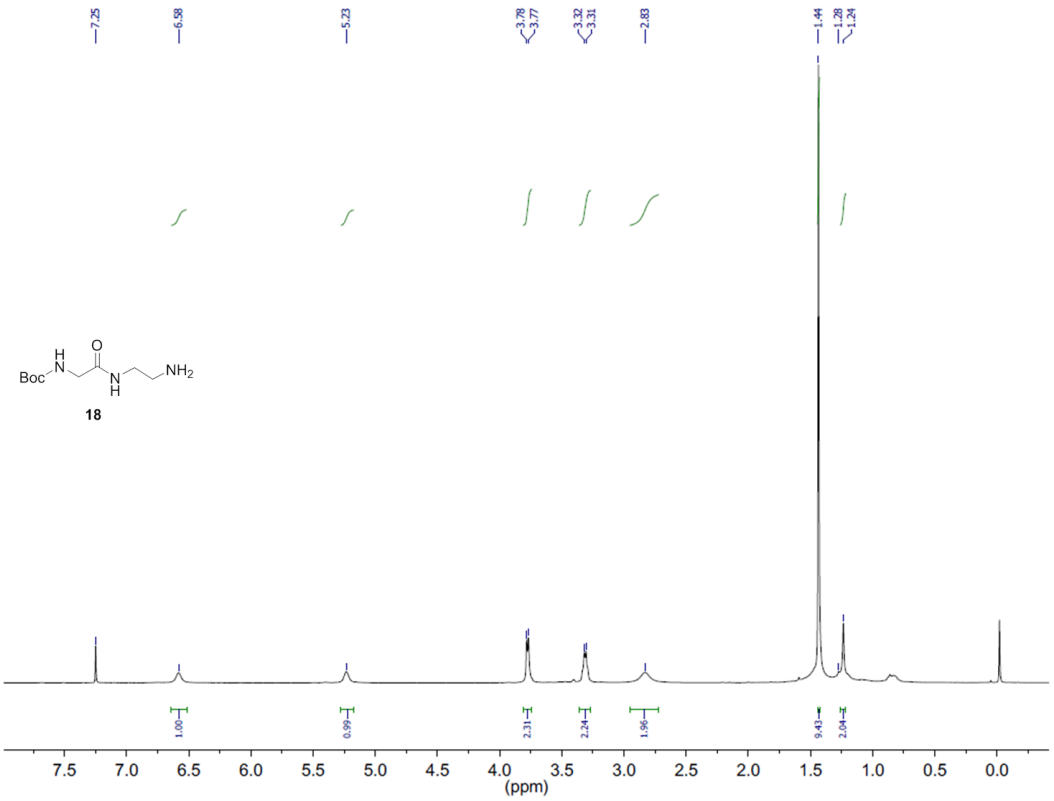
7.25
6.98
5.23
3.78
3.77
3.32
3.31
2.83
1.44
1.28
1.24
Boc
NH2
18
1.00
0.99
2.31
2.24
1.96
9.43
2.04
7.5 7.0 6.5 6.0 5.5 5.0 4.5 4.0 3.5 3.0 2.5 2.0 1.5 1.0 0.5 0.0
(ppm)

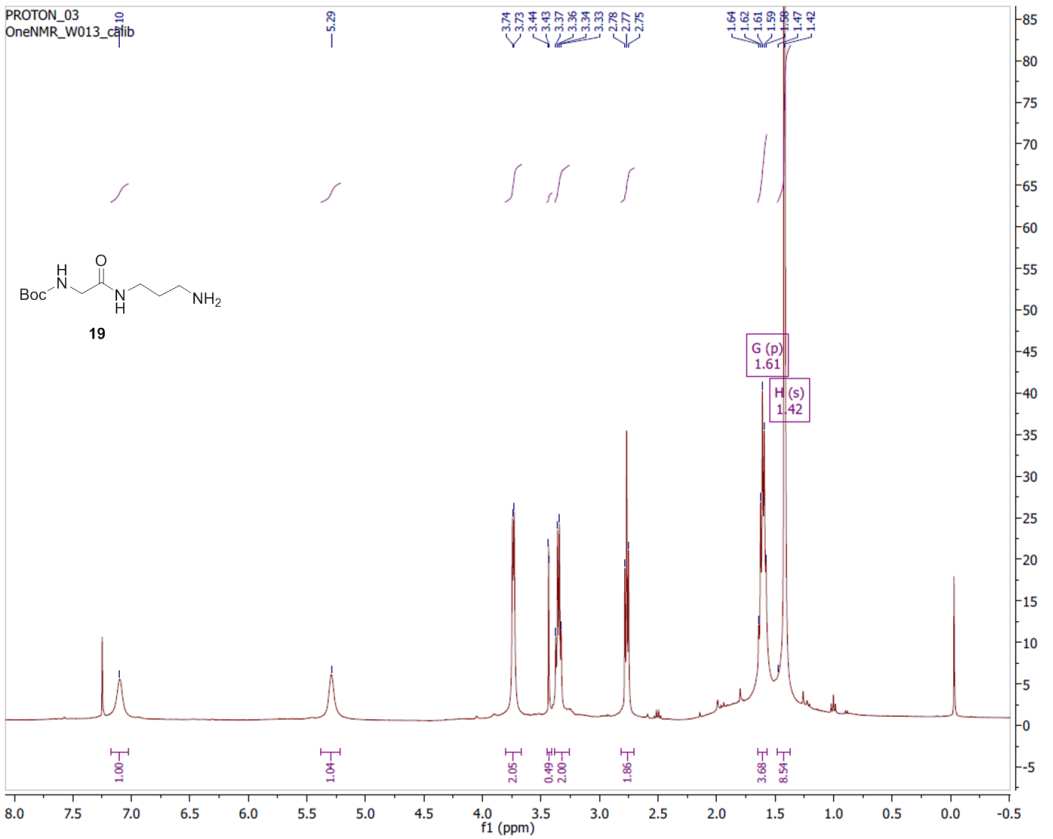
PROTON_03
OneNMR_W013_calib
5.29
3.74
3.73
3.44
3.43
3.37
3.36
3.34
3.33
2.78
2.77
2.75
1.64
1.62
1.61
1.59
1.47
1.42
Boc
NH2
19
G (p)
1.61
H (s)
1.42
1.00
1.04
2.05
0.49
2.00
1.86
3.68
8.54
8.0 7.5 7.0 6.5 6.0 5.5 5.0 4.5 4.0 3.5 3.0 2.5 2.0 1.5 1.0 0.5 0.0 -0.5
f1 (ppm)

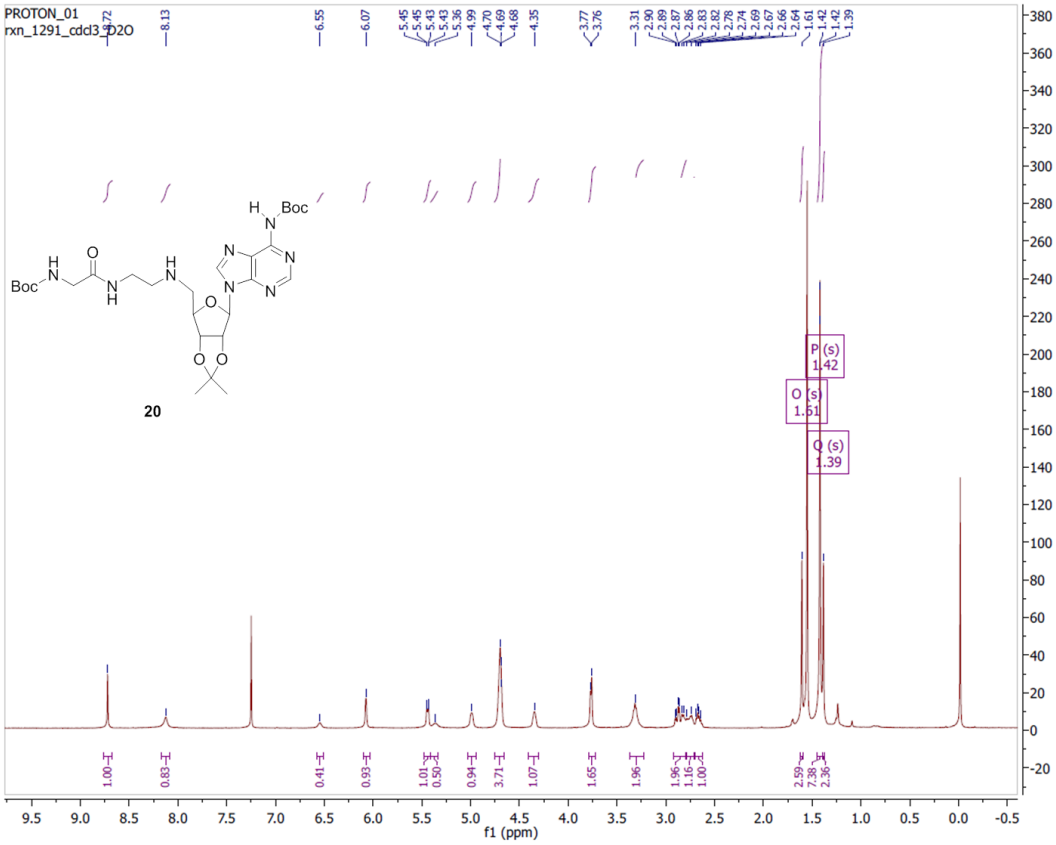
PROTON_01
rxn_1291_cdd3_D2O
P (s)
1.42
O (s)
1.51
Q (s)
1.39
f1 (ppm)

20

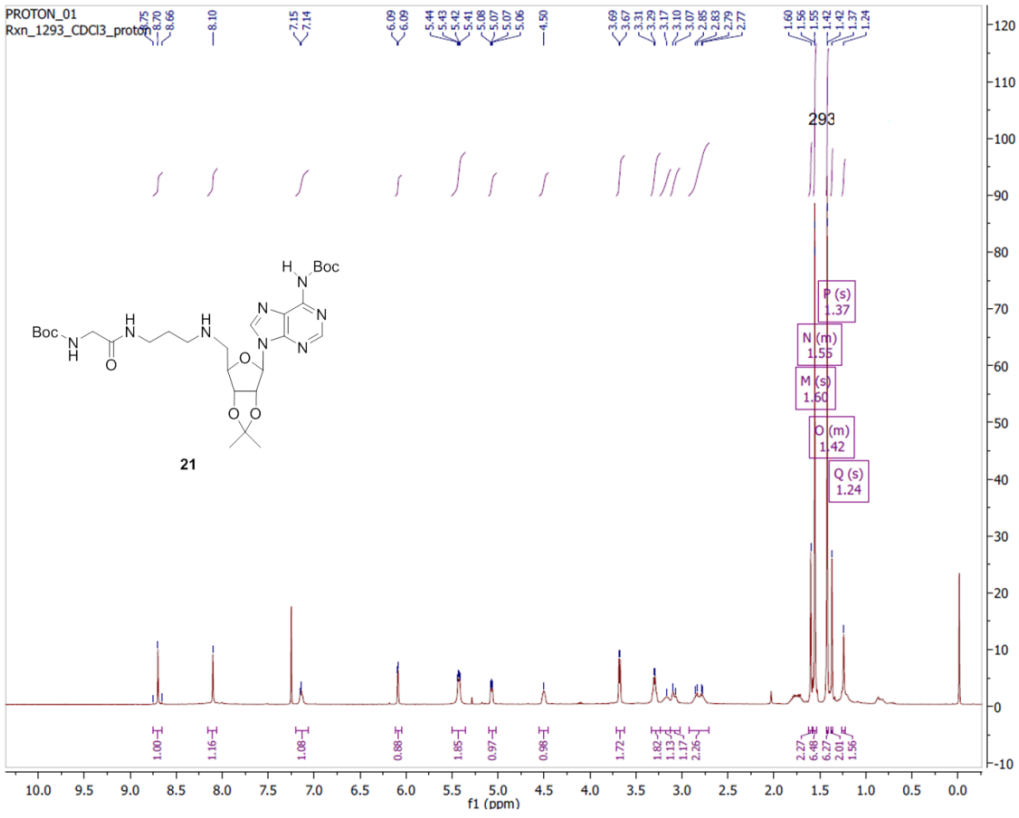
PROTON_01
Rxn_1293_CDCl3_proton
293
P (s)
1.37
N (m)
1.55
M (s)
1.50
O (m)
1.42
Q (s)
1.24
f1 (ppm)

21